EGE UNIVERSITY GRADUATE SCHOOL OF APPLIED AND NATURAL SCIENCES

(MASTER OF SCIENCE THESIS)

REMOVAL OF BORON FROM SEAWATER BY ION EXCHANGE AND MEMBRANE PROCESSES

SARPER SARP

Department of Chemical Engineering
Department Code : 603.01.00

Date of Presentation : 31.07.2006

Supervisors : Prof. Dr. Nalan KABAY
Prof. Dr. Mithat YÜKSEL

II

Sarper SARP tarafından **Yüksel Lisans** tezi olarak sunulan "**Removal of boron from seawater by ion exchange and membrane processes**" başlıklı bu çalışma, E.Ü. Lisansüstü Eğitim ve Öğretim Yönetmeliği ile E.Ü. Fen Bilimleri Enstitü Eğitim ve Öğretim Yönergesi'nin ilgili hükümleri uyarınca tarafımızdan değerlendirilerek savunmaya değer bulunmuş ve **31.07.2006** tarihinde yapılan tez savunma sınavında aday oybirliği/oyçokluğu ile başarılı bulunmuştur.

		İmza
Jüri Başkanı	: Prof. Dr. Nalan KABAY	.....
Üye	: Prof. Dr. Ümran YÜKSEL	.....
Üye	: Prof. Dr. Mehmet SAĞLAM	.....

IV

ÖZET

İYON DEĞİŞTİRME VE MEMBRAN PROSESLERLE DENİZ SUYUNDAN BOR GİDERİLMESİ

SARP, Sarper

Yüksek Lisanas Tezi, Kimya Mühendisliği Bölümü

Tez Yöneticileri: Prof. Dr. Nalan KABAY

Prof. Dr. Mithat YÜKSEL

Temmuz, 2006, 192 sayfa

Ters ozmoz desalinasyon prosesi, deniz suyundan içme suyu üretmek için güvenilir ve etkin bir yöntemdir. Dünya Sağlık Örgütü'nün belirlediği düzenlemelere göre, içme suyundaki bor konsantrasyonu 0.5 mg/L yi geçmemelidir. Bu değer hali hazırda işletilmekte olan ters ozmoz tesisleri için ulaşılması çok zor bir değerdir. Bu yüzden daha etkin bor uzaklaştırma teknolojileri geliştirilmelidir

Bu çalışmada, borun farklı çözeltilerden (model deniz suyu, içerisine H_3BO_3 eklenmiş, doğal deniz suyundan elde edilmiş ters ozmoz çıkış suyu, model ters ozmoz çıkış suyu, 1.5 mg B/L ve 5 mg B/L derişiminde standart bor çözeltileri), şelatlayıcı, ticari reçineler (Diaion CRB 02 ve Dowex-XUS 43594.00) yardımıyla uzaklaştırılması incelenmiştir.

Çalışmalar; kesikli, sürekli ve iyon değiştirme-membran filtrasyon hibrit olmak üzere üç farklı yöntemle gerçekleştirilmiştir.

Bu çalışmalarda, optimum reçine miktarı, kinetik testler ve kolon sorpsiyon-sıyırma çalışmaları yapılmıştır. Bu çalışmalardan elde edilen verilerle;

- Tanecik boyutunun bor uzaklaştırma üzerine etkisi (0.355-0.500 mm ve 45-125 μm),
- Adsorpsiyon izotermleri (Freundlich ve Langmuir),
- Reçinelerin kinetik performansları,
- Çözelti konsantrasyonun, reçinelerin kinetik performanslarına etkisi,
- Çözeltideki tuz bileşiminin reçinenin kinetik ve kolon performansına etkisi
- İyon değiştirme kinetik basamakları,
- İyon değiştirme hızı tayin basamakları (Sonsuz Çözelti Hacmi ve Reaksiyona Girmemiş Çekirdek Modelleri)
- Akış hızının salıverme kapasitesine etkisi,

incelenmiştir. Bu çalışmaların ışığında iyon değiştirme-membran filtrasyon hibrit proses denemeleri yapılmış ve bu yöntemle sürekli ve etkin bir bor uzaklaştırması sağlanmıştır.

Anahtar Sözcükler: Bor, desalinasyon, iyon değiştirme, mebran filtrasyonu, hibrit proses.

ABSTRACT

REMOVAL OF BORON FROM SEAWATER BY ION EXCHANGE AND MEMBRANE PROCESSES

SARP, Sarper

Master Science Thesis, Department of Chemical Engineering

Supervisors: Prof. Dr. Nalan KABAY

Prof. Dr. Mithat YÜKSEL

July, 2006, 192 pages

Reverse osmosis (RO) membrane desalination process is an efficient and reliable technology for the production of drinking water from seawater. According to the WHO regulations, the boron concentration should be lower than 0.5 mg/L in drinking water. In the literature it was reported that, the concentration limit of boron in drinking water is very low for conventional reverse osmosis desalination plants equipped with commercially available membranes. Therefore, more efficient separation technologies are needed for boron removal.

In this study, removal of boron from different solutions (model seawater, H_3BO_3 added natural seawater RO permeate, model RO permeate, standard solutions of 1.5 mg B/L and 5 mg B/L solutions) with two commercial chelating resins (Diaion CRB 02 and Dowex-XUS 43594.00) was studied.

Experiments were performed with tree different methods; batch studies, column mode sorption-elution studies and sorption-membrane filtration hybrid studies.

According to these studies:

- Effect of particle sizes on boron removal (0.355-0.500 mm ve 45-125 μm),
- Adsorption isotherms (Freundlich and Langmuir),
- Kinetic performances of the resins,
- Effect of the boron concentration on kinetic performances of resins,
- Effect of salt composition of the solution on kinetic and column performances of resins,
- Sorption kinetic orders,
- Rate determining steps of the sorption (Infinite Solution and Unreacted Core Models)
- Effect of SV (space velocity) on breakthrough capacities

were investigated. Efficient and continuous boron removal was achieved by hybrid process with the guiding of the obtained results.

Key words: Boron, desalination, ion exchange-membrane filtration, hybrid process.

TEŞEKKÜR

Bu çalışma finansal olarak Ortadoğu Desalinasyon Araştırma Merkezi (MEDRC) tarafından 04-AS-004 No'lu projeyle desteklenmiştir. Sağladıkları maddi destekten dolayı Ortadoğu Desalinasyon Araştırma Merkezi'ne teşekkürlerimi sunarım.

Bu çalışma, aynı zamanda Ege Üniversitesi Rektörlüğü Bilimsel Araştırma Proje Saymalığı tarafından 2005 BIL 014 ve 2005 MUH 033 No'lu projelerle de desteklenmiştir. Katkılarından ötürü Ege Üniversitesi Rektörlüğü Bilimsel Araştırma Proje Saymanlığı'na teşekkürlerimi sunarım.

Tez çalışmamın başarıya ulaşmasında büyük bir özveri ile bütün imkanlarını önüme seren, bana yeni ufuklar açan tez danışman hocam Sayın Prof. Dr. Nalan KABAY'a; değerli bilgi ve tecrübeleriyle çalışmalarıma ışık tutan, büyük desteğini gördüğüm ve bir baba kadar sevip saygı duyduğum hocam Sayın Prof. Dr. Mithat YÜKSEL'e saygı ve şükranlarımı sunmayı bir borç bilirim.

Yüksek lisans çalışmalarım esnasında dört ay süreyle eğitim stajında bulunmak üzere gittiğim Güney Kore'deki Gwangju Enstitude of Science and Technology'e ve bu enstitüdeki desteklerinden ötürü Sayın Prof. Dr. Jaeweon Cho'ya; gerek Kore'deki bilimsel çalışmalarda gerekse sosyal alanda yardımlarını biran olsun esirgemeyen, değerli microHM ailesine minnettarım.

Tezimi inceleyerek verdikleri katkılardan ötürü Sayın Prof. Dr. Ümran Yüksel ve Sayın Prof. Dr. Mehmet Sağlam'a teşekkürlerimi sunarım.

Avicenne Proje Laboratuarı'ndaki yardımlarından ve dostuklarından dolayı Yard. Doç. Müşerref Arda'ya, Araştırma Görevlileri İdil Yılmaz ve Özgür Arar'a, Dr. Saba Samatya'ya ve Özlem Kırmızısakal'a teşekkür ederim.

Bora seçimli reçineleri sağlayan Dow Chemicals, Germany (M. Busch) ve Mitsubishi Chemicals, Japan firmalarına, ters ozmoz çıkış suyu örneklerini teminlerinden dolayı Doç. Dr. Mehmet Kitiş ve Araştırma Görevlisi Hasan Köseoğlu'na ve AAS ile yapılan ölçümlerdeki yardımlarından ötürü Mehmet Akçay'a teşekkürü bir borç bilirim.

Bu noktaya gelmemdeki büyük emeklerinden ve özverilerinden dolayı başta annem olmak üzere aileme, hayatımın son 7 ayında her daim yanımda olan ve kalanında da yanımda olmasını istediğim Sema ŞİRİN'e sonsuz teşekkürler.

Sarper SARP

TABLE OF CONTENTS

ÖZET V

ABSTRACT VII

TEŞEKKÜR IX

LIST OF FIGURES XV

LIST OF TABLES XXV

NOMENCLATURE XXVII

1. INTRODUCTION 1
   1.1 Boron 1
      1.1.1 History and sources of boron 2
      1.1.2 Chemistry in nature 4
      1.1.3 Industrial uses of boron 5
      1.1.4 Health effects of boron 7
         1.1.4.1 Plants 7
         1.1.4.2 Microorganisms 8
         1.1.4.3 Aquatic organisms 8
         1.1.4.4 Animals 9
         1.1.4.5 Humans 10
      1.1.5 Regulations and guidelines for boron 11
         1.1.5.1 U.S. EPA Contaminant Candidate List (CCL) 11
         1.1.5.2 World Health Organization Guideline 12
         1.1.5.3 European Union 12

1.1.5.4 Canada 13
1.1.5.5 New Zealand 13
1.1.6 Importance of boron in Turkey 13
1.2 Desalination 14
1.2.1 Sewater desalination 14
1.2.1.1 Multi effect distillation (MED) 16
1.2.1.2 Multi stage flash (MSF) evaporation 17
1.2.1.3 Reverse Osmosis (RO) 18
1.3 Removal of Boron from Seawater 20
1.3.1 Reverse osmosis 20
1.3.2 Ion exchange 23
1.3.3 Hybrid process 26
1.4 Ion Exchange Technology 28
1.4.1 Ion exchange phenomenon 28
1.4.2 Synthesis of ion exchange resins 33
1.4.3 Properties and characterization of ion exchange resins 35
1.4.4 The kinetics of ion exchange 39
1.4.5 Ion exchange operational techniques 47
1.4.5.1 Batch operation 48
1.4.5.2 Column operation 48
1.4.5.3 Ion exchange capacity 50
2. EXPERIMENTAL 52
2.1 Materials 52
2.1.1 Ion exchange resins 52
2.1.2 Chemicals 53
2.1.3 Solutions 53
2.1.4 Equipments 56
2.2 Methods 57
2.2.1 Batch mode sorption studies 57

2.2.1.1 Effect of pH on removal of boron from 5 mg B/L solution 57
2.2.1.2 Effect of resin amount on removal of boron from model seawater 57
2.2.1.3 Effect of resin amount on removal of boron from H_3BO_3 added natural seawater RO permeate solution 58
2.2.1.4 Effect of resin amount on removal of boron from 1.5 mg B/L solution 58
2.2.1.5 Effect of resin amount on removal of boron from 5 mg B/L solution 58
2.2.1.6 Kinetic tests using model saewater 59
2.2.1.7 Kinetic tests using NaCl + H_3BO_3 solution 59
2.2.1.8 Kinetic tests using H_3BO_3 added natural seawater RO permeate solution 59
2.2.1.9 Kinetic tests using 1.5 mg B/L solution 60
2.2.1.10 Kinetic tests using 5 mg B/L solution 60
2.2.2 Column mode sorption-elution studies 60
2.2.3 Sorption-membrane filtration hybrid method 62
2.3 Chemical Analysis 64
2.3.1 Boron analysis 64
3. RESULTS AND DISCUSSION 66
3.1 Removal of Boron from Model Seawater 66
3.1.1 Effect of resin amount on removal of boron from model seawater as a function of resin particle size 66
3.1.2 Sorption isotherms of boron removal from model seawater 70
3.1.3 Kinetic performance of the resins in model seawater 80
3.1.4 Column mode sorption-elution studies of the resins in model seawater 98
3.2 Removal of Boron from NaCl + H_3BO_3 Solution 101

3.2.1 Kinetic performance of the resin in NaCl + H_3BO_3 Solution....101
3.2.2 Column mode sorption-elution studies of the resins in NaCl + H_3BO_3 solution....106
3.3 Removal of Boron from H_3BO_3 Added Natural Seawater RO Permeate Solution....108
3.3.1 Effect of resin amount on removal of boron from H_3BO_3 added natural seawater RO permeate solution....108
3.3.2 Sorption isotherms of removal of boron from H_3BO_3 added natural seawater RO permeate solution....110
3.3.3 Kinetic performance of the resins in H_3BO_3 added natural seawater RO permeate solution....114
3.3.4 Column mode sorption-elution studies of the resins in H_3BO_3 added natural seawater RO permeate solution....123
3.4 Removal of Boron by Sorption-Membrane Filtration Hybrid Method....127
3.4.1 Effect of resin amount on removal of boron from 1.5 and 5 mg B/L solutions....127
3.4.2 Kinetic performance of the resins in 1.5 and 5 mg B/L solutions....129
3.4.3 Effect of pH on removal of boron from 5 mg B/L solution....129
3.4.4 Removal of boron by sorption-membrane filtration hybrid method with 1.5 mg B/L, 5 mg B/L and model RO permeate solutions....130
4. CONCLUSIONS....136
APPENDIX-I....141
APPENDIX-II....162
REFERENCES....181
CURRICULUM VITAE....192

LIST OF FIGURES

Figure	Page
1.1 Distribution of polyborate species as a function of pH, 0.40M boric acid.	5
1.2 Operation principle of multi effect ditillation.	17
1.3 Operation principle of multi stage flash evaporation	18
1.4 Flow Diagram of Conventional Single Stage RO Seawater Desalination System (Water Recovery 40%)	19
1.5 Boron rejection with FILMTEC membrane elements as a function of pH	22
1.6 Temperature dependence of permeate TDS and boron rejection	22
1.7 Impact of average permeate flux on boron permeate concentration	23
1.8 Structure of the boron selective resin	24
1.9 Capturing of boric acid	25
1.10 Conjugate acid form consumes eluant acid	26
1.11 Overview of the hybrid process options	27
1.12 A cation exchange resin structure	29
1.13 Styrene-divinylbenzene copolymer	34
1.14 Radial concentration profiles for ideal particle diffusion control (schematic)	40
1.15 Breakthrough curve of column operation	50
2.1 Flow-sheet of column mode sorption-elution studies	61
2.2 Flow-sheet of sorption-membrane filtration hybrid method	63
2.3 Calibration curve of boron by curcumine method	65

LIST OF FIGURES

Figure	Page
3.1 Removal of boron from model seawater solution by boron selective resins (0.355-0.500 mm)	69
3.2 Removal of boron from model seawater solution by boron selective resins (45-75 μm)	69
3.3 Effect of particle size of resins for boron removal from model seawater solution	70
3.4 Equilibrium isotherm for loading B onto Diaion CRB 02 (0.355-0.500 mm)	72
3.5 Equilibrium isotherm for loading B onto Dowex-XUS 43594.00 (0.355-0.500 mm)	72
3.6 Linearized form of Langmuir isotherm for Diaion CRB 02 (0.355-0.500 mm)	73
3.7 Linearized form of Langmuir isotherm for Dowex-XUS 43594.00 (0.355-0.500 mm)	74
3.8 Linearized form of Freundlich isotherm for Diaion CRB 02 (0.355-0.500 mm)	74
3.9 Linearized form of Freundlich isotherm for Dowex-XUS 43594.00 (0.355-0.500 mm)	75
3.10 Equilibrium isotherm for loading B onto Diaion CRB 02 (45-75 μm)	76
3.11 Equilibrium isotherm for loading B onto Dowex-XUS 43594.00 (45-75 μm)	76
3.12 Linearized form of Langmuir isotherm for Diaion CRB 02 (45-75 μm).	77

LIST OF FIGURES

Figure	Page
3.13 Linearized form of Langmuir isotherm for Dowex-XUS 43594.00 (45-75 μm)	78
3.14 Linearized form of Freundlich isotherm for Diaion CRB 02 (45-75 μm)	78
3.15 Linearized form of Freundlich isotherm for Dowex-XUS 43594.00 (45-75 μm)	79
3.16 Comparison of kinetic performances of Diaion CRB 02 and Dowex-XUS 43594.00 (0.355-0.500 mm) for B removal	80
3.17 Comparison of kinetic performances of Diaion CRB 02 and Dowex-XUS 43594.00 (45-75 μm) for B removal	81
3.18 Effect of particle size on kinetic performance for B removal	81
3.19 Lagergren pseudo-first-order kinetics for B adsorption on Diaion CRB 02 (0.355-0.500 mm)	85
3.20 Ho pseudo-second-order kinetics for B adsorption on Diaion CRB 02 (0.355-0.500 mm)	85
3.21 Comparison of second order kinetic models in predicting q_t for B adsorption on Diaion CRB 02 (0.355-0.500 mm).	86
3.22 Lagergren pseudo-first-order kinetics for B adsorption on Dowex-XUS 43594.00 (0.355-0.500 mm)	86
3.23 Ho pseudo-second-order kinetics for B adsorption on Dowex-XUS 43594.00 (0.355-0.500 mm)	87

LIST OF FIGURES

Figure	Page
3.24 Comparison of second order kinetic models in predicting q_t for B adsorption on Dowex-XUS 43594.00 (0.355-0.500 mm)	87
3.25 Lagergren pseudo-first-order kinetics for B adsorption on Diaion CRB 02 (45-75 μm)	88
3.26 Ho pseudo-second-order kinetics for B adsorption on Diaion CRB 02 (45-75 μm)	88
3.27 Comparison of second order kinetic models in predicting q_t for B adsorption on Diaion CRB 02 (45-75 μm).	89
3.28 Lagergren pseudo-first-order kinetics for B adsorption on Dowex-XUS 43594.00 (45-75 μm)	89
3.29 Ho pseudo-second-order kinetics for B adsorption on Dowex-XUS 43594.00 (45-75 μm).	90
3.30 Comparison of second order kinetic models in predicting q_t for B adsorption on Dowex-XUS 43594.00 (45-75 μm).	90
3.31 Kinetic behavior of Diaion CRB 02 (0.355-0.500 mm) based on Unreacted Core Models.	94
3.32 Kinetic behavior of Diaion CRB 02 (0.355-0.500 mm) based on Infinite Solution Models.	95
3.33 Kinetic behavior of Dowex-XUS 43594.00 (0.355-0.500 mm) based on Unreacted Core Models	95
3.34 Kinetic behavior of Dowex-XUS 43594.00 (0.355-0.500 mm) based on Infinite Solution Models	96
3.35 Kinetic behavior of Dowex-XUS 43594.00 (45-75 μm) based on Unreacted Core Models	96

LIST OF FIGURES

Figure	Page
3.36 Kinetic behavior of Dowex-XUS 43594.00 (45-75 μm) based on Infinite Solution Models.	97
3.37 Breakthrough curves of boron selective resin (Diaion CRB02) for boron removal from model seawater solution as a function of SV	99
3.38 Elution curves of boron selective resin (Diaion CRB02) for boron removal from model seawater solution as a function of SV	99
3.39 Breakthrough curves of boron selective resin (Dowex-XUS 43594.00) for boron removal from model seawater solution as a function of SV	100
3.40 Elution curves of boron selective resin (Dowex-XUS 43594.00) for boron removal from model seawater solution as a function of SV	100
3.41 Comparison of the kinetic performance of boron selective resin (Diaion CRB02) with NaCl+H_3BO_3 and model seawater solutions	102
3.42 Lagergren pseudo-first-order kinetics for B adsorption on Diaion CRB 02 (0.355-0.500 mm) in NaCl + H_3BO_3 solution	103
3.43 Ho pseudo-second-order kinetics for B adsorption on Diaion CRB 02 (0.355-0.500 mm) in NaCl + H_3BO_3 solution	103
3.44 Comparison of second order kinetic models in predicting q_t for B adsorption on Diaion CRB 02 (0.355-0.500 mm) in NaCl + H_3BO_3 solution	104

LIST OF FIGURES

Figure	Page
3.45 Kinetic behavior of Diaion CRB 02 (0.355-0.500 mm) in NaCl + H_3BO_3 solution based on Unreacted Core Models	105
3.46 Kinetic behavior of Diaion CRB 02 (0.355-0.500 mm) in NaCl + H_3BO_3 solution based on Infinite Solution Models	105
3.47 Breakthrough curves of boron selective resin (Diaion CRB02) for boron removal from NaCl + H_3BO_3 and model seawater solution.	107
3.48 Breakthrough curves of boron selective resin (Diaion CRB02) for boron removal from NaCl + H_3BO_3 and model seawater solution	107
3.49 Removal of boron from H_3BO_3 added natural seawater RO permeate solution by boron selective resins (0.355-0.500 mm).	110
3.50 Equilibrium isotherm for loading B onto Diaion CRB 02 (0.355-0.500 mm) in H_3BO_3 added natural seawater RO permeate solution	111
3.51 Equilibrium isotherm for loading B onto Dowex-XUS 43594.00 (0.355-0.500 mm) in H_3BO_3 added natural seawater RO permeate solution	111
3.52 Linearized form of Langmuir isotherm for Diaion CRB 02 (0.355-0.500 mm), in H_3BO_3 added natural seawater RO permeate solution	112
3.53 Linearized form of Langmuir isotherm for Dowex-XUS 43594.00 (0.355-0.500 mm), in H_3BO_3 added natural seawater RO permeate solution	112

LIST OF FIGURES

Figure Page

3.54 Linearized form of Freundlich isotherm for Diaion CRB 02 (0.355-0.500 mm), in H_3BO_3 added natural seawater RO permeate solution 113

3.55 Linearized form of Freundlich isotherm for Dowex-XUS 43594.00 (0.355-0.500 mm), in H_3BO_3 added natural seawater RO permeate solution 113

3.56 Comparison of kinetic performances of Diaion CRB 02 and Dowex-XUS 43594.00 (0.355-0.500 mm) for B removal with H_3BO_3 added natural seawater RO permeate solution. 114

3.57 Comparison of kinetic performances of the resin Diaion CRB 02 (0.355-0.500 mm) with model seawater and H_3BO_3 added natural seawater RO permeate solution 115

3.58 Lagergren pseudo-first-order kinetics for B adsorption on Diaion CRB 02 (0.355-0.500 mm) in H_3BO_3 added natural seawater RO permeate solution 117

3.59 Ho pseudo-second-order kinetics for B adsorption on Diaion CRB 02 (0.355-0.500 mm) in H_3BO_3 added natural seawater RO permeate solution 117

3.60 Comparison of second order kinetic models in predicting q_t for B adsorption on Diaion CRB 02 (0.355-0.500 mm) in H_3BO_3 added natural seawater RO permeate solution. 118

3.61 Lagergren pseudo-first-order kinetics for B adsorption on Dowex-XUS 43594.00 (0.355-0.500 mm) in H_3BO_3 added natural seawater RO permeate solution 118

LIST OF FIGURES

Figure	Page
3.62 Ho pseudo-second-order kinetics for B adsorption on Dowex-XUS 43594.00 (0.355-0.500 mm) in H_3BO_3 added natural seawater RO permeate solution	119
3.63 Comparison of second order kinetic models in predicting q_t for B adsorption on Dowex-XUS 43594.00 (0.355-0.500 mm) in H_3BO_3 added natural seawater RO permeate solution.	119
3.64 Kinetic behavior of Diaion CRB 02 (0.355-0.500 mm) in H_3BO_3 added natural seawater RO permeate solution based on Unreacted Core Models	121
3.65 Kinetic behavior of Diaion CRB 02 (0.355-0.500 mm) in H_3BO_3 added natural seawater RO permeate solution based on Infinite Solution Models	121
3.66 Kinetic behavior of Dowex-XUS 43594.00 (0.355-0.500 mm) in H_3BO_3 added natural seawater RO permeate solution based on Unreacted Core Models	122
3.67 Kinetic behavior of Dowex-XUS 43594.00 (0.355-0.500 mm)) in H_3BO_3 added natural seawater RO permeate solution based on Infinite Solution Models	122
3.68 Breakthrough curves of boron selective resin (Diaion CRB02) for boron removal from H_3BO_3 added natural seawater RO permeate solution as a function of SV	124
3.69 Elution curves of boron selective resin (Diaion CRB02) for boron removal from H_3BO_3 added natural seawater RO permeate solution as a function of SV	125

LIST OF FIGURES

Figure	Page
3.70 Breakthrough curves of boron selective resin (Dowex-XUS 43594.00) for boron removal from H_3BO_3 added natural seawater RO permeate solution as a function of SV	125
3.71 Elution curves of boron selective resin (Dowex-XUS 43594.00) for boron removal from H_3BO_3 added natural seawater RO permeate solution as a function of SV	126
3.72 Removal of boron by Diaion CRB 02 (45-125 μm), as afunction B concentration.	128
3.73 Comparison of kinetic performances of Diaion CRB 02 (45-125 μm) for B removal as a function of B concentration	129
3.74 Efffect of pH on boron removal from 5 mg B/L solution with Diaion CRB 02 (0.355-0.500 mm)	130
3.75 Blank curves of the permeate solutions in 1.5 mg B/L, 5 mg B/L and model RO permeate solutions	132
3.76 Boron removal by using sorption-membrane filtration hybrid method with Diaion CRB 02 (45-125μm)	132
3.77 Boron removal by using sorption-membrane filtration hybrid method with Diaion CRB 02 (45-125 μm).	133
3.78 C/C_0 vs time plots obtained by using sorption-membrane filtration hybrid (45-125 μm, Diaion CRB 02) and batch (0.355-0.500 mm, Diaion CRB 02) methods	134
3.79 C/C_0 vs time plots obtained by using sorption-membrane filtration hybrid and batch methods with Diaion CRB 02 (45-125 μm)	134

XXIV

LIST OF TABLES

Table	Page
1.1 Important refined borate products and mineral concentrates	3
2.1 Typical chemical and physical characteristic of Diaion CRB 02	52
2.2 Typical chemical and physical characteristic of Dowex-XUS 43594.00	52
2.3 Composition of model seawater solution	55
2.4 Composition of NaCl + H_3BO_3 solution.	55
2.5 Composition of H_3BO_3 added natural seawater RO permeate solution.	55
2.6 Composition of model RO permeate solution	56
3.1 Effect of Resin Amount on Removal of Boron from Model Seawater by Diaion CRB 02 and Dowex-XUS 43594.00 (0.355-0.500 mm)	67
3.2 Effect of Resin Amount on Removal of Boron from Model Seawater by Diaion CRB 02 and Dowex-XUS 43594.00 (45-75 μm).	68
3.3 Diffusional and reaction models	93
3.4 Evaluation of kinetic models for Diaion CRB 02 and Dowex-XUS 43594.00 (0.355-0.500 mm and 45-75 μm).	98
3.5 Column data for boron removal from model seawater solution.	101
3.6 Evaluation of kinetic models for Diaion CRB 02 (0.355-0.500 mm) in NaCl + H_3BO_3 solution	106

LIST OF TABLES

Table	Page
3.7 Column data for boron removal from model seawater solution.	108
3.8 Effect of Resin Amount on removal of boron from H_3BO_3 added natural seawater RO permeate solution by Diaion CRB 02 and Dowex-XUS 43594.00 (0.355-0.500 mm)	109
3.9 Evaluation of kinetic models for Diaion CRB 02 and Dowex-XUS 43594.00 (0.355-0.500 mm) in H_3BO_3 added natural seawater RO permeate solution.	123
3.10 Column data for boron removal from H_3BO_3 added natural seawater RO permeate solution	127
3.11 Effect of resin amount on removal of boron from 1.5 and 5 mg B/L solutions by Diaion CRB 02 (45-125 μm)	128

NOMENCLATURE

a	:	specific surface area (m^2/m^3), stoichiometric coefficient
b	:	constant in Langmuir equilibrium (m^3/kg)
C	:	concentration of the solute in the solvent (kg/m^3)
C_{A0}	:	solute concentration in the bulk solution (M)
C_0	:	initial concentration (mg/L)
C_{s0}	:	concentration of the solid reactant at the bead's unreacted core (M)
d_p	:	particle diameter (m)
D	:	diameter of the packed bed column (m)
$\bar{D}$	:	inter-diffusion coefficient in the ion exchange resin
D_0	:	inter-diffusion coefficient in the film
$D_{e,r}$	:	effective diffusion coefficient in the solid phase (m^2/s)
F	:	surface area (m^2)
H	:	height of the sorbent layer in packed bed column (m)
J	:	permeate flux (m^3/m^2s)
k	:	kinetic constant (s^{-1})
K_{mA}	:	mass-transfer coefficient of the solute through the liquid film (m/s)
k_s	:	reaction constant based on surface (m/s)
m	:	mass of the solute (kg)
P	:	pressure drop during the flow in the column (Pa)
q	:	solute concentration in the sorbent (kg/kg)
r_0	:	average particle radius (mm)
X	:	concentration of fixed groups

v	:	superficial velocity of the feed in columns
V_b	:	Breakthrough volume (mL)
V_{eq}	:	Equilibrium volume (mL)

Greek Letters

δ	:	film thickness (m)
ε	:	porosity
η	:	membrane-sorption efficiency
μ	:	viscosity (Pa s)
τ	:	tortuosity
α_B^A	:	separation factor

1. INTRODUCTION

1.1 Boron

Boron is an ubiquitous element in rocks, soil, and water. Most of the earth's soils have <10 ppm boron, with high concentrations found in parts of the western United States and in other sites stretching from the Mediterranean to Kazakhstan. The average soil boron concentration is 10 to 20 ppm, with large areas of the world boron deficient. Boron concentrations in rocks range from 5 ppm in basalts to 100 ppm in shales, and averages l0 ppm in the earth's crust overall. Soils have boron concentrations of 2 to 100 ppm. Seawater contains an average of 4.6 ppm boron, but ranges from 0.5 to 9.6 ppm. Freshwaters normally range from <0.01 to 1.5 ppm, with higher concentrations in regions of high boron soil levels (Morgan, 1980; Woods, 1994). Food is the primary source of boron that is ingested by humans. A recent study indicates that the average adult in the United States consumes about 1 mg boron per day in diet (Meacham and Hunt, 1998). The richest sources of boron include fruits and nuts. Wine is also a major contributor (Parks and Edwards, 2005).

Highly concentrated, economically sized deposits of boron minerals, always in the form of compounds with boron bonded to oxygen, are rare and generally are found in arid areas with a history of volcanism or hydrothermal activity. Such deposits are being exploited in Turkey, the United States, and several other countries (Matterson, 1980). Borate-mineral concentrates and refined products are produced and sold worldwide. They are used in a myriad ways: in glass and related vitreous applications, in laundry bleaches, in fire retardants, as micronutrients in fertilizers and for many other purposes, as well (Woods, 1994).

The varied chemistry and importance of boron is dominated by the ability of borates to form trigonal as well as tetrahedral bonding patterns and to create complexes with organic functional groups, many of biologic importance.

1.1.1 History and sources of boron

The Babylonians have been credited with importing borax from the Far East over 4000 years ago for use as a flux for working gold. Mummifying, medicinal and metallurgic applications of boron are sometimes attributed to the ancient Egyptians. None of this very old borax history has been verified, but solid evidence exists that tinkar (i.e., $Na_2B_4O_7•10H_2O$, tincal, the mineral borax) was first used in the eighth century around Mecca and Medina, having been brought there (and to China) by Arab traders (Travis et al., 1984). The use of borax flux by European goldsmiths dates to about the l2th century.

The earliest source of borax is believed to have been Tibetan lakes. The borax was transported in bags tied to sheep, which were driven over the Himalayas to India.

Volatility of boric acid with steam is believed by geologists to be the primary mechanism for the formation of borate deposits (Matterson, 1980). Prime examples of this are the geysers (soffioni) in Tuscany, which were an important source of boric acid in Europe from about 1820 to the 1950s (Woods, 1994).

The borate industry in Turkey commenced in 1865 with mining of the calcium borate pandermite (priceite, $4CaO•5B_2O_3•7H_2O$). At about the same time, several borate deposits were found in California and Nevada, including ulexite ($Na_2O•2CaO•5B_2O_3•l6H_2O$) and colemanite ($2CaO•3B_2O_3•5H_2O$) in Death Valley. These minerals could be converted to borax by reaction with trona ($Na_2CO_3•NaHCO_3•2H_2O$) (Woods, 1994).

The Kramer deposit, at what is now Boron, California, in the Mojave Desert, was discovered in 1913, first as a colemanite ore source. In l925, tincal ore was found and in l926, the new mineral rasorite (kernite, $Na_2O•2B_2O_3•4H_2O$) was encountered (Travis et al., 1984). It is the largest borate deposit outside of Turkey and has supplied a sizable portion of world borate demand for over 50 years.

Turkey has supplied colemanite for many years to boric acid producers in Europe. Sodium borates were discovered at Kirka in l960 and other deposits have since been found and developed in Anatolia. As a result, today Turkey is the largest producer of borate products in the world (Sprague, 1992), exporting mineral concentrates of tincal, colemanite, and ulexite, plus refined borax decahydrate, borax pentahydrate ($Na_2O•2B_2O_3•5H_2O$) anhydrous borax ($Na_2O•2B_2O_3$) and boric acid ($B(OH)_3$) (Parks and Edwards, 2005).

Table 1.1 gives a list of the commercially important refined borate products and mineral concentrates.

Table 1.1 Important refined borate products and mineral concentrates

Substance	**%B_2O_3**	**Place**
Tincal Conite	47.8	Turkey, Argentina, USA
Tincal	36.5	Turkey
Cernite (Razorite)	50.9	USA, Argentina
Ulexite	43.0	Turkey, USA
Colemanite	50.9	Turkey, USA, Mexico
Pandermite	49.8	Turkey
Borasite	62.2	Turkey
Hydroborasite	50.5	Turkey
Sassolite (natural)	56.4	Italy
Datolite	26.7	Russia, China

1.1.2 Chemistry in nature

In nature, boron is found in the form of boric acid, borate (i.e., salt of boric acid), or as a borosilicate mineral (Holleman and Wiberg, 2001). Boric acid, H_3BO_3 (or $B(OH)_3$), behaves as a weak Lewis acid in aqueous solution (Power and Woods, 1997). It accepts hydroxide ion from water and releases a proton into solution according to the following equilibrium equation ($K_a=5.8\times10^{-10}$; $pK_a=9.24$ at 25°C) (Dean, 1987):

$$B(OH)_3 + H_2O \rightarrow B(OH)_4^- + H^+$$

Boric acid dissociation is a function of pH; above pH 9.24 the anion, $B(OH)_4^-$, is predominant, while below pH 9.24 the uncharged species is predominant. Boric acid is soluble in water (5.5 g/100 g solution at 25°C), and its solubility increases with temperature (Waggott, 1969). At concentrations below 0.02 M (216 mg/L as B) only the mononuclear species $B(OH)_3$ and $B(OH)_4^-$ are present. Polynuclear ions or ringed structures can exist at higher concentrations (Power and Woods, 1997). Figure 1.1 shows the distribution of the polynuclear ions of boron with respect to pH.

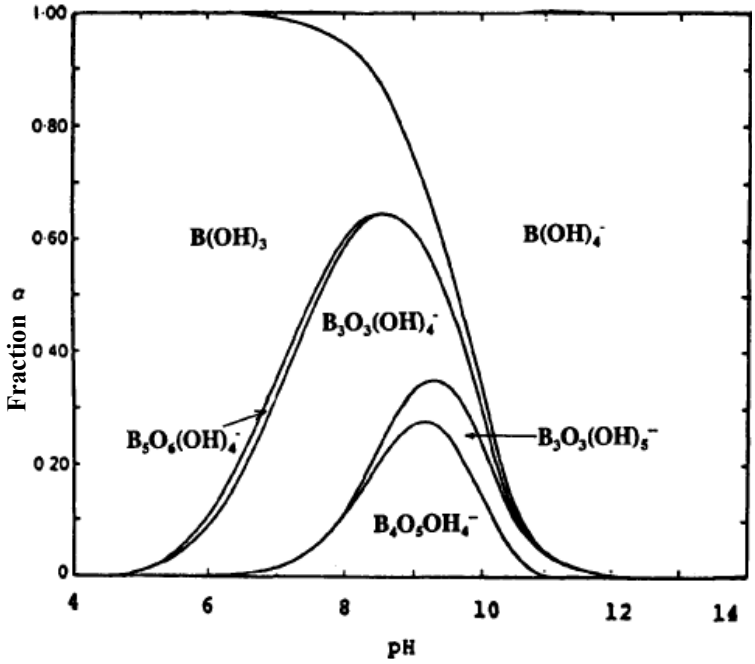


Figure 1.1 Distribution of polyborate species as a function of pH, 0.40M boric acid (Anderson et al., 1964)

1.1.3 Industrial uses of boron

Boron has many uses worldwide. The principal industrial uses of boron compounds are in the production of fiberglass insulation, borosilicate glass, and detergents. Other uses include fertilizers, metallurgy, and nuclear shielding (Power and Woods, 1997).

Boron is used in the fiberglass and glass industries because of its mechanical qualities. Boron oxide lowers the expansion coefficient in glass, and therefore borosilicate glass has an increased shock resistance. Boron also gives glass increased mechanical strength and increased drawing quality, which is especially useful in the manufacture of fiberglass (Woods, 1994).

Boron is used in the manufacture of detergents and bleaches as well. Boron in the form of sodium perborates is added to detergents as a bleaching agent. The hydrolysis of sodium perborate forms the hydroperoxide ion (Parks and Edwards, 2005). This is only effective at temperatures above 60°C unless an activator is present. It also has been added to diaper pails and to animal litter to reduce odor, since it prevents the formation of ammonia by inhibiting the urease enzyme (Woods, 1994).

Boron has varied uses as a result of its nuclear properties. Elemental boron is used in alloys for nuclear reactor control rods because of its large neutron capture cross section (Waggott, 1969). This same property has led the medical establishment to use ^{10}B in a procedure known as boron neutron capture therapy in the treatment of cancer patients (Hawthorne, 1993).

A recent innovation utilizing boron is the fuel cell as patented by Millennium Cell, Inc. Sodium borohydride is dissolved in water and passed over a catalyst, producing liquid borax and hydrogen gas. The hydrogen can then be used in a fuel cell, where it is converted into electricity and water (Parks and Edwards, 2005). The borohydride fuel cell's advantage is that hydrogen is produced on demand and there is no need to store it as is the case with other fuel cells. An obvious drawback is the need to recycle the borax back into its borohydride form (ABC News, 2001). Currently, Rohm and Haas is the only producer of sodium borohydride in the United States. A fairly complex reaction sequence is utilized in borohydride production, including converting boric acid to trimethylborate (TMB), converting sodium to sodium hydride, and then reacting the TMB and sodium hydride to make sodium borohydride (Mannsville Chemical Products Corp., 1999). Still, some designers believe this may be a viable technology in the next decade (Avril, 2002).

1.1.4 Health effects of boron

1.1.4.1 Plants

There is a small range between boron deficiency and boron toxicity in plants (Parks and Edwards, 2005). Boron has been shown to play a role in carbohydrate metabolism, sugar translocation, pollen germination, hormone action, normal growth and functioning of the apical meristem, nucleic acid synthesis, and membrane structure and function (Howe, 1998). Symptoms of boron deficiency include discontinuance of root and leaf growth, bark splitting, retardation of enzyme reactions, reduced pollen germination, and even death (Versar, Inc., 1975; Wells and Whitton, 1977; WHO, 1998). The initial stages of boron toxicity in plants include yellowing of leaf tips progressing into the leaf blade. Death of chlorotic tissue occurs followed by leaf loss. This ultimately results in a loss of photosynthetic capacity and a loss in plant productivity (Lovatt and Dugger, 1984; WHO, 1998).

Boron deficiency may occur in heavy-textured soils with high pH because under these conditions boron is readily adsorbed (Howe, 1998). Boron toxicity may also occur in boron-rich soils or in soils that have been exposed to boron-contaminated irrigation waters or the excess application of boronrich fertilizers, sewage sludge, and fly ashes (Nable et al., 1997). Some plants are more sensitive to boron than others (Parks and Edwards, 2005). Sensitive plants can tolerate irrigation waters with only 0.3 mg/L boron, while very tolerant plants may be able to survive where 4 mg/L boron irrigation water is used (Keren and Bingham, 1985).

1.1.4.2 Microorganisms

Toxicity thresholds (TTs) were determined for various microorganisms in a study by Bringmann and Kuhn (1980). They found that the bacteria Pseudomonas putida had a TT of 290 mg/L boron. Toxicity threshold was defined as the concentration at which the inhibitory action of a chemical leads to a >3% difference in the quantity of organisms versus a control group (Parks and Edwards, 2005). The green alga Scendesmus quadricauda had a TT of 0.16 mg/L, while the protozoan Entosiphon sulcatum had a TT of 0.28 mg/L (Bringmann and Kuhn, 1980).

Activated sewage treatment was not affected by a boron concentration of 20 mg/L (Howe, 1998). Banerji et al. (1968), on the other hand, observed a significant decrease in chemical oxygen demand (COD) removal at concentrations greater than 10 mg/L on aerobic activated sludge biological treatment. Banerji et al. (1968) observed no effects on settling at concentrations below 100 mg/L boron, while other researchers observed activated sludge settling problems at a concentration of 0.05 mg/L (Banerji et al., 1968). Banerji (1969) also observed a twofold reduction in the endogenous respiration of activated sludge at a boron concentration of 100 mg/L.

1.1.4.3 Aquatic organisms

The acute toxicity of boron to various fish has been the focus of a number of studies. The most sensitive freshwater fish identified thus far is the rainbow trout (Oncorhynchus mykiss). Initial studies in reconstituted water indicated a lowest observed effect concentration (LOEC) of 0.1 mg/L. The LOEC is the lowest observed concentration at which there is a significant increase in the frequency of an adverse reproductive or developmental effect in comparison to a control group (Parks and Edwards, 2005). Subsequent tests in

natural waters (with boron amendments), however, indicated that the LOEC ranged from 1.1 to 1.73 mg/L. Major trout hatcheries commonly use waters containing up to 1 mg/L boron with no apparent problems (Butterwick et al., 1989; Howe, 1998).

A recent study by Pillard et al. (2002) evaluated the toxicity of boron to the mysid shrimp (Americamysis bahia) in saline water. This species was chosen because it is the most common marine invertebrate required in whole-effluent toxicity (WET) tests and it has proven to be more sensitive to ion toxicity than other WET organisms (Parks and Edwards, 2005). Pillard et al. (2002) observed a no-observed-adverse-effect level (NOAEL) of 275 mg/L boron in water with a salinity of 10 ppt (parts per thousand) and 170 mg/L boron in water with a salinity of 20 ppt (Pillard et al., 2002). The NOAEL is the highest concentration at which there is not a significant increase in the frequency of an adverse reproductive or developmental effect in comparison to a control group. (The NOAEL can differ significantly from the LOEC, depending on the magnitude of the concentrations tested.)

1.1.4.4 Animals

Boron is nutritionally important to animals. Boron has been found to enhance the maturation of the growth plate in the long bones in chicks (Hunt, 1994). Boron also influences brain activity in mature rats (Penland and Eberhardt, 1993). In rats, a lack of boron has also decreased the absorption of calcium, magnesium, and phosphorus (Hegsted et al., 1991). Another study substantiated this finding by discovering that boron supplementation to boron deficient chicks increased femur calcium, phosphorus, and magnesium concentrations (Hunt, 1994).

A study on rabbits indicated boron is not able to penetrate intact skin but is readily absorbed through broken skin (Draize and Kelly, 1959; Moore, 1997).

Many studies have been made on rats, mice, rabbits, ducks, and dogs (e.g., Price et al., 1990, 1991, 1994; Fail et al., 1990, 1991; Smith and Anders, 1989; Weir and Fisher, 1966, 1972) and are summarized extensively in Moore (1997). Moore concluded that a NOAEL of 9.6 mg B/kg body weight/day was appropriate based on developmental toxicity in rats, the most sensitive organism in the studies reviewed. Data indicated NOAELs for female and male reproductive toxicity were 24 and 17 mg/kg body weight/day, respectively (Moore, 1997).

1.1.4.5 Humans

Boron has not been established to be an essential element in the human diet because a specific biochemical function for it has not been identified (Nielsen, 1997). However, there is strong circumstantial evidence that this may be the case. Boron is important in the metabolism and utilization of calcium in humans (Nielsen, 1994). Other benefits of boron include improvement of brain function, psychomotor response, and the response to estrogen ingestion in postmenopausal women (Nielsen, 1994). There is evidence that boron plays a role in healthy bones and joints (Newnham, 1994). The Newnham study and various others (Havercroft and Ward, 1991; Shah and Vohora, 1990; Travers et al., 1990) illustrate that boron can be effective in preventing and treating various forms of arthritis.

A skin irritation study similar to the Draize and Kelly (1959) study on rabbits was conducted on humans in 1998 and resulted in a similar conclusion. Wester et al. (1998) determined that 0.1 to 0.2% of applied borates (either boric acid, borax, or disodium octaborate) absorbed through human skin. Treatment of the skin with sodium lauryl sulfate (SLS), a known skin irritant, resulted in a slight increase on boron absorbed but not enough to be statistically significant .

No human studies are available that effectively assess developmental toxicity. Harchelroad and Peskind (1993) reported that the oral ingestion of 250 g boric acid by a woman in her second trimester of pregnancy had no effect on her offspring. Her blood boron level was 7.9 mg/L at 5 h after ingestion and decreased to 0.42 mg/L after 28 h.

Several studies detail the elimination of boron in urine. In one study 98.7% of an injected 600-mg dose of boric acid was eliminated in the first 5 days (Jansen et al., 1984; Moore, 1997). Oral doses have also been shown to be almost entirely eliminated in the urine. Janson and Schou (1984) found that 92 to 94% was eliminated in the first 4 days, and more than 50% was excreted in the first day.

Studies indicate that most soft tissues in the human body contain similar levels of boron to that in blood. Bone tends to have a higher amount, as well as fingernails, toenails, and hair (Forbes et al., 1954; Abou-Shakra et al., 1989).

Murray (1995) critically reviewed existing toxicologic and pharmacokinetic data on boron and made a risk assessment regarding human health. He used the NOAEL value of 9.6 mg B/kg/day determined by Price et al. (1994) along with an average body weight of 60 kg and various uncertainty factors to determine the acceptable daily intake of boron to be 18 mg B/day (Murray, 1995).

1.1.5 Regulations and guidelines for boron

1.1.5.1 U.S. EPA Contaminant Candidate List (CCL)

The U.S. Environmental Protection Agency (U.S. EPA) is required by the Safe Drinking Water Act (SDWA) to establish a list of contaminants to

assist in setting priorities for its drinking water program. This list, called the Candidate Contaminant List (CCL), was published in 1998 and includes boron (U.S. EPA, 2003). Boron, however, was not selected as a priority for regulatory determination due to insufficient data and information on treatment options.

1.1.5.2 World Health Organization Guideline

The World Health Organization (WHO) did not address boron in its 1958, 1963, or 1971 International Standards for Drinking-Water. In 1984 the WHO determined that no action was required for boron. However, in 1993 the WHO established a health-based guideline of 0.3 mg/L for boron. This value was raised to 0.5 mg/L in 1998 primarily because the treatment technology at that time precluded the ability to achieve 0.3 mg/L in areas with high natural boron levels. Furthermore, in 2000 it was decided to leave the guideline at 0.5 mg/L until data from ongoing research becomes available that may change the current view of boron toxicity or boron treatment technology (WHO, 2003).

1.1.5.3 European Union

The European Union is currently comprised of 15 countries in Europe and is in the process of accepting 13 additional eastern and southern European countries. The European Union established a value of 1.0 mg/L for boron in 1998 for the quality of water intended for human consumption (Council of the European Union, 1998). After 2000 the EU suggested a value of 0.5 mg/L for boron in drinking water.

1.1.5.4 Canada

The interim maximum acceptable concentration (IMAC) for boron in Canada is 5 mg/L. The Canadians have established this value on the basis of practical treatment technology. They believe available technologies are inadequate to reduce boron concentrations to less than 5 mg/L. They will review this IMAC periodically as new data becomes available (Health Canada, 2002).

1.1.5.5 New Zealand

New Zealand has established a drinking water standard for boron of 1.4 mg/L. This maximum acceptable value (MAV) was calculated using a tolerable daily intake (TDI) approach, which identifies the dose below which no major adverse health effects are likely to occur from a lifetime consumption of two liters of water per day (New Zealand Ministry of Health, 2000).

1.1.6 Importance of boron in Turkey

Turkey has the largest boron reserve which is approximately 90 million tons in the world. It was estimated that Turkey has about 70% of the known reserves of the world. But a boron production portion in Turkey is 31%. The known borate reserves in Turkey are located in four main districts, namely Emet, Bigadic¸ Kırka and Mustafakemalpasa (Öztürk and Kavak, 2005).

Boron pollution is a severe problem for Turkey. Wastes from the boron mines and boric acid plants are the main sources of the pollution (Yurdakoç et al., 2005). In addition to this, geothermal waters contain high levels of boron concentration in west Anatolia in Turkey. The Denizli-Kizildere geothermal power plant is the first and only geothermal power plant established for

electricity production in Turkey. Geothermal water in this field contains boron of approximately 20-30 mg/L (Kabay et al., 2004). Boron removal was studied using N-Glucamine type resins Diaion CRB 02 and Purolite S108 from the geothermal wastewater of Kızıldere, Turkey (Badruk et al., 1999). Also the usage of the seawater, by the tourism centers in the Mediterranean cost, for producing tap water makes removal of boron important (Öztürk and Kavak, 2005).

1.2 Desalination

Desalination is a process that removes dissolved minerals (including but not limited to salt) from seawater, brackish water, or treated wastewater. A number of technologies have been developed for desalination, including reverse osmosis (RO), distillation, electrodialysis, and vacuum freezing.

As the requirement for fresh water increases worldwide, there is a need for more and more plants that are able to treat non-conventional water sources. Sea water has become an important source of fresh water in many arid regions. This feature provides an overview of recent process improvements in seawater desalination using reverse osmosis, multi-stage flash, multi-effect distillation and electrodialysis (Bruggen, 2003).

1.2.1 Sewater desalination

Seawater contains high concentrations of salts. It has electrical conductivity (EC) levels of around 55 dSm^{-1} (total dissolved solids ~35,000 mg L^{-1}) and sodium (Na^{+}) concentration of more than 450 mmol L^{-1} (~10,400 mg L^{-1}). Without treatment to reduce its salt content, humans or animals cannot use seawater directly for consumption, as this would severely affect their health; nor can untreated seawater be used to produce crops (Qadir et al., 2003). The

same is true of highly brackish groundwater containing elevated levels of various types of salts (Qadir et al., 2006).

Desalination, a process that converts seawater or highly brackish groundwater into good-quality freshwater, has been practiced for over 50 years. The scarcity of freshwater has provided a driving force for the use of this approach in arid and semi-arid regions and in countries bordering seas or salt lakes. The largest producers of freshwater from seawater are the Middle Eastern countries, including Saudi Arabia (which produces one-tenth of world's desalinated water), the United Arab Emirates, Kuwait, Bahrain, Qatar, and Oman. However, several other countries have a compelling need to desalinate seawater and highly brackish groundwater to produce freshwater (Qadir et al., 2006).

These countries are not all located in the arid and semiarid areas: some simply have dense population concentrations and high levels of industry and tourism, resulting in local drinking water resources being either inadequate or becoming unfit for consumption. Currently, desalination plants operate in more than 120 countries worldwide (Voutchkov, 2004).

Estimates show that each day desalination plants throughout the world produce about 30x106 m^3 of freshwater; about 20x106 m^3 from seawater and the remainding from highly brackish groundwater (Pearce, 2004). This suggests that the total amount of freshwater produced each year from desalination is around 11x109 m^3 (Qadir et al., 2006).

Over the past 20 years or so, desalination has become a reliable and convenient method for water production in many arid regions around the world. A number of trends in technologies for desalination have resulted in a significantly lower cost for the water that is produced. One of the most important innovations in the 1980s was the breakthrough of membrane technology, for reverse osmosis, as an alternative to traditional distillation

processes multi-effect distillation (MED) and multi-stage flash (MSF) evaporation (Bruggen, 2003).

During the 1990s, the focus in desalination was mainly on process improvements. The robustness of MED increased so that it became more attractive than MSF, and progress in reverse osmosis technology resulted in a growing market share for membrane desalination (Bruggen, 2003).

The most innovative improvement today is the integration of membrane applications and distillation into a hybrid desalination system. As a result, membrane technology and distillation processes have found a collaboration where each has its own place – reverse osmosis and MED for standalone applications, MSF and reverse osmosis for application in hybrid systems. Nanofiltration may also play an important role as a complement to distillation or even reverse osmosis (Bruggen, 2003).

1.2.1.1 Multi effect distillation (MED)

The oldest distillation process is MED (Semiat, 2000). It is based on evaporation of water from brine by heat transfer from condensing steam (Figure 1.2). The steam produced in this way is used in a subsequent step or 'effect', which operates at a slightly lower pressure and temperature so that the energy retrieved from the condensing steam can be used for further evaporation of the brine from the preceding effect. Only in the first stage, fresh or 'primary' steam, generated independent of the distillation process, is used. The number of effects that can be obtained ranges from 8 to 16 for MED. A high number of effects is the aim because it is a measure of the process efficiency (the fresh water/primary steam ratio approximately equals the number of effects minus one) (Semiat, 2000; Bruggen, 2003).

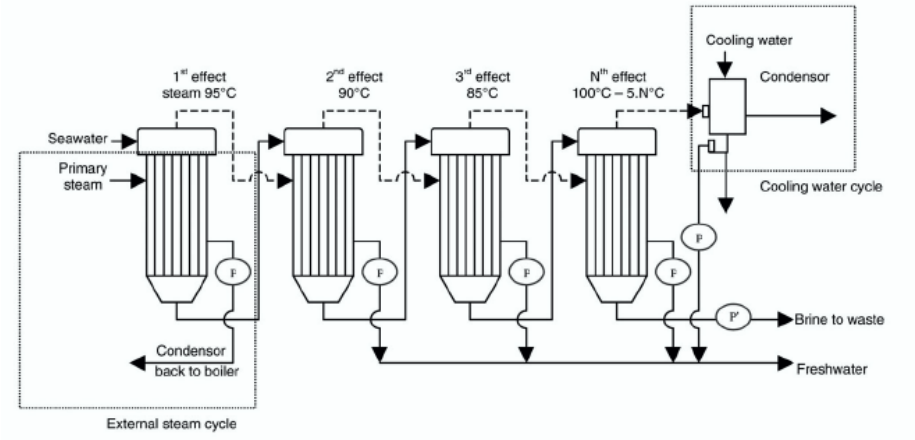


Figure 1.2 Operation principle of multi effect ditillation (Bruggen, 2003)

The number of effects is limited by a maximal top brine temperature of 120°C in the first effect, above which scaling occurs, and by the temperature difference with the cooling water in the last effect.

1.2.1.2 Multi stage flash (MSF) evaporation

MSF evaporation technique consists of a series of flash chambers where the evaporation of the brine results from a pressure drop and not from heat exchange with condensing steam (Figure 1.3). The steam fraction obtained is condensed by heat exchange with sea water, which results in an effective preheating. Contact between heat exchanging surfaces and the brine is limited, which means that corrosion and erosion problems are avoided, the process is more reliable and easier to operate than MED, and it has a longer service lifetime (Oldfield and Todd, 1999; Malik et al., 1999).

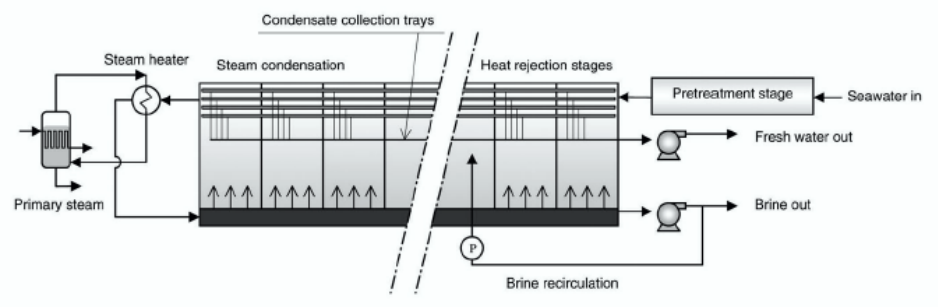


Figure 1.3 Operation principle of multi stage flash evaporation (Bruggen, 2003)

1.2.1.3 Reverse Osmosis (RO)

In order to reduce energy costs, the seawater reverse osmosis process as developed in the 1970s. This is a more energy-efficient process, which makes use of tightly bound semipermeable membranes, through which seawater is forced at very high pressures. Only the water molecules are able to pass through these membranes, as they are smaller than almost all the impurities (including salts) contained in seawater. The separated impurities and some residual water are then discharged as brine, usually into the ocean. Advances in membrane technologies have also led to the emergence of membrane configurations with different performance parameters. A conventional system of RO seawater desalination system generally consists of pretreatment part, high-pressure pump and RO modules (Figure 1.4) (Qadir et al., 2006).

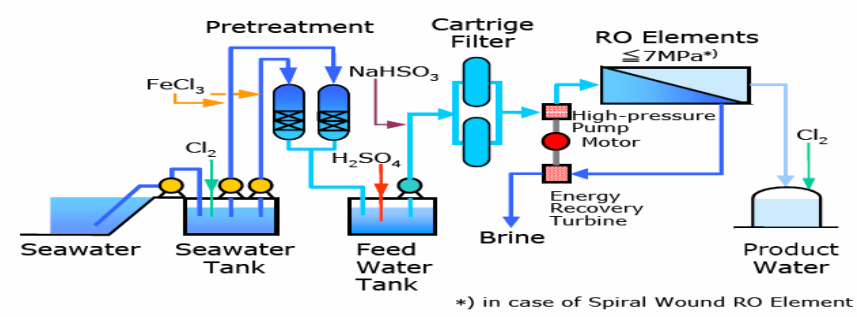


Figure 1.4 Flow Diagram of Conventional Single Stage RO Seawater Desalination System (Water Recovery 40%) (Kurihara et al., 1999)

This method of desalination became popular during the 1990s, as it has a lower operating cost than thermal desalination processes. Since then, the construction of new reverse osmosis plants has accelerated significantly (Qadir et al., 2006). Interestingly, most of the large desalination plants constructed during the last 10 years, or currently undergoing construction, are delivered under public–private partnership arrangements using the build–own–operate–transfer method of project implementation. In addition, the trend has been towards building fewer seawater desalination plants but ensuring that those built have a large capacity, rather than building a large number of smaller facilities with less capacity. This is a result of the benefits offered by larger capacities and centralization (Voutchkov, 2004).

The reverse osmosis plants do have advantages over distillation plants. These include the fact that feed water for reverse osmosis plants generally does not have to be heated, so the thermal impacts of discharges are lower. In addition, reverse osmosis plants have fewer problems with corrosion and usually have lower energy requirements than distillation plants. They also tend to have higher recovery rates, which can be as high as 45% in the case of seawater. Reverse osmosis process can also remove unwanted contaminants such as pesticides and bacteria. In the case of simple distillation, chemical contaminants with boiling points below that of water are condensed along with the water.

Finally, reverse osmosis plants take up less surface area than distillation plants for the same amount of freshwater produced (Qadir et al., 2006).

1.3 Removal of Boron from Seawater

1.3.1 Reverse osmosis

It is well known that boron compounds in seawater do not dissociate into ions at low or natural pH. Therefore, boron rejection in SWRO desalination systems is low and the process is not adequate to produce permeate complying with the required quality standards (0.4-l.0 mg/l boron).

At elevated pH, the rejection increases up to 98-99% at pH 11 (Magara et al., 1998; Glueckstern and Priel, 2003). However, at high pH potential precipitation of calcium carbonate and magnesium hydroxide must be avoided. The practical limit of the feed pH for a second desalination stage, desalination of the permeate of the first SWRO desalination stage, is about 10. However, use of advanced antiscalants permits raising the pH up to 10.3-10.5, corresponding to a brackish membrane rejection rate of 96-97%. The precipitation potential of calcium carbonate and magnesium hydroxide in seawater systems is obviously much higher and the limitation on a rising pH is much more severe (Glueckstern and Priel, 2003).

Field tests in Eilat (Red Sea) indicate scale-free operation up to about pH 9 without the use of scale inhibitors, However, at this stage, only short-term tests were performed, not enough to draw reliable conclusions regarding operation at an elevated pH (Glueckstern and Priel, 2003).

Regarding increasing pH in seawater systems, at the range of 8-9, boron rejection has been already remarkably increased compared to desalination of

low salinity water such as SWRO permeate undergoing additional desalination by brackish water RO membranes. This is due to relatively better ionization of boric acid in high salinity solutions such as seawater at this pH range.

According to data in various references (Stumm and Morgan, 1981; Glueckstern and Priel, 2003), the pH required for 50% ionization of boric acid in low salinity water is about 9.5, while in seawater, the required pH for the same rate of ionization is about 8.5.

Boron rejection by RO membranes is affected by pH, permeate flux and temperature (Figures 1.4-1.6) (Busch et al., 2003). The boron rejection of the currently applied SWRO systems, at nominal test conditions, is 85-90%. This corresponds to about 78-80% boron rejection in operation of commercial SWRO systems. Thus, for typical Mediterranean seawater containing 5-6 ppm of boron, operation at 50% recovery will produce permeate containing 1.6-2.0 ppm of boron. Recently developed SWRO membranes (Ando et al., 2001) with improved boron rejection are supposed to operate at a nominal rejection of 92-94%, corresponding to an actual rejection of 85-87% in commercial systems. These membranes would produce permeate with much lower boron content, typically in a range of 0.9-1.2 ppm, at initial operating conditions at a temperature not exceeding 25^{o}C. Pilot tests of two advanced SWRO membrane types performed by Mekorot in Eilat indicated somewhat lower boron rejection, in the range of 82-85% (Busch et al. 2003).

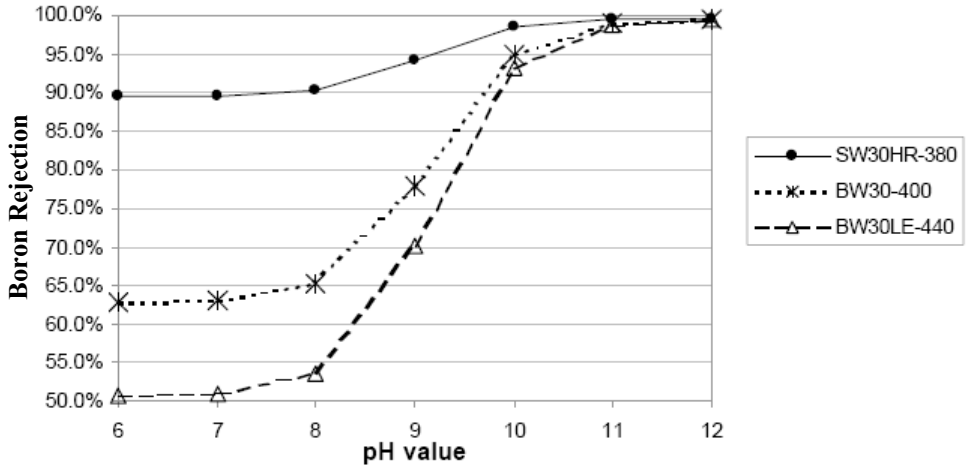


Figure 1.5 Boron rejection with FILMTEC membrane elements as a function of pH (Busch et al. 2003).

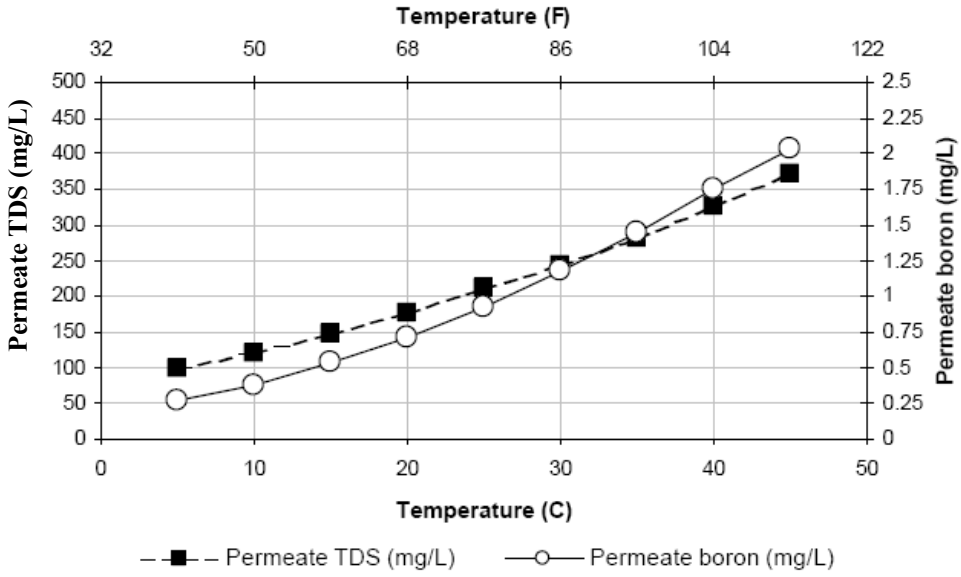


Figure 1.6 Temperature dependence of permeate TDS and boron rejection (Busch et al. 2003).

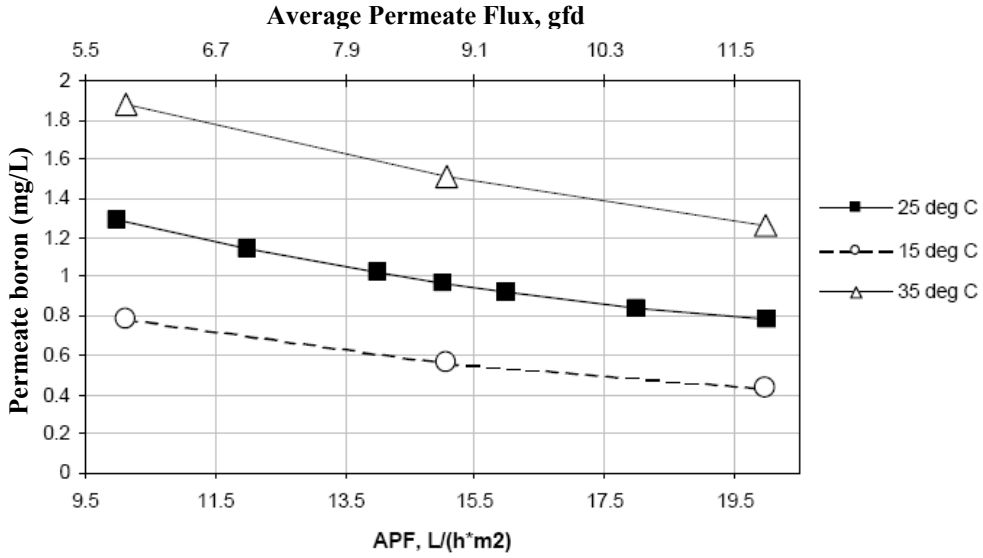


Figure 1.7 Impact of average permeate flux (APF) on boron permeate concentration (Busch et al. 2003).

1.3.2 Ion exchange

In the case of ion-exchange processes, the weak dissociation of boron salts requires the use of a strong basic ion-exchanger and all anions of the solution will be retained, resulting in a very high regeneration cost. A boron-specific ion-exchanger is therefore the only solution for achieving economic boron removal (Kunin and Preuss, 1964).

Today's commercial Boron Selective Resins (BSRs) are primarily classified as macroporous cross linked polystyrenic resins, functionalized with N-methyl-D-glucamine (1-amino-1-deoxy-D-glucitol; NMG) group (Figure 1.8).

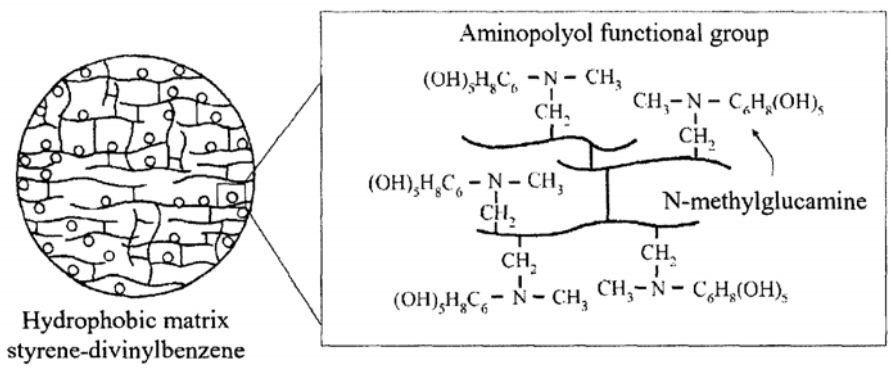


Figure 1.8 Structure of the boron selective resin (Soto and Camacho, 2005).

While today's BSRs may possess as much as 0.9 moles of NMG per liter of resin volume, their operating capacities for boron are typically somewhat lower. Usable operating capacity depends strongly on the concentration of boron in the feed, the operational flow rate, the efficiency of regeneration, and the outlet boron concentration cut-off limit (Marston et al., 2005).

In contrast to standard ion exchange processes, the NMG moieties of BSR capture boron via a covalent chemical reaction and an internal coordination complexation. Over a wide range of pH, boric acid "adds" across one of the cis-diol pairs of the functional group to form this relatively stable cis-diol borate ester complex (Figure 1.9) (Marston et al., 2005).

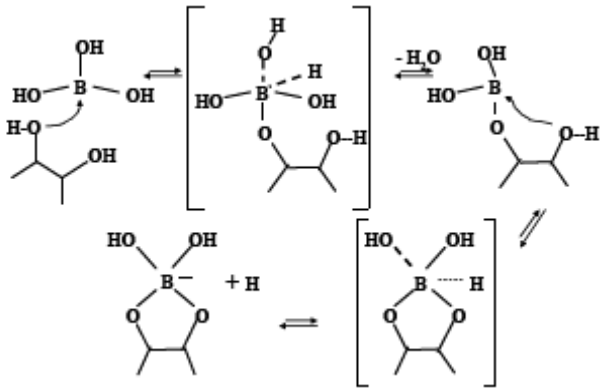


Figure 1.9 Capturing of boric acid (Marston et al., 2005).

In a boron removal process, once the BSR has achieved its maximum boron loading, the polymer bound cis-diol borate ester complex is subsequently hydrolyzed and the boron eluted from the resin via an acid rinse (the exact reverse of the loading reaction). This boron liberating hydrolysis is relatively facile at pH less than about 1.0; therefore, relatively high acid concentrations of acid are required for the complete and rapid elution of the boric acid from BSR (Marston et al., 2005).

Since the NMG functional group is linked to the styrenic backbone through a tertiary nitrogen bridging atom, extra acid is required in the elution step. Up to about 0.9 moles of acid per liter of BSR is needed, simply to accommodate the tertiary amine atom's appetite for hydronium ion while it reacts with the acid to form a conjugate acid salt (Figure 1.10). As a result of the high acid consumption by NMG nitrogens, much more acid is required for elution process than would be required to achieve the hydrolysis alone. Only after the bridging nitrogen atoms of the NMG have been protonated, can acid accumulate around the bound cis-diol borate ester complex to an extent great enough to accelerate the boron liberating hydrolysis reaction (Marston et al., 2005).

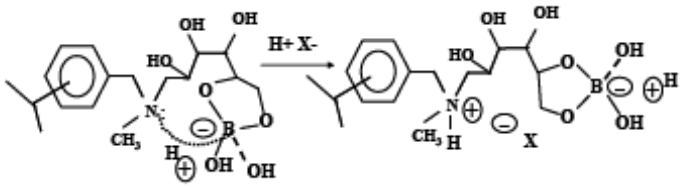


Figure 1.10 Conjugate acid form consumes eluant acid (Marston et al., 2005).

Essentially complete boron elution can be achieved in a little more than two bed volumes of total eluant. This method differs markedly from the widely applied method (Kunin and Preuss, 1964) which utilizes several bed volumes of 1N sulphuric acid and several bed volumes of rinse water. Different concentrations of sulphiric acid were also investigated (Samatya, 2002)

Recepoglu and Beker (1991) and later, Nadav (1999) investigated the possibility of a single stage elution without alkaline regeneration. Both concluded that with low buffering feed such as SWRO permeate, a two stage (acid then base) elution/regeneration protocol similar to the classic conditions of Kunin and Preuss (1964) yields the best performance, while a single stage (acid elution only) process, may be economic in cases having highly buffering feed-stocks.

1.3.3 Hybrid process

The boron problem has most frequently been encountered in ultrapure water production and sea water desalination. However the limit for boron for UPW industry is very low (in ppt range) and any discussion and reference to UPW water is outside the scope of this paper. For potable and irrigation needs, various plants have been designed to reach very low limits, of down to 0.4 mg/L B. The plants so far designed for boron removal to very low limits had been

previously described in detail by Redondo et al. (2003). Figure 1.11 shows an overview of the previously mentioned design options (Busch et al., 2005).

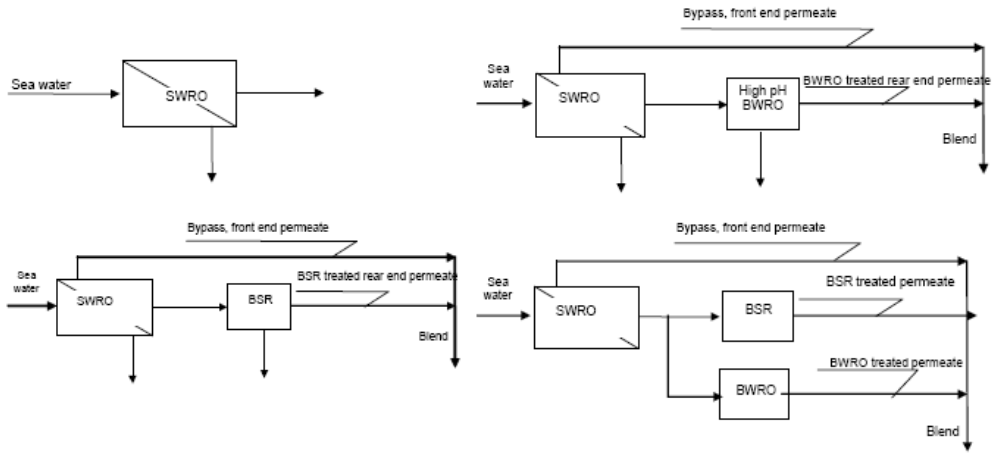


Figure 1.11 Overview of the hybrid process options (Busch et al., 2005).

Despite recent claims that very high boron rejection membranes might enable low boron contents cost-effectively (Taniguchi et al., 2004), most systems use multiple stages to achieve efficient and safe boron removal to low limits at competitive costs. The most frequent solution uses brackish water reverse osmosis (BWRO) membranes treatment with increased pH on a part of the seawater permeate (usually from the rear end of the seawater system). Instead of 2nd stage treatment by brackish water membranes, the previously described boron-selective resin (BSR) has also been proposed for various plants, in combination with BWRO 2nd pass treatment, but until very recently, only limited experience was available with this technology and the option was treated with caution (Busch et al., 2005).

In some cases the BSR units are included in the design to treat a part of the SW permeates to reduce the levels of boron and the balance quantity is treated by 2nd pass BWRO units. This approach would ensure that the final

treated quality of the blended water is within limits for both TDS and boron. The first step of sizing the 2nd stage BSR or BWRO unit is to calculate the flow rate that has to be treated, and based on the current trend and boron limit specification in treated waters, it may be said that a BSR or BWRO unit can be designed to treat 20-80% of the SW permeate (Busch et al., 2005).

1.4 Ion Exchange Technology

1.4.1 Ion exchange phenomenon

Ion exchangers are insoluble materials carrying reversibly exchangeable ions. These ions can be stoichiometrically exchanged for other ions of the same sign when the ion exchanger is in contact with an electrolyte solution. They are polymers carrying fixed functional groups (Zagarodni, 1997) (Figure 1.12).

The fixed groups are either permanently ionized so that they always possess a formal charge, or are capable of ionization or acceptance of protons to from the charged site. The resin interacts with mobile ions from an external solution. Ions of opposite charge to that on the resin, and which are exchanged by the resin, are known as counter-ions, while ions of the same charge as that of the exchange sites are known as co-ions. The polymeric network of the resin is known as the matrix (Bolto and Pawlowski, 1987).

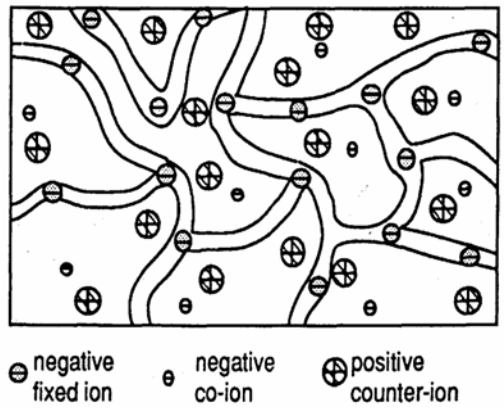


Figure 1.12 A cation exchange resin structure (Zagarodni, 1997).

Basic requirements of ion exchange resins are:

1. Resin must be highly polymeric and sufficiently crosslinked.
2. Resin must be of high exchange capacity.
3. Resin must be as stable as possibly chemically and physically.
4. Resin must be sufficiently hydrophilic.
5. Resin must be of granulation tuned to envisaged application.
6. Resin in swollen state should be denser than water (Bolto and Pawlowski, 1987).

The ionizable group attached to resin structure determines the functional capability of the exchanger. According to their functional groups, ion exchangers are divided into three groups:

Cation exchange resins:

Strongly Acid Type: The most important cation exchange resins are those of the *sulfonic acid type* ($-SO_3H$), which are used in acid, neutral, or

alkaline solution. The resins are widely used for the uptake and chromatographic separation of ampholytic substances, e.g., amino acids (Samuelson, 1963).

Weakly Acid Type: These cation exchange resins possess *carboxylic acid groups* (-COOH) as the functional species. Being of weak electrolyte character, the carboxylic acid groups dissociate to varying extents depending on the pH level. They are essentially undissociated at pH 3 and below, dissociation increases with increase in pH until by pH 10 until they are fully dissociated. Carboxylic acid resins are very stable thermally. This type of resin used for separation of basic amino acids and the separation of strong organic bases from weak ones (Samuelson, 1963).

Anion exchange resins:

Strongly Basic Type: Generally, resins of the strongly basic resin type are much more useful than weakly basic resins. Anion-exchange resins of the strong basic type are usually based on *quaternary ammonium groups* ($-N^{+}R_3OH^{-}$), connected to the aromatic rings of styrene-DVB copolymers via a methylene group. In general, strong base resins are very much less stable than strong acid resins. This type of resins used for the uptake and chromatographic separation of complex metal ions (Bolto and Pawlowski, 1987).

Weakly Basic Type: Weak base resins can possess *tertiary* ($-NR_2$), *secondary* (-NHR) or *primary* ($-NH_2$) *amino groups*, or mixtures of the same. The matrix can be as for strong base resins, although there are other matrices employed specifically for weak base resins. In acid medium, a weakly basic resin in the free-base form is a valuable tool for the removal of acids from solutions of various non-electrolytes. These resins are preffered when solutes which are unstable at high pH are present in solution (Samuelson, 1963).

Chelating ion exchangers: Compared with sulfonic acid resins the chelating resins show superior selectivity in their sorption of various metallic

cations. The published data show that the affinities for alkali metals are low, whereas most multivalent cations are held very strongly by the chelating resins (Samuelson, 1963).

These are weak acid cation exchangers consisting of iminodiacetate, aminomethyl and phosphonic functional groups in sodium form. These groups impart to the resin properties similar to those of ethylenediaminetetra-acetic acid (EDTA), in that the resin can form strong complexes with heavy metal ions. These resins have optimum porosity and surface area that give excellent operating capacities (Samuelson, 1963).

Certain resins can exchange both cations and anions, and are termed as *amphoteric ion* exchangers (Bolto and Pawlowski, 1987).

According to their material, ion exchangers are divided into two groups:

1. Inorganic ion exchangers: Most inorganic materials are crystalline alumosilicates with cation exchange properties. Characteristic representatives of this group of materials are the *zeolites* which are the best known of these, and included the minerals: analcite ($Na[Si_2AlO_6]_2.6H_2O$), chabazite ($Ca,Na[Si_2AlO_6]_2.6H_2O$), harmotome ($K,Ba[Si_5Al_2O_{10}].5H_2O$), heulandite ($Ca[Si_3AlO_8].5H_2O$), natrolite ($Na_2[Si_3Al_2O_{10}].2H_2O$) (Bolto and Pawlowski, 1987).

2. Organic ion exchangers: The majority of organic resins have a matrix of an irregular, three-dimensional network of macromolecular hydrocarbon chains. In most cases, this consists of a copolymer of styrene and divinylbenzene (DVB), with the latter providing the crosslinking. The properties of the resins are determined all else by the ion-exchange groups present on the matrix. In general, these may be divided into three groups: cation exchangers (strong acid or weak acid groups); anion exchangers (strong base or weak base groups);

specific ion exchangers (selective chelating groups) as mentioned before (Bolto and Pawlowski, 1987).

According to their physical structures, ion exchange resins are divided into five groups:

1. Gel Resins: The organic ion exchangers first developed were so-called gel resins. They have an essentially homogeneous distribution of water throughout the resin matrix (Bolto and Pawlowski, 1987).

Gel resins are homogenous crosslinked polymers and are the most common resins available. Gel resins usually have higher operating efficiencies and cost less. There are no permanent pore structures for the gel type resins. These pores are generally considered to be quite small and are referred as gelular pores or molecular pores. The pore structures are determined by the distance between the polymer chains and crosslinks which vary with the crosslink level of the polymer, the polarity of the solvent and the operating conditions. The gel type resins are generally translucent (Desilva, 1999).

2. Macroporous resins: Macroporous resins are made with large pores that permit access to interior exchange sites. Macroporous resins are manufactured by a process that leaves a network of pathways throughout the bead. This sponge like structure allows the active portion of the bead to contain a high level of DVB crosslinking without affecting the exchange kinetics. Unfortunately, it also means that the resin has a lower capacity because the beads contain less exchange sites (Desilva, 1999).

Macroporous copolymers, being highly crosslinked, are generally tougher than their gel equivalents and are more resistant to physical breakdown through mechanical forces, osmotic volume changes, and chemical degradation of crosslinking through the action of oxidizing agents (Harland, 1994).

3. Isoporous resins: It is claimed that some of the disadvantages of macroporous resins can be overcome by the synthesis of isoporous resins, in which the matrix has a substantially uniform network, free of highly crosslinked regions (Bolto and Pawlowski, 1987).

4. Microporous resins: Microporous is the term used to describe polymer particles manufactured with a low level of cross-linker. Improved rates of exchange can be obtained by using smaller particles, which make a larger surface area available. Powdered ion exchangers are employed in what has been termed precoat filters. However, because they are very fine particles (even though they are present in a coagulated form) they cause a high pressure loss in operation. Because of the high pressure loss, they can not be employed in a column system (Bolto and Pawlowski, 1987).

5. Magnetic resins: The difficulties of handling small, rapidly reacting resin beads can be surmounted by incorporating a magnetic filler such as the iron oxide γ-Fe_2O_3 within the particles. The magnetized resin beads then flocculate strongly to give agglomerates, which have settling rates comparable to those of normal sized beads. The flocs, which are held together by magnetic forces, are readily broken up by agitation so that the fast exchange rates associated with the small size of the resin particles can be achieved. Magnetic resins therefore combine some of the handling characteristics of conventional resin beads with the reaction rates of small particles (Bolto and Pawlowski, 1987).

1.4.2 Synthesis of ion exchange resins

The majority of ion exchange resins are made by the copolymerization of styrene and divinylbenzene (DVB) (Figure 1.13). The styrene molecules provide the basic matrix of the resin, while the DVB is used to crosslink the polymers to allow for the general insolubility and toughness of the resin. The degree of crosslinking in the resin's three-dimensional array is important because it

determines the internal pore structure, which will have a large effect on the internal movement of exchanging ions (Helfferich, 1962).

Typically a styrene and DVB mixture containing a polymerization initiator is dispersed as spherical liquid droplets in water. The styrene and DVB, both liquids at the start, are put into a chemical reactor with roughly the same amount of water. The suspension is continuously stirred and heated. A surfactant is also present to keep everything dispersed. The styrene/DVB begin to form large globules of material, and as the speed of agitation increases, the globules break up into smaller droplets until reaching the size of about a milimeter. At this point, the polymerization reaction is initiated by the addition of benzoyl peroxide, which causes styrene/DVB molecules to form the resultant small plastic beads. The divinylbenzene is a crosslinking agent that gives the beads their physical strength, and without which the styrene would be water-soluble. Higher DVB content gives the bead additional strength, but the additional crosslinking can hinder kinetics by making the bead too resistant to the shrinking and swelling necessary during normal operation (Desilva, 1999).

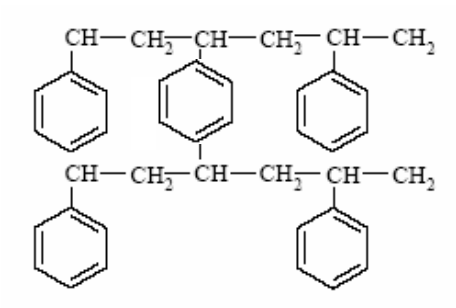


Figure 1.13 Styrene-divinylbenzene copolymer

There are three parameters defining the chemical structure of an ion-exchange resin (Marinsky, 1966):

1. The nature of the exchange grouping,

2. The degree of cross-linking, usually defined by the percentage of cross-linking agent used in the preparation of the cross-linked matrix,
3. The number of exchange groups per unit amount of exchanger.

Active groups are attached to provide chemical functionality to the bead. Each active group has a fixed electrical charge, which is balanced by an equivalent number of oppositely charged ions, which are free to exchange with other ions of the same charge. Strong acid cation resins are formed by treating the beads with concentrated sulphuric acid (process called sulphonation) to form permanent, negatively charged sulphonic-acid groups throughout the beads. Important here is the fact that the exchange sites thus formed are located throughout the bead. The ion exchange process is not a surface phenomenon; more than 99% of the capacity of anion exchange material is found in the interior of the bead (Desilva, 1999).

Strong base anion resins are activated in two steps process that consists of chloromethylation followed by amination. The two steps process begins with the same styrene/DVB material as is used for cation resins. The only difference is that the amount of DVB used is less to allow for a more porous bead. The first reaction step is the attachment of a chloromethyl group to each of the benzene rings in the bead structure (Desilva, 1999).

This intermediate chloromethylated plastic material needs to be reacted with an amine in a process called amination. The type of amine used determines the functionality of the resin (Desilva, 1999).

1.4.3 Properties and characterization of ion exchange resins

Matrix: Framework of ion exchanger, the so-called matrix, consists of an irregular, macromolecular, three-dimensional network of hydrocarbon chains. The matrix of the resin is hydrophobic. However, hydrophilic components are

introduced by the incorporation of ionic groups such as $-SO_3^-H^+$ (Helfferich, 1962).

The common choice is between "styrene-divinylbenzene" or "acrylic-divinylbenzene" copolymer. In the case of the cation exchange resins, selection is easily made since the acrylic products are weakly acidic whilst the styrenic resins are strongly acidic. Therefore for cation exchange the choice of copolymer is primarily decided by the process application and operating pH. The situation is very different with anion exchange resins since the two types of matrix pertain to products of both weak and strong functionality. Here anion exchange resins are concerned the choice between an acrylic resin and its styrenic equivalent is often made on considerations of operating exchange capacity, physical strength, and fouling resistance to complex high molecular weight organic anions (Harland, 1994).

Crosslinking: Crosslinking influences not only the solubility but the mechanical stability, exchange capacity, water uptake and swelling behavior, volume change in different forms of loading, selectivity, and chemical as well as oxidation resistance of ion exchangers. The amount of crosslinking depends on the proportions of different monomers used in the polymerization step. Practical ranges are 4 % to 16 %. Exchangers with low degree of crosslinking are soft and mechanically unstable (in the swollen state), while highly crosslinked products are hard and brittle with an increased sensitivity to osmotic influences (Desilva, 1999):

Swelling: The volume change which takes place during transference from one medium to another is known as swelling. This swelling is produced by the osmotic pressure in the interior of the ion exchanger against the external, more dilute solution, so that the solvent uptake producing the swelling. Absolute swelling takes place when air-dried resin becomes wet. During absolute swelling a certain quantity of water is taken up by the exchanger. Swelling is influenced by the matrix structure, i.e., the degree of crosslinking as discussed above. If the

water contains an electrolyte, swelling depends also on the electrolyte concentration. When this concentration increases, the moisture uptake will increase, since the osmotic pressure difference between the external and internal solution is then smaller (Desilva, 1999).

Ionic Form: Most ionic forms may be prepared by passing a large excess of an appropriate acid, alkali, or salt solution through a column of resin over 20-30 minutes. The ease of resin conversion generally increases with decreasing particle size, decreasing crosslinking, and decreasing charge of the ion being displaced (Harland, 1994).

pH Range: The pH range is very much dependent upon the strength of the functional group, but the following guidelines could be applied (Harland, 1994):

1. Strong acid cation: any pH
2. Weak acid cation: > 4
3. Strong base anion: any pH
4. Weak base anion (tertiary): < 9

Chemical stability: At the macroscopic level, the chemical stability of modern resins at normal ambient temperatures is excellent, being insoluble in all common organic solvents and electrolyte solutions. Two principle exceptions are resin breakdowns caused by sustained exposure to ionizing nuclear radiation and powerful chemical oxidizing agents such as nitric, chromic (VI) acid, chlorate (V) ions, halogens, and peroxy compound (Harland, 1994).

Thermal stability: Over a temperature range, the stability characteristics of resins in common use may be summarized as follows (Harland, 1994):

• **Cation exchange resins:** Cation exchange resins are generally quite stable, especially if they are in their salt forms.

• **Anion exchange resins:** Strong base and weak base materials are also most stable in their salt forms compared with their hydroxide and free base forms, respectively. The effect of increased temperature is to accelerate the loss of exchange capacity, in which respect acrylic anion exchangers whether weak or strong base are significantly more unstable than their styrenic counterparts.

Physical appearance:

- Gel resins: usually shiny beads, clear to transmitted light.

- Macroporous resins: usually dull beads of opaque or translucent appearance.

Resin particle size: It is a major part of the fluid flow and effectiveness of separation of systems. For example, condensation type resins are generally broken granules. On the contrary, polymerization-type resins are small beads that are uniformally packed. To measure the grain size a mesh is used to keep out larger particles. In addition, for certain processes grain size is extremely important to efficiency. One such process is separations carried out by chromotography. The major point of study of grain size is that it determines the fluid resistance of an ion exchange column made from ion exchange resin. This can be the key to success of an industrial operation (Desilva, 1999).

The bead size range of conventional products is 300 μm to 1200 μm with a true mean value of approximately 700 μm (Harland, 1994).

Resin Density: The density of the any dry, water free resin is generally smaller for anion exchangers than cation exchangers. The density of water swollen resin depends on the type counter ion, swelling capacity and on the degree of crosslinking, besides the density of dry resin. Furthermore, it should be noted that bulk density is different than the density of the swollen resin. These

densities are important because operation is dependent upon the resins (Harland, 1994).

1.4.4 The kinetics of ion exchange

An understanding of the kinetics of ion exchange reactions has application in two broad areas. Firstly, it helps to understand the nature of the various fundamental ionic transport mechanisms, which control or contribute to the overall exchange rate. Secondly, derived numerical parameters such as rate constants, mass transfer coefficients, or diffusion coefficients found from a rate investigation are of value when making projections concerning the dynamic behaviour of columns and process design (Harland, 1994).

In the general theory described by Boyd, Adamson and Myers the overall transport of mass may be divided into three steps (Samuelson, 1963);

1. Mass-transfer in the external solution up to the surface of the resin particles (film diffusion)

2. Diffusion inside the resin phase (particle diffusion)

3. Chemical exchange in the vicinity of the exchange groups

Figure 1.14 shows the radial concentration profiles of the exchanging species. The right sides of the diagrams show the profiles of species A (initially in the ion exchanger) and the left sides those of species B (initially in the solution). The various curves are for different contact times, t (Helfferich, 1962).

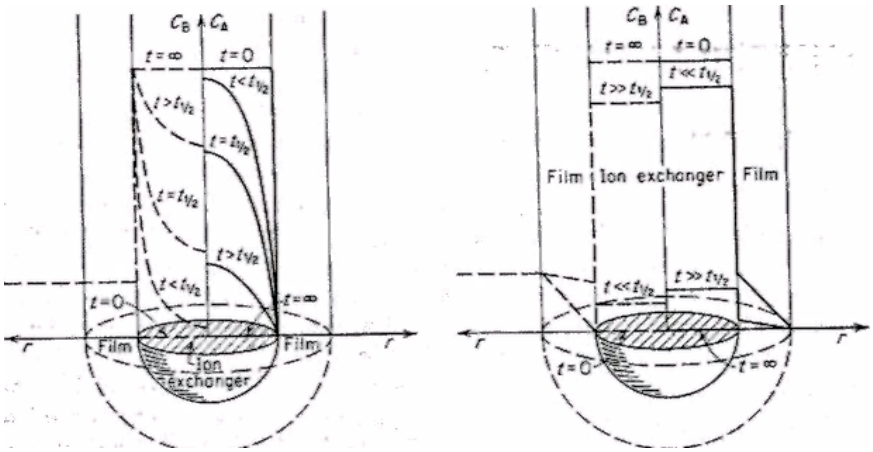


Figure 1.14 Radial concentration profiles for ideal particle diffusion control (schematic) (Helfferich, 1962)

Two main rate–determining steps in kinetics of ion exchange could be given as:

$$\frac{X\bar{D}\delta}{CD_0 r_0}(5+2\alpha_B^A) \qquad << 1 \quad \text{particle diffusion control} \qquad (1.1)$$

$$\frac{X\bar{D}\delta}{CD_0 r_0}(5+2\alpha_B^A) \qquad >> 1 \quad \text{film diffusion control} \qquad (1.2)$$

X**:** concentration of fixed groups

C: solution concentration

$\bar{D}$: inter-diffusion coefficient in the ion exchange resin

D_0 : inter-diffusion coefficient in the film

r_0 : bead radius

δ : film thickness

α_B^A: separation factor

Rate laws can be derived by applying the diffusion equations to ion exchange systems. In general case, the differential equations and boundary conditions are nonlinear due to complications arising from diffusion-induced electric forces, selectivity, specific interactions and changes in swelling (Helfferich, 1962).

The following diffusion kinetic treatments are applicable for idealized ion exchange, i.e., they are only strictly true for isotropic exchange in a system which is in equilibrium expect for isotropic distribution. It is also assumed that all exchanger beads are spherical and have uniform size (Helfferich, 1962).

Diffusion processes are usually described in terms of Fick's first law:

$$J_i = -D \text{ grad } C_i \qquad (1.3)$$

where J_i is the flux (in moles per unit time and unit cross section) of the diffusing species i, C_i is its concentration (in moles per unit volume), and D is the diffusion coefficient (Helfferich, 1962).

- ***Particle Diffusion***

In the case of particle diffusion control, concentration gradients will exist in the ion exchange bead. A quasi-homogenous model is assumed to derive the rate laws. The theoretical treatment of the diffusion within the solid phase is considered as occurring through a homogenous spherical electrolyte gel. The flux of the isotope A (J_A) in the ion exchanger is given by;

$$J_A = -\overline{D}\ \text{grad}\ \overline{C_A} \qquad (1.4)$$

where $\overline{D}$ is self diffusion coefficient of species and $\overline{C_A}$ is the concentration of species in the resin phase (Helfferich, 1962).

The time dependence of the concentration is interrelated with the flux by material balance (Fick's second law, termed the condition of continuity)

$$\frac{\partial \overline{C_A}}{\partial t} = -\text{div}\ J_A \qquad (1.5)$$

where t is time.

The combination of Eqn. (1.4) and Eqn. (1.5) for systems with spherical geometry and with a constant diffusion coefficient gives

$$\frac{\partial \overline{C_A}}{\partial t} = \overline{D}\left(\frac{\partial^2 \overline{C_A}}{\partial r^2} + \frac{2}{r}\frac{\partial \overline{C_A}}{\partial r} \right) \qquad (1.6)$$

where r is radial space coordinate (distance from the bead center) (Helfferich, 1962).

This equation must be solved under the appropriate initial condition, all ions A are in the ion exchanger at a uniform concentration $\overline{C_A}^{o}$, and no A is in the solution:

$r > r_o,\ t = 0 \qquad \overline{C_A}(r) = 0$

$0 < r \le r_o,\ t = 0 \qquad \overline{C}_A(r) = \overline{C_A^o} = \text{const.} \qquad (1.7)$

The first and simpler condition applies when the concentration of A in the solution remains negligible throughout the process. This is true when a solution of constant composition is continuously passed through a thin layer of beads or in the case of batch operation if, the solution volume is so large (Helfferich, 1962).

$$\overline{C}\overline{V} << CV \qquad (1.8)$$

where $\overline{V}$ and V are total volume of ion exchange material and solution respectively. This condition is called the "infinite solution volume". The infinite solution volume condition thus is,

$$r = r_o,\ t > 0 \qquad \overline{C_A}(t) = 0 \qquad (1.9)$$

Under this initial and infinite solution volume condition, the equation may be solved and integrated to give:

$$X = 1 - \frac{6}{\pi^2}\sum_{n=1}^{\infty}\frac{1}{n^2}\exp\left(-\frac{\overline{D}t\pi^2 n^2}{r_o^2}\right) \qquad (1.10)$$

where X is the fractional attainment of equilibrium.

A simplified expressions of this equation is given by the Vermeulen's approximation (Vermeulen, 1953).

$$X = \left(1 - \exp\left(-\frac{\overline{D}\pi^2}{r_o^2}t\right)\right)^{1/2} \qquad (1.11)$$

The half time $t_{1/2}$ of ion exchange is readily calculated from Eqn. (1.11). The substitution X = 0.5 gives;

$$t_{1/2} = 0.03\frac{r_o^2}{D} \qquad (1.12)$$

Secondly, the "finite solution volume" condition which does not meet the condition (1.8). The solution obtained by Peterson is;

$$X = \frac{w+1}{w}\left[1 - \frac{1}{\alpha-\beta}\left[\alpha\exp(\alpha^2\tau)(1+\text{erf }\alpha\ \tau^{1/2}) - \beta\exp(\beta^2\tau)(1+\text{erf }\beta\ \tau^{1/2}\right]\right] \qquad (1.13)$$

where α and β are the roots of the equation $X^2 + 3wX - 3w = 0$ (Helfferich, 1962).

- **Film Diffusion**

The rate laws for film-diffusion controlled isotopic exchange is derived under the following assumptions:

1. Interdiffusion in the film is treated as quasi-stationary, i.e.; it is assumed that diffusion across the film is fast as compared with the concentration changes at the film boundaries.

2. The film is treated as a planar layer (one-dimensional diffusion).

This is admissible if the film thickness is much smaller than the bead radius. Under this condition, the momentary flux (J_A) constant throughout the film and from Eqn. (1.3) is given by

$$J_A = D\frac{\Delta C_A}{\delta} \qquad (1.14)$$

where ΔC_A is concentration difference between the boundaries of the film and δ is the film thickness (Helfferich, 1962).

Time dependence is obtained from material balance;

$$-\frac{dQ_A}{dt} = FJ_A \qquad (1.15)$$

where F is the total surface area of the ion exchanger.

The equilibrium condition at the interface

$$\frac{\overline{C_A}}{C_A'} = \frac{\overline{C}}{C} \qquad (1.16)$$

Combination of Eqn. (1.15) and Eqn. (1.16) gives after substitution;

$$-\frac{dC_A'}{dt} = \frac{3C}{r_o \overline{C}} J_A \qquad (1.17)$$

Eqn. (1.16) and Eqn. (1.17) are solved under the appropriate initial and boundary conditions. The simple initial condition corresponding to uniform initial concentration $\overline{C_A}^o$ in the ion exchanger and no A in the solution is;

$$r = r_o,\ t = 0 \qquad C_A' = \frac{\overline{C_A}^o C}{\overline{C}}$$

$$r \geq r_o,\ t = 0 \qquad C_A(r, t) = 0 \qquad (1.18)$$

The boundary condition in the case of "infinite solution volume" condition

$$r \geq r_o + \delta,\ t \geq 0 \qquad C_A(r, t) = 0 \qquad (1.19)$$

The mathematical solution under the conditions (1.17) to (1.18) is,

$$X = 1 - \exp\left(-\frac{3DCt}{r_o \delta \overline{C}}\right) \qquad (1.20)$$

with a half time of ion exchange :

$$t_{1/2} = 0.023 \frac{r_o \delta \overline{C}}{DC} \qquad (1.21)$$

The rate thus is proportional to the diffusion coefficient in the film and to the concentration of the solution and is inversely proportional to the bead radius, the film thickness, and the counter-ion concentration in the ion exchanger (Helfferich, 1962).

In the case of "finite solution volume", the condition (1.19) replaces by;

$$r \geq r_o + \delta, \quad t > 0 \qquad C_A(r,t) = \frac{\overline{V}}{V}\left(\overline{C_A}^{\,o} - \overline{C_A}(t)\right) \qquad (1.22)$$

The solution to this case is given by:

$$X = 1 - \exp\left(-\frac{3D(\overline{V}\overline{C} + VC)}{r_o \delta \overline{C} V} t\right) \qquad (1.23)$$

- **Chemical Reaction Kinetics**

Chemical reaction between the fixed ion exchange sites is one of the general ion exchange mechanisms. In certain cases, chemical reaction kinetics can control

the ion exchange. This is seen to be the case in some chelating and solvent impregnated type ion exchange resins (Helfferich, 1962).

The kinetic concept of a "shell progressive" mechanism can be described in terms of the concentration profile of a liquid reactant containing a counter ion A advancing into a spherical bead of a partially substituted ion exchanger. As the reaction progresses in the bead, the material balance of counterion A follows Fick's diffusion equation with spherical coordinates. In this case, the relationship between reaction time and degree of conversion gives the following expressions (Liberti, 1987).

When the fluid film is controlling

$$t = \frac{ar_o C_{so}}{3C_{Ao} K_{mA}} X \qquad (1.24)$$

When the diffusion through the reacted layer control

$$t = \frac{ar_o^2 C_{so}}{6D_{e,r} C_{Ao}} \left[3 - 3(1-X)^{2/3} - 2X\right] \qquad (1.25)$$

When the chemical reaction control

$$t = \frac{r_o}{k_s C_{Ao}} \left[1 - (1-X)^{1/3}\right] \qquad (1.26)$$

1.4.5 Ion exchange operational techniques

Ion exchange reaction starts when an ion exchanger is placed in an electrolyte solution contain a counter ion, which is different from the counter ion on ion exchanger. During the ion exchange reaction the counter ion on the resin

is partially or totally replaced by the counter ion contained in the solution (Zagorodni, 1997).

1.4.5.1 Batch operation

The comparison of various ion-exchange resins with respect to their relative equilibrium and kinetic behaviour can be performed by batch techniques, i.e., by following the change in composition of an electrolyte solution in contact with an ion-exchange resin. The kinetic behaviour may be approximated by observing the change in composition of the solution as a function of time (Kunin, 1960).

In batch contact, a method with only slight usefulness, maximum removal (neutralization, etc.) is limited by the equilibrium relationship between resin and solutes. When viscous solutions are being processed or when the equilibria are irreversible (neutralization, etc.), batch contact may offer some advantages (Kunin, 1960).

Since ion exchange is a form of sorption from a solution, it is possible to describe the equilibrium of ions between the solid and solute phases by different equations and isotherms which are *Langmuir* and *Freundlich isotherms* and related correlations are taken into account (Samuelson, 1963).

1.4.5.2 Column operation

Ion-exchange materials are frequently tested for performance in a given application by small-scale column tests (Kunin, 1960). The solution is passed through a fixed bed of ion exchanger, which is packed in column, usually of glass. The solution which enters the column, is called the influent and the liquor leaving the column the effluent. Three types of column operations are; *down*

flow, up flow and counter flow. Most beds operate with down flow operation (Samuelson, 1963).

Column operation conveniently suffices for complete removal. In equilibrium operation, the solution continuously contacts with resin and consequently there is a high driving force for the removal of solute from solution. In order to achieve maximum removal, the resin in the column must be most highly regenerated (Kunin, 1960).

A solution is passed through a bed of ion exchanger beads where its composition is changed by ion exchange reaction. The composition of the effluent and its change with time (or volume passed) depends on (Samuelson, 1963):

- The properties of the ion exchanger
- Composition of the feed solution
- Operating conditions

A typical breakthrough curve during a column operation is given in Figure 1.15.

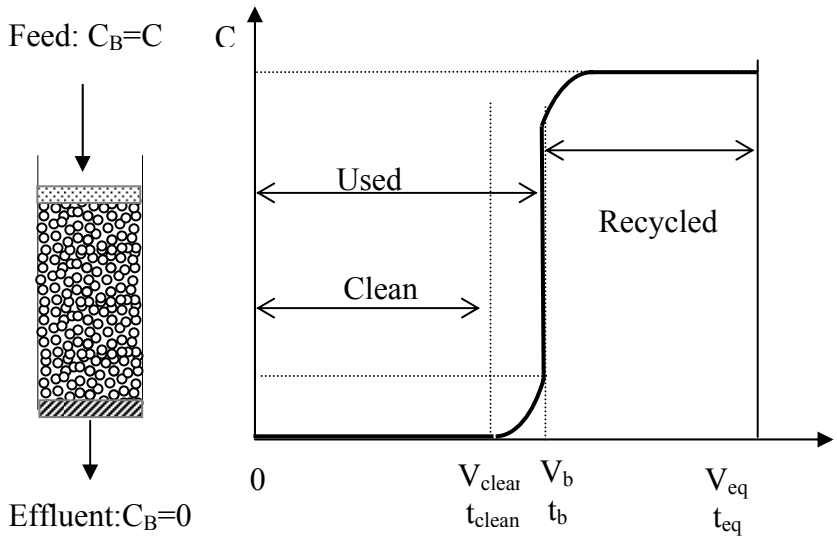


Figure 1.15 Breakthrough curve of column operation (Zagorodni, 1997)

1.4.5.3 Ion exchange capacity

Capacity and related data are primarily used for two purposes: lon characterizing of ion-exchange materials and for use in the numerical calculation of ion-exchange operations (Helfferich, 1962).

Ion exchange capacity could be defined as concentration of fixed functional groups per specified amount of ion exchanger (Zagarodni, 1997).

Ion exchange capacities can be classified as (Kunin, 1960):

1. Anion exchange capacity
2. Cation exchange capacity
3. Breakthrough capacity
4. Saturation column capacity

Taking into consideration the breakthrough curve given in Figure 1.15 and types of capacities given above, the following equations could be formulated:

$$\textbf{Breakthrough Capacity} = \int_{0}^{Vb} (C_0 - C)dV$$

$$\textbf{Total Capacity} = \int_{0}^{V_{eq}} (C_0 - C)dV$$

$$\textbf{Degree of the Column Utilization} = \frac{\int_{0}^{V_b} (C_0 - C)dV}{\int_{0}^{V_{eq}} (C_0 - C)dV}$$

2. EXPERIMENTAL

2.1 Materials

2.1.1 Ion exchange resins

The N-glucamine type chelating resins; Diaion CRB 02 and Dowex-XUS 43594.00 supplied by Mitsubishi Chemicals, Japan and Dow Chemicals, Germany respectively. Their characteristics are summarized in Tables 2.1 and 2.2.

Table 2.1 Typical chemical and physical characteristic of Diaion CRB 02

Constitutional type	Highly porous
Ion form as shipped	OH-form
Shipping density (g/dm^3) (app.)	635
Moisture content (%)	50-60
Exchange capacity	Acid 0.6 meq/cm^3 (min)
Screen grading	118-300 μ
Effective size (mm)	0.355-0.500
Uniformity coefficient	1.6 (max)
Operating temperature (^{o}C)	100 ^{o}C (max) OH-form
Effective pH range	6-10

Table 2.2 Typical chemical and physical characteristic of Dowex-XUS 43594.00

Total exchange capacity (min)	0.7 eq/L
Water retention capacity (%)	51-59
Mean particle size (μm)	550 ± 50
Uniformity coefficient	1.1 (max)
Whole uncracked beads (min) (%)	90
Total swelling (%)	24-28
Shipping weight (lbs/ft^3) (app.)	41
Total boron capacity (g B/L)	3.4-4.0

2.1.2 Chemicals

- H_3BO_3: 99.8 %, Merck
- H_2SO_4: 95-97 %, d:1.84 g/L, J.T. Baker
- HCl: 37 %, d:1.19 g/L, Merck
- CH_3COOH: 99-100 %, d:1.06 g/L, Carlo Erba
- Curcumine: $C_{12}H_{26}O_6$, Natural, Wako
- NaOH: 99 %, (solid-pulp), J.T. Baker
- $NaHCO_3$: 99.5-100.5 %, UPARC
- $CaCl_2.2H_2O$: 99-103 %, Riedel-de Haën
- $MgCl_2.6H_2O$: 98 %, Merck
- NaCl: 99.8 % Riedel-de Haën
- pH=4 and pH=7 buffer, Metrohm

2.1.3 Solutions

- **100 mg/L B solution:** 0.5719 g H_3BO_3 is dissolved in deionized water and diluted to 1L

- **Standard boric acid solutions:** Standard solutions of 0.05, 0.1, 0.5, 1.0, 1.5, 2.0 mg B/L is prepared from 100 mg B/L boric acid stock solution.

- **Curcumine Solution (0.075%):** the solution was prepared on the day of use by dissolving 0.075 g curcumine in 100 mL of glacial acetic acid and stored in a polyethylene bottle.

- **H_2SO_4: CH_3COOH (1:1) Solution:** Equal volumes of the two acids are mixed.

- **Sodium Acetate Buffer Solution:** 200 g sodium acetate was dissolved with 250 ml glacial acetic acid and diluted with deionized water to 1 L. (pH ~ 4.5).

- **Model Seawater Solution (MSW):** Model seawater solution was prepared with certain amounts of $NaHCO_3$, $CaCl_2.2H_2O$, $MgCl_2.6H_2O$, NaCl and H_3BO_3 and diluted with deionized water. The composition of the model seawater is given in Table 2.3.

- **NaCl + H_3BO_3 Solution:** NaCl + H_3BO_3 solution was prepared with certain amounts of NaCl and H_3BO_3 and diluted with deionized water. The composition of the solution is given in Table 2.4.

- **H_3BO_3 added RO Permeate:** H_3BO_3 was added to natural seawater RO permeate (RO permeates were provided by Associate Prof. Mehmet Kitiş, Süleyman Demirel University, Isparta, Turkey) to adjust the B concentration in the RO permeate to 1.5 mg/L. The composition of the solution is given in Table 2.5.

- **1.5 and 5.0 mg B/L Solutions:** 1.5 and 5.0 mg B/L solutions were prepared from 100 mg B/L boric acid stock solution (pH 6.01 and 5.58 respectively).

- **Model RO Pearmeate:** Model RO permeate solution was prepared with the composition which is given in Table 2.6 and deionized water.

Table 2.3 Composition of model seawater solution.

pH	B (mg/L)	HCO_3 (mg/L)	Mg (mg/L)	Ca (mg/L)	NaCl (mg/L)
8.2	5.0	163	1500	400	35000

Table 2.4 Composition of NaCl + H_3BO_3 solution.

pH	B (mg/L)	NaCl (mg/L)
8.2	5.0	35000

Table 2.5 Composition of H_3BO_3 added natural seawater RO permeate solution.

pH	6.53
Conductivity	1728 µS/cm
Salinity	0.7
TDS	828 mg/L
Cl^-	511 mg/L
SO_4^{2-}	LDL*
F^-	LDL
Ca^{2+}	11.6 mg/L
Mg^{+2+}	25.3 mg/L
Na^+	274.6 mg/L
B	1.5 mg/L (Original B: 0.77 mg/L)
HCO_3^-	13 mg/L

*LDL: Lower than detection limit

Table 2.6 Composition of model RO permeate solution.

pH	6.53
Cl^-	511 mg/L
Ca^{2+}	11.6 mg/L
Mg^{+2+}	25.3 mg/L
Na^+	274.6 mg/L
B	1.5 mg/L
HCO_3^-	13 mg/L

2.1.4 Equipments

- **Glass column :** ID=0.7 cm, h=10 cm
- **Hollow fiber membrane:** Polypropylene, ID=1.5 mm
- **Membrane module:** ID=0.7 cm, h=15 cm
- **Vacuum oven:** Gallen Kamp
- **Shaker:** Memmert
- **Peristaltic pumps:** Ismatec, ISM 597A-03516 and Masterflex, Easyload II
- **Fraction collector:** Iwaki FRC-2100
- **Spectrophotometer:** Jasco SSE-343, V-530 UV/VIS Spectrophotometer
- **Sample container:** Glass cell, b: 1 cm
- **Atomic absorption spectrophotometer:** Varian 10 Plus, Atomic Absorption Spectrophotometer

- **Ion Chromatography:** Shimadzu 10 Ai Ion Chromatography
- **pH meter:** Metrohm 694
- **Magnetic Stirrer:** Velp Scientifica Strirrer DLH

2.2 Methods

2.2.1 Batch mode sorption studies

2.2.1.1 Effect of pH on removal of boron from 5 mg B/L solution

In this study, 0.1 g dry Diaion CRB02 (0.355-0.500 mm) resin was contacted with 50 mL of 5 mg/L boron solution at various pH values (pH=7, 8, 9, 10) at 30 ^{o}C for 48 h with continuous shaking.

2.2.1.2 Effect of resin amount on removal of boron from model seawater

Optimum resin amounts for boron removal from model seawater were determined by using Diaion CRB02 (0.355-0.500 mm and 45-75 μm) and Dowex-XUS 43594.00 (0.355-0.500 mm and 45-75 μm). Various dry resins amounts (0.0125 g, 0.025 g, 0.05 g, 0.075 g, 0.1 g, 0.125 g and 0.15 g for 0.355-0.500 mm sized resins and 0.005 g, 0.01 g, 0.015 g, 0.025 g, 0.03 g, 0.04 g, 0.05 g, 0.06 g, 0.07 g, 0.075 g, 0.1 g for 45-75 μm sized resins) were contacted with 50 mL of model seawater at 30 ^{o}C for 48 h with continuous shaking.

2.2.1.3 Effect of resin amount on removal of boron from H_3BO_3 added natural seawater RO permeate solution

Optimum resin amounts for boron removal from model seawater were determined by using Diaion CRB02 (0.355-0.500 mm) and Dowex-XUS 43594.00 (0.355-0.500 mm). Various dry resins amounts (0.01 g, 0.02 g, 0.03 g, 0.04 g, 0.05 g, 0.07 g for Diaion CRB 02 resin and 0.01 g, 0.02 g, 0.03 g, 0.04 g, 0.05 g for Dowex-XUS 43594.00 resin) were contacted with 50 mL of H_3BO_3 added natural seawater RO permeate solution at 30 ^oC for 48 h with continuous shaking.

2.2.1.4 Effect of resin amount on removal of boron from 1.5 mg B/L solution

Optimum resin amounts for boron removal from 1.5 mg B/L solution were determined by using Diaion CRB02 (45-125 μm). Various dry resins amounts (0.005 g, 0.01 g, 0.015 g, 0.02 g and 0.025 g) were contacted with 50 mL of 1.5 mg B/L solution at 30 ^oC for 48 h with continuous shaking.

2.2.1.5 Effect of resin amount on removal of boron from 5 mg B/L solution

Optimum resin amounts for boron removal from 5 mg B/L solution were determined by using Diaion CRB02 (45-125 μm). Various dry resins amounts (0.01 g, 0.025 g, 0.05 g, 0.075 g and 0.1 g) were contacted with 50 mL of 5 mg B/L solution at 30 ^oC for 48 h with continuous shaking.

2.2.1.6 Kinetic tests using model saewater

Kinetic tests were carried out in a 500 mL of three neckled glass flask placed in a water bath at 25^{o}C. The model seawater in the flask was agitated on a mechanical stirrer with 200 RPM to prevent the resin model seawater from settling. Samples were withdrawn from the vessel at regular time intervals (3, 5, 10, 15, 20, 30, 45, 60, 90, 120, 150, 180, 240, 300, 360, 420, 480, 540, 600 660, 720, 1440 min.). Kinetic tests were performed by using 1.0 g of dry Diaion CRB02 and Dowex-XUS 43594.00 (0.355-0.500 mm) and 0.5 g of dry Diaion CRB02 and Dowex-XUS 43594.00 (45-75 μm).

2.2.1.7 Kinetic tests using NaCl + H_3BO_3 solution

This study was done for investigating the salt effect other than NaCl on the kinetic performance of the resin. Samples were withdrawn from the vessel at regular time intervals (3, 5, 10, 15, 20, 30, 45, 60, 90, 120, 150, 180, 240, 300, 360, 420, 1440 min.). Kinetic tests were performed by using 1 g of dry Diaion CRB02 (0.355-0.500 mm) and 500 mL of NaCl + H_3BO_3 solution.

2.2.1.8 Kinetic tests using H_3BO_3 added natural seawater RO permeate solution

Samples were withdrawn from the vessel at regular time intervals (3, 5, 10, 15, 20, 30, 45, 60, 90, 120, 150, 180, 240, 300, 360, 420, 1440 min.). Kinetic tests were performed by using 0.5 g of dry Diaion CRB02 (0.355-0.500 mm) and 0.5 g of dry Dowex-XUS 43594.00 (0.355-0.500 mm) and 500 mL of H_3BO_3 added (1.5 mg B/L) natural seawater RO permeate solution.

2.2.1.9 Kinetic tests using 1.5 mg B/L solution

Samples were withdrawn from the vessel at regular time intervals (3, 5, 10, 15, 20, 30, 45, 60, 90, 120, 150, 180, 1440 min.). Kinetic tests were performed by using 0.15 g of dry Diaion CRB02 (0.355-0.500 mm) and 500 mL of 1.5 mg B/L solution.

2.2.1.10 Kinetic tests using 5 mg B/L solution

Samples were withdrawn from the vessel at regular time intervals (3, 5, 10, 15, 20, 30, 45, 60, 90, 120, 150, 180, 1440 min.). Kinetic tests were performed by using 0.5 g of dry Diaion CRB02 (0.355-0.500 mm) and 500 mL of 5 mg B/L solution.

2.2.2 Column mode sorption-elution studies

In order to get some information about column performances of chelating resins on removal of boron from various solutions (model seawater, NaCl + H_3BO_3 and H_3BO_3 added natural seawater RO permeate solutions), chelating resins Diaion CRB 02 and Dowex-XUS 43594.00 were used for column mode sorption and elution studies.

In these studies, a glass column with an internal diameter of 0.7 cm and height of 10 cm was employed. The resins in the 0.355-0.500 mm of particle size range were used for the column studies.The resin beads were immersed into deionized water for 24 h before being packed into the column.

The column was packed with 0.5 mL wet-settled volume of resins. The solutions which contains boron was delivered by down-flow to the column at

room temperature using a peristaltic pump at different SV values (10, 15, 20 h^{-1}). Each successive 3 mL (6 BV) fractions of the effluent were collected using a fraction collector. Breakthrough curves were obtained by analysis of these successive fractions. Resin packed into the column was washed with deionized water after sorption step. The boron loaded to the resin was eluted with 5 % H_2SO_4 at SV 10 h^{-1}. The column elution profiles were obtained by analysis of each successive 2 mL (4 BV) fractions of eluates. Flow-sheet of column-mode sorption-elution studies is shown in Figure 2.1.

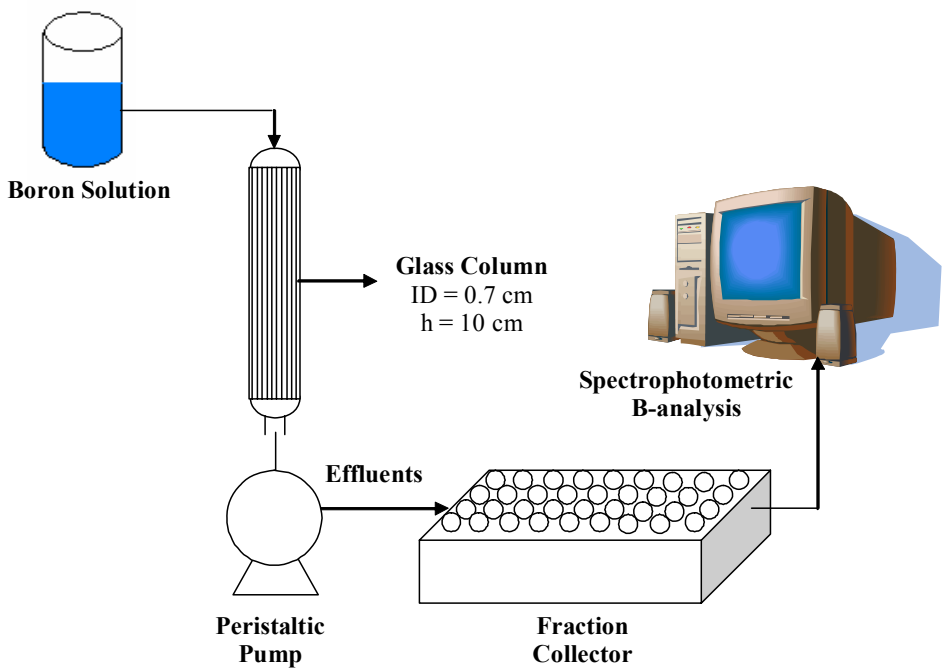


Figure 2.1 Flow-sheet of column mode sorption-elution studies.

2.2.3 Sorption-membrane filtration hybrid method

In sorption-membrane filtration hybrid method, powdered Diaion CRB 02 (45-125 μm) and boron solution (1.5 and 5 mg B/L) suspension was passed through a membrane module containing hollow fiber membranes (Polypropylene, ID=1.5 mm). The permeates were taken from the module at regular time intervals (0, 5, 10, 15, 20, 30, 40, 60, 80, 100, 120 min). The blank of the studies were obtained without resin at same conditions. The flowsheet of the system is given at Figure 2.2.

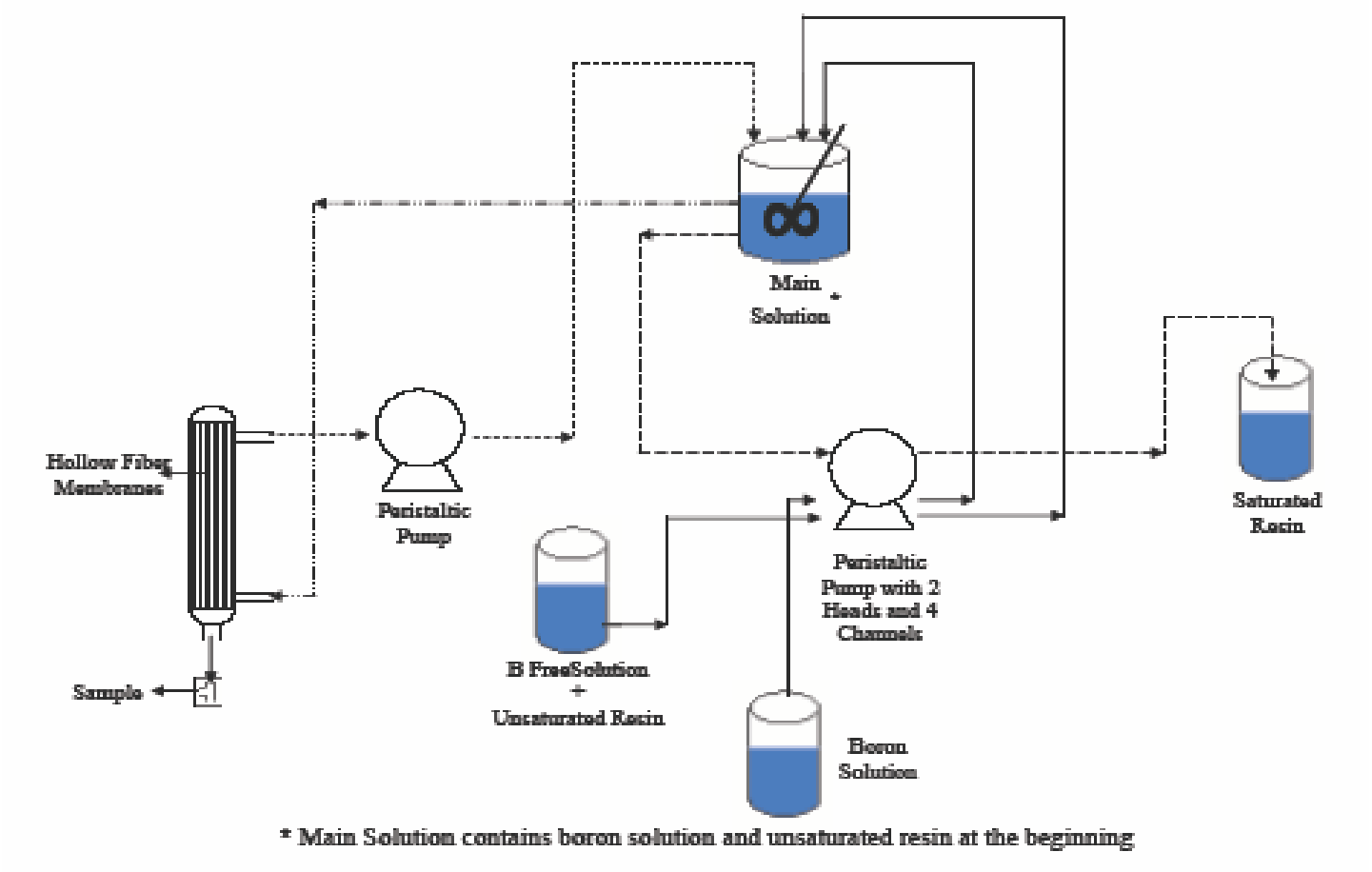


Figure 2.2 Flow-sheet of sorption-membrane filtration hybrid method.

2.3 Chemical Analysis

2.3.1 Boron analysis

The analysis of boron was performed spectrophotometrically using Curcumine Method.

A 0.5 mL of supernatant is taken from the standart solutions (0.05-2.00 mg B/L) and samples into polyethylene bottle. 3 mL of 0.075% Curcumine solution and 3 mL H_2SO_4:CH_3COOH (1:1) solution were added over the supernatant. Then the mixture was shaken on a shaker at 30 ^oC for 1 h to get homogenous mixture. After 1 h, 10 mL CH_3COONa buffer solution was added to this mixture. Samples were left to cool for a while and then absorbance of samples were measured at λ_{max}= 543 nm by means of Jasco SSE-343, V-530 UV/VIS Model Spectrophotometer.

Before beginning measurement of absorbances of the samples, the absorbances of blank, 0.05, 0.1, 0.5, 1.0, 1.5 and 2.0 mg B/L of standart solutions were measured to obtain the calibration curve (Figure 2.3). The calibration curve was obtained everyday. After the calibration curve was drawn, absorbances of samples were measured.

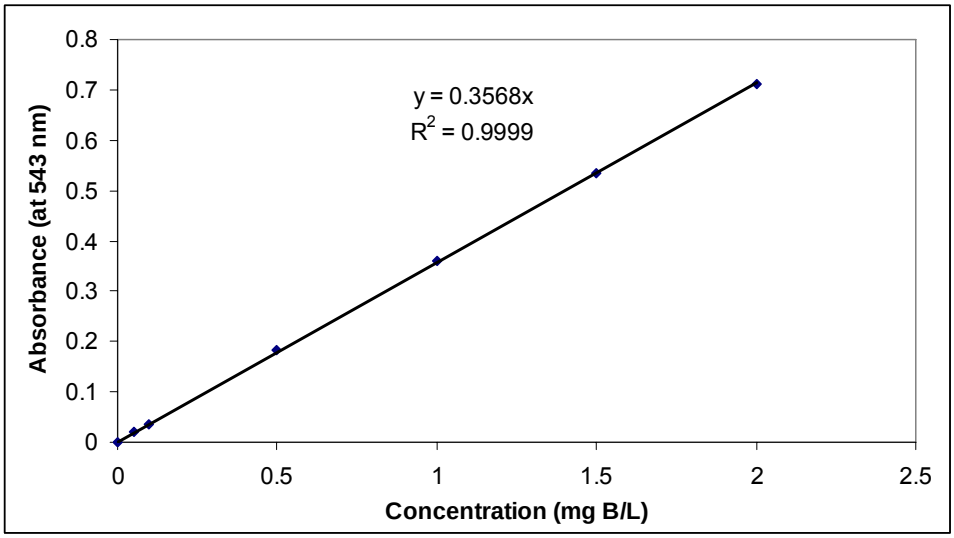


Figure 2.3 Calibration curve of boron by curcumine method.

3. RESULTS AND DISCUSSION

3.1 Removal of Boron from Model Seawater

3.1.1 Effect of resin amount on removal of boron from model seawater as a function of resin particle size

Optimum resin amounts for boron removal from model seawater were determined by using Diaion CRB02 (0.355-0.500 mm and 45-75 μm) and Dowex-XUS 43594.00 (0.355-0.500 mm and 45-75 μm).

Table 3.1 and Figure 3.1 show that boron removal increased with increasing resin amounts from 0.0125 g to 0.1000 g/50 mL for both Diaion CRB 02 and Dowex-XUS 43594.00 (0.355-0.500 mm). But boron removal had a plateau for the resin amounts between 0.1250 g to 0.1500 g/50 mL According to these results, optimum resin amount was found as 2 g resin/L for both Diaion CRB 02 and Dowex-XUS 43594.00 (0.355-0.500 mm) resins.

Table 3.2 and Figure 3.2 show that boron removal increased with increasing resin amounts from 0.005 g to 0.050 g/50 mL for both Diaion CRB 02 and Dowex-XUS 43594.00 (45-75 μm). But boron removal had a plateau for the resin amounts between 0.060 g to 0.100 g/50 mL for both resins. According to these results, optimum resin amount was found as 1 g resin/L for both Diaion CRB 02 and Dowex-XUS 43594.00 (45-75 μm) resins.

Figure 3.3 gives the comparison of optimum resin amounts for two resins at two different particle sizes. By reducing the resin particle size, the optimum resin amounts decreased from 2 g resin/L to 1 g resin/L for Diaion CRB 02 and Dowex-XUS 43594.00.

Table 3.1 Effect of Resin Amount on Removal of Boron from Model Seawater by Diaion CRB 02 and Dowex-XUS 43594.00 (0.355-0.500 mm)

Resin	Resin Amount (g/50 mL)	Boron Removal (%)	Boron Removal (mg B)
Diaion CRB 02	0.0125	40.24	0.101
	0.0250	65.96	0.165
	0.0500	85.12	0.213
	0.0750	90.00	0.225
	0.1000	94.88	0.237
	0.1250	97.87	0.245
	0.1500	100	0.250
Dowex-XUS 43594.00	0.0125	39.36	0.098
	0.0250	65.85	0.165
	0.0500	78.04	0.195
	0.0750	89.14	0.223
	0.1000	93.29	0.233
	0.1250	95.85	0.240
	0.1500	100.00	0.250

Table 3.2 Effect of Resin Amount on Removal of Boron from Model Seawater by Diaion CRB 02 and Dowex-XUS 43594.00 (45-75 μm).

Resin	Resin Amount (g/50 mL)	Boron Removal (%)	Boron Removal (mg B)
Diaion CRB 02	0.005	19.00	0.048
	0.010	34.34	0.086
	0.015	50.67	0.127
	0.025	77.00	0.193
	0.030	81.95	0.205
	0.040	93.85	0.235
	0.050	97.55	0.244
	0.060	98.08	0.245
	0.070	99.29	0.248
	0.075	100.0	0.250
	0.100	100.0	0.250
Dowex-XUS 43594.00	0.005	24.67	0.062
	0.010	45.00	0.113
	0.015	64.67	0.162
	0.025	84.08	0.210
	0.030	87.36	0.218
	0.040	95.47	0.239
	0.050	99.56	0.249
	0.060	97.43	0.244
	0.070	99.39	0.248
	0.075	100.0	0.250
	0.100	100.0	0.250

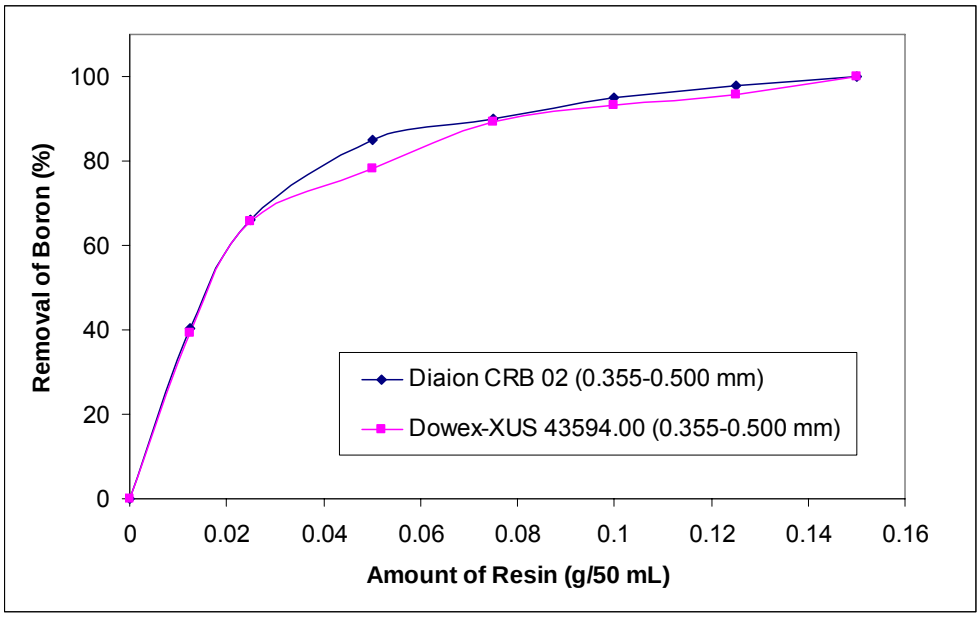


Figure 3.1 Removal of boron from model seawater solution by boron selective resins (0.355-0.500 mm).

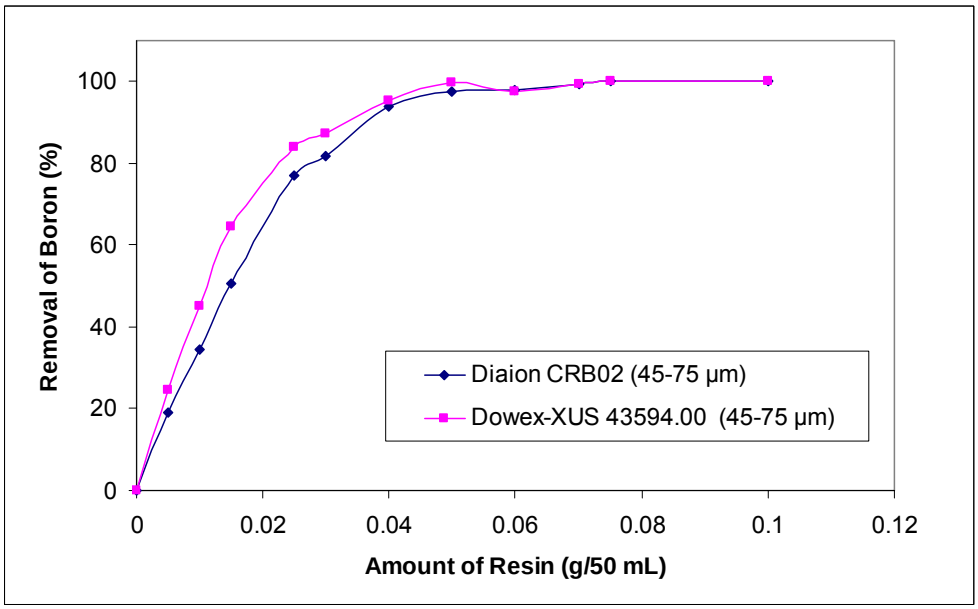


Figure 3.2 Removal of boron from model seawater solution by boron selective resins (45-75 µm).

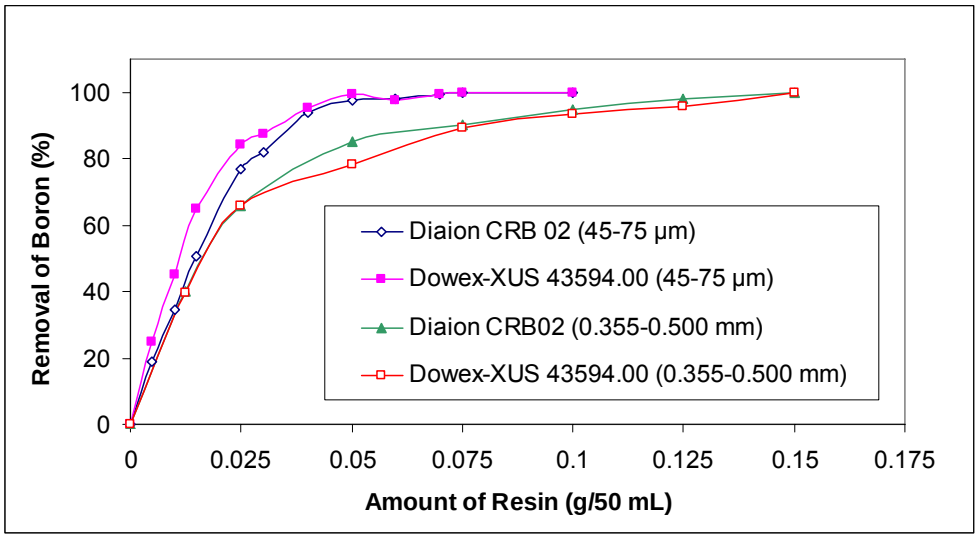


Figure 3.3 Effect of particle size of resins for boron removal from model seawater solution.

3.1.2 Sorption isotherms for boron removal from model seawater

1. Langmuir Model: In the Langmuir model for low concentrations, adsorption is proportional to solute concentration, and hence, in this range this equation reduces to Henry's equation, and approaches a constant value at high concentrations. Langmuir model is based on the following assumptions (Yılmaz, 2003):

- Only monomolecular adsorption takes place
- Adsorption is localized, that is; the bonding to the adsorbent is sufficiently strong to prevent displacement of the adsorbed molecules along the surface.
- Heat of adsorption is independent of surface coverage because of homogeneous surfaces, whose adsorption sites are energetically equivalent.

Langmuir isotherm model is represented as (Yılmaz, 2003)**;**

$$\frac{C_e}{Q_e} = \frac{1}{Q_o b} + \frac{C_e}{Q_o}$$

where C_e is the equilibrium concentration (mg/L), Q_e is the amount of ion (such as B) sorbed on the resins (mg B/g-dry resin), Q_o is a constant indicates the adsorption capacity of resins (mg B/g-dry resin), b is a constant indicates energy of adsorption (L/mg).

Freundlich Model: The Freundlich model is an empirical isotherm equation and is suitable for highly heterogeneous surfaces. When this equation fits to data at high and moderate concentrations, it provides a poor fit for adsorption data at low concentrations. Since for highly heterogeneous surfaces, extremely low concentrations are required to attain the Henry's law region. Freundlich equation does not reduce to Henry's law at concentrations approaching zero (Yılmaz, 2003).

Freundlich isotherm implies a logarithmic decrease in the heat of adsorption with surface coverage. The dependence of heat of adsorption on surface coverage has its basis in the energetic heterogeneity of most solid surfaces. The first sites on a surface to be occupied are those, which attract adsorbate molecules most strongly and with the greatest release of energy. Thus the heat of adsorption decreases with surface coverage (Yılmaz, 2003).

The equation for Freundlich isotherm model is as**;**

$$Q_e = K_f C_e^{(1/n)}$$

where C_e is the equilibrium concentration (mg/L), Q_e is the amount of ion (such as B) sorbed on the resins (mg B/g-dry resin), K_f is a constant indicates the rate of adsorption, n is a constant indicates the degree of favorability of adsorption.

The equilibrium relationships for Diaion CRB 02 and Dowex-XUS 43594.00 (0.355-0.500 mm) are also shown in Figures 3.4 and 3.5 respectively.

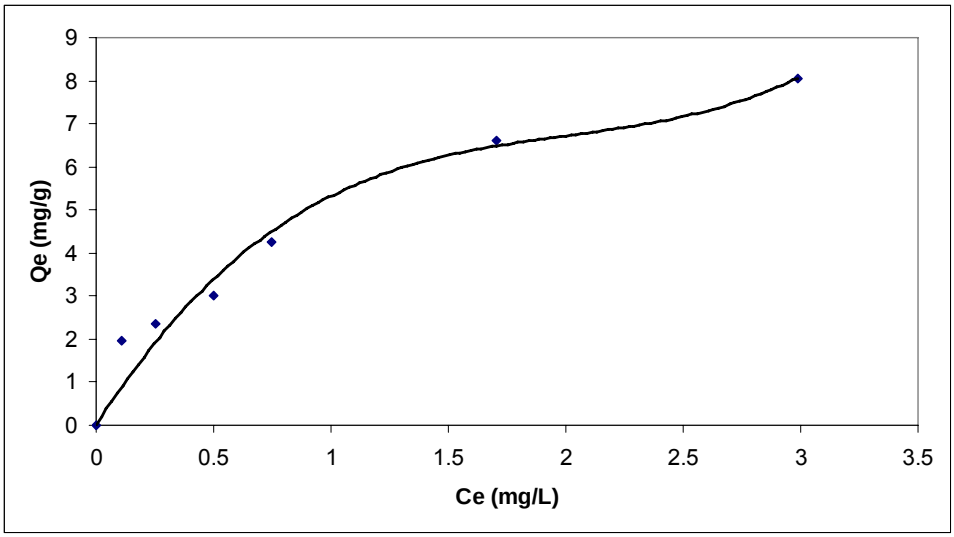


Figure 3.4 Equilibrium isotherm for loading B onto Diaion CRB 02 (0.355-0.500 mm).

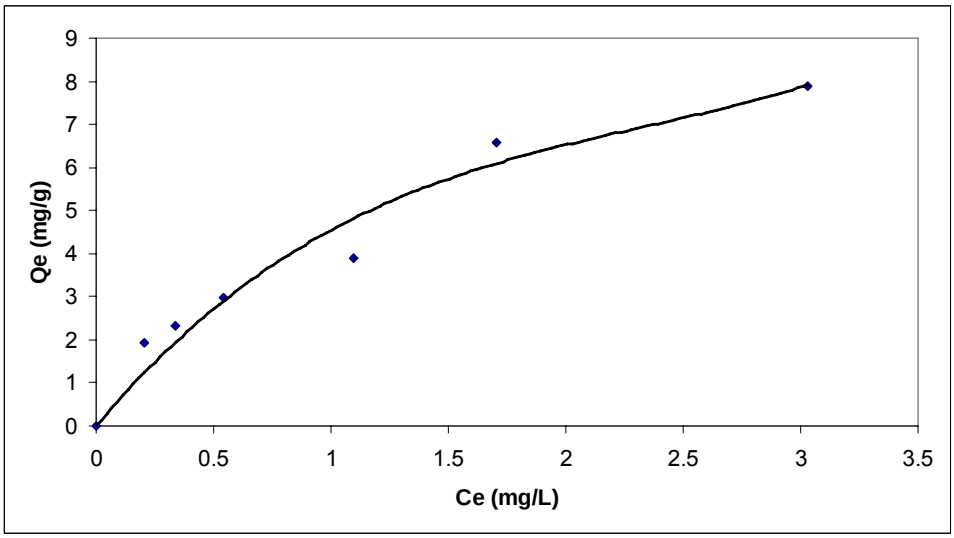


Figure 3.5 Equilibrium isotherm for loading B onto Dowex-XUS 43594.00 (0.355-0.500 mm).

The linearized fitting curves of for Diaion CRB 02 and Dowex-XUS 43594.00 (0.355-0.500 mm) are given for Langmuir isotherm in Figures 3.6 and

3.7 respectively. The linearized fitting curves of for Diaion CRB 02 and Dowex-XUS 43594.00 (0.355-0.500 mm) are given for Freundlich isotherm in Figures 3.8 and 3.9 respectively. Equilibrium data were obtained for B adsorption onto Diaion CRB 02 and Dowex-XUS 43594.00 resins (0.355-0.500 mm). Results were tabulated in Appendix-I section, respectively.

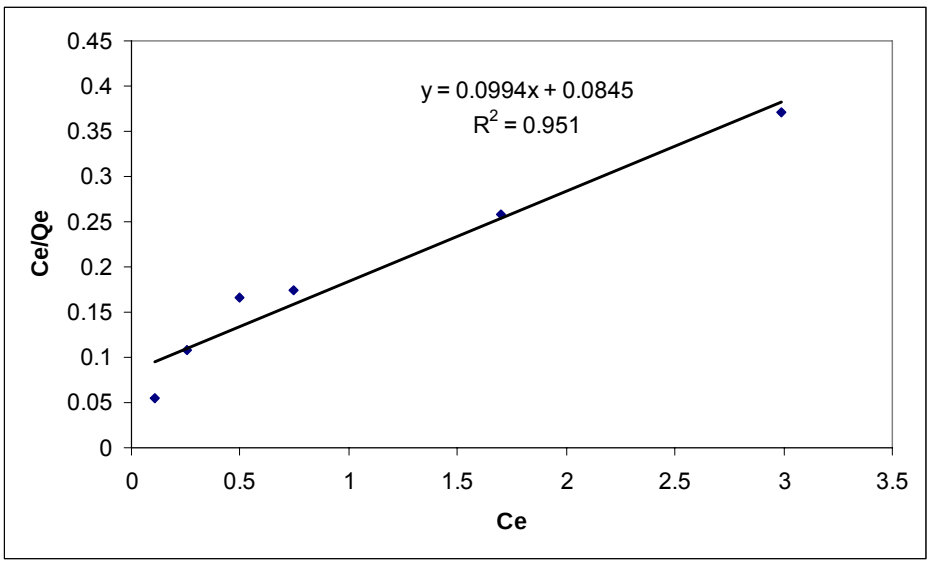


Figure 3.6 Linearized form of Langmuir isotherm for Diaion CRB 02 (0.355-0.500 mm).

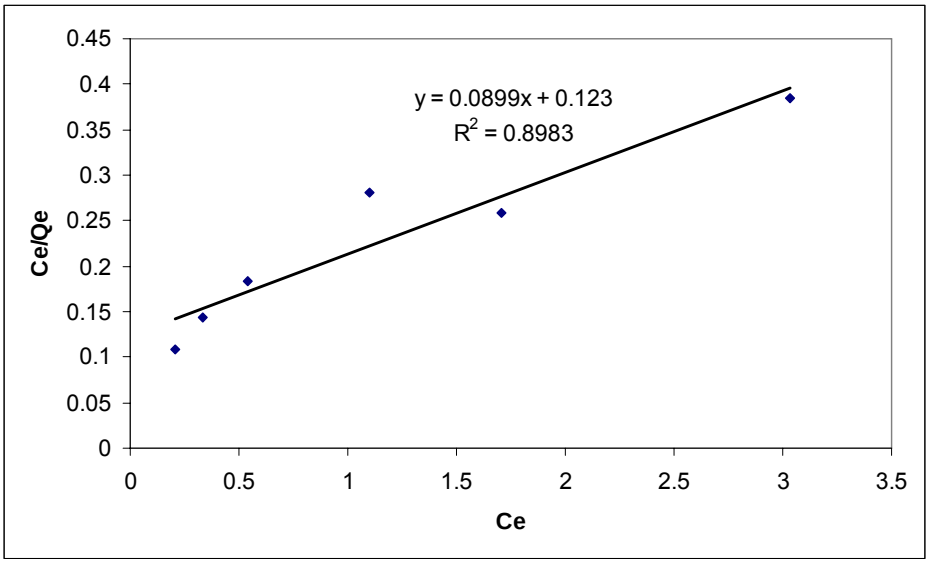


Figure 3.7 Linearized form of Langmuir isotherm for Dowex-XUS 43594.00 (0.355-0.500 mm).

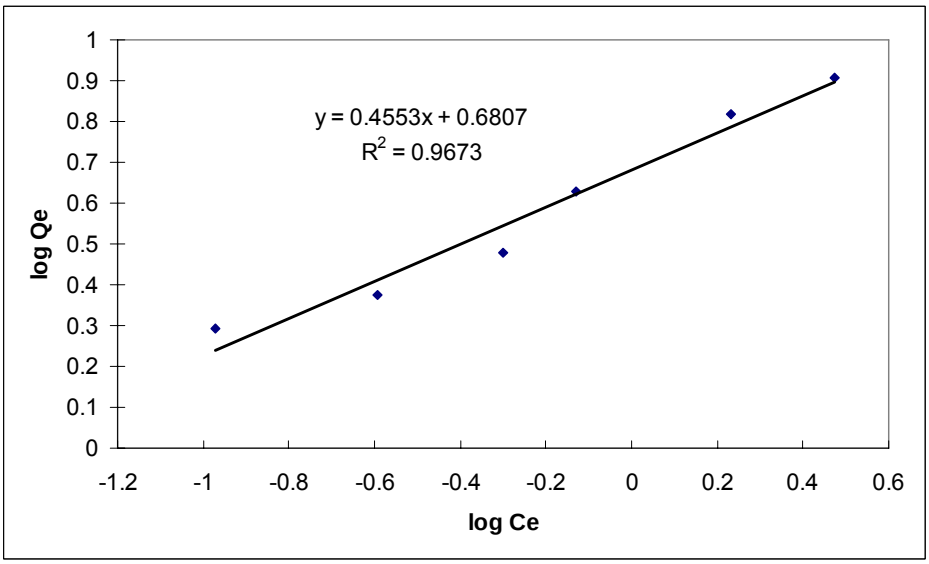


Figure 3.8 Linearized form of Freundlich isotherm for Diaion CRB 02 (0.355-0.500 mm).

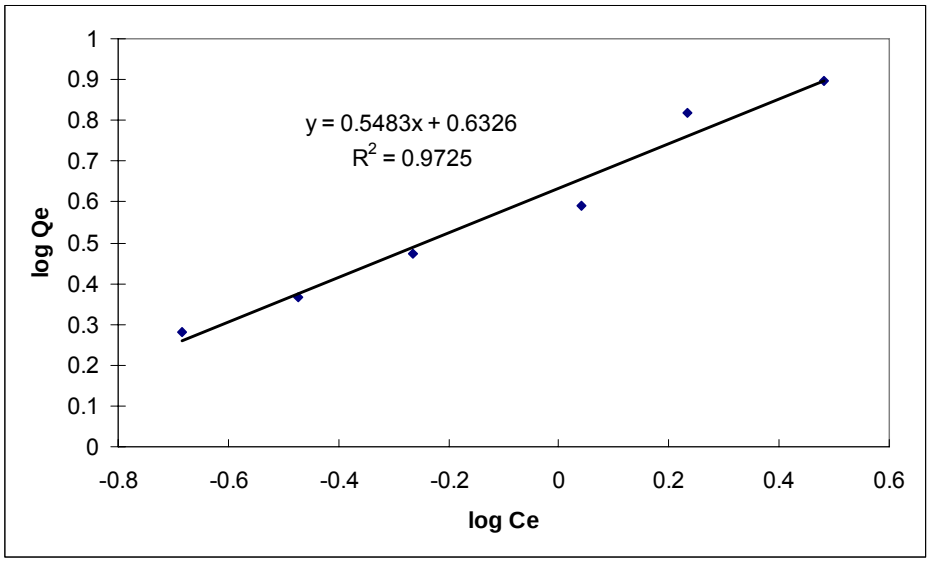


Figure 3.9 Linearized form of Freundlich isotherm for Dowex-XUS 43594.00 (0.355-0.500 mm).

The equilibrium relationships for Diaion CRB 02 and Dowex-XUS 43594.00 (45-75 μm) are also shown in Figures 3.10 and 3.11 respectively.

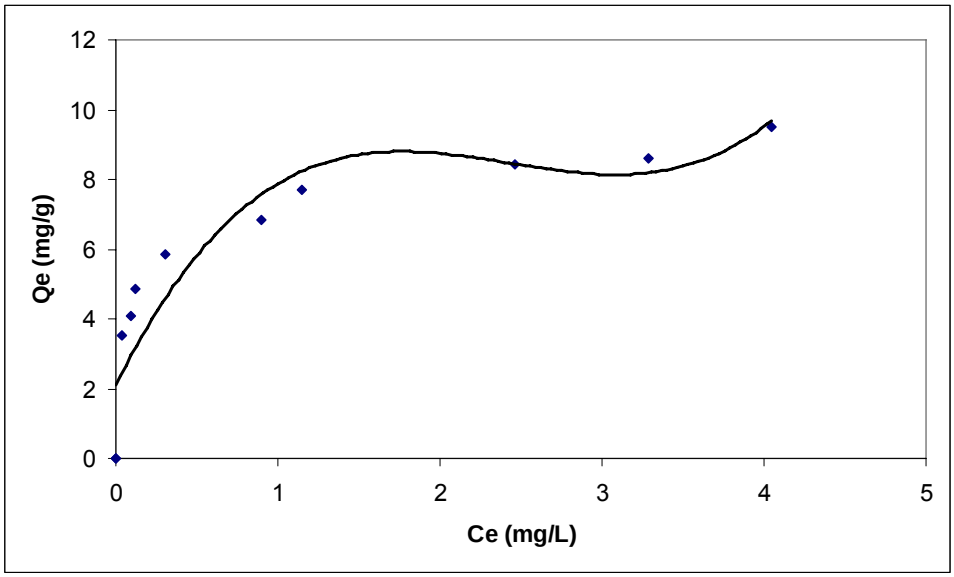


Figure 3.10 Equilibrium isotherm for loading B onto Diaion CRB 02 (45-75 μm).

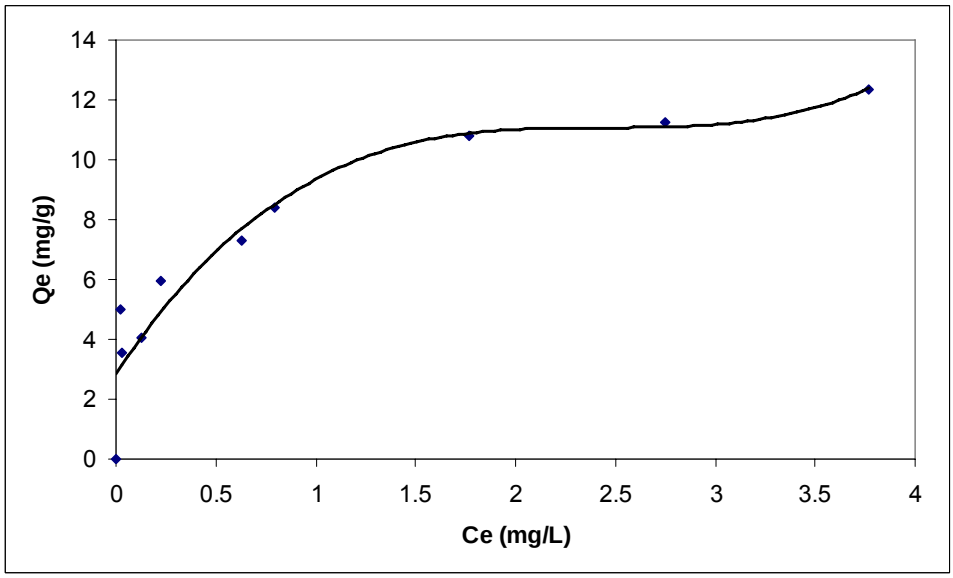


Figure 3.11 Equilibrium isotherm for loading B onto Dowex-XUS 43594.00 (45-75 μm).

The linearized fitting curves of for Diaion CRB 02 and Dowex-XUS 43594.00 (45-75 μm) are given for Langmuir isotherm in Figures 3.12 and 3.13 respectively. The linearized fitting curves of for Diaion CRB 02 and Dowex-XUS 43594.00 (45-75 μm) are given for Freundlich isotherm in Figures 3.14 and 3.15 respectively. Equilibrium data were obtained for B adsorption onto Diaion CRB 02 and Dowex-XUS 43594.00 resins (45-75 μm). Results were tabulated in Appendix-I section, respectively.

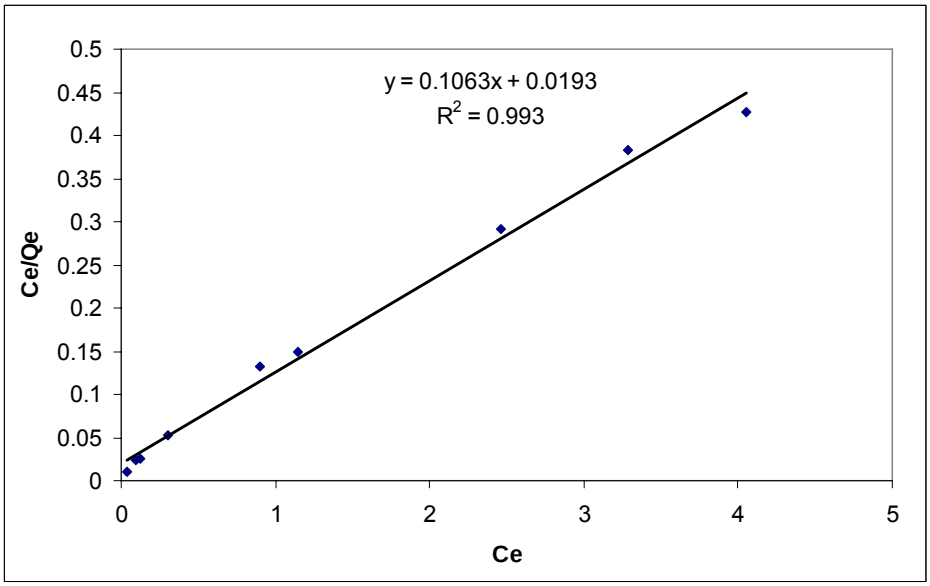


Figure 3.12 Linearized form of Langmuir isotherm for Diaion CRB 02 (45-75 μm).

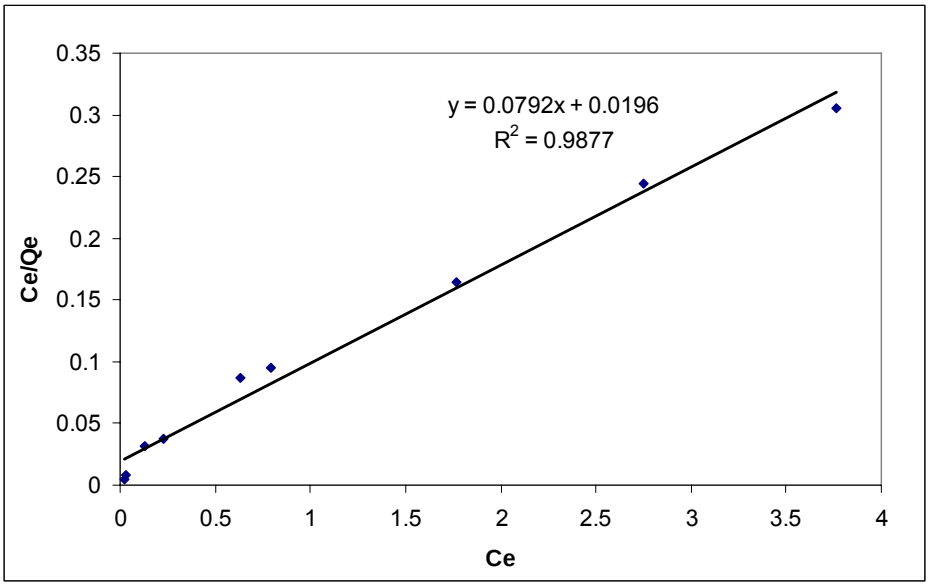


Figure 3.13 Linearized form of Langmuir isotherm for Dowex-XUS 43594.00 (45-75 μm).

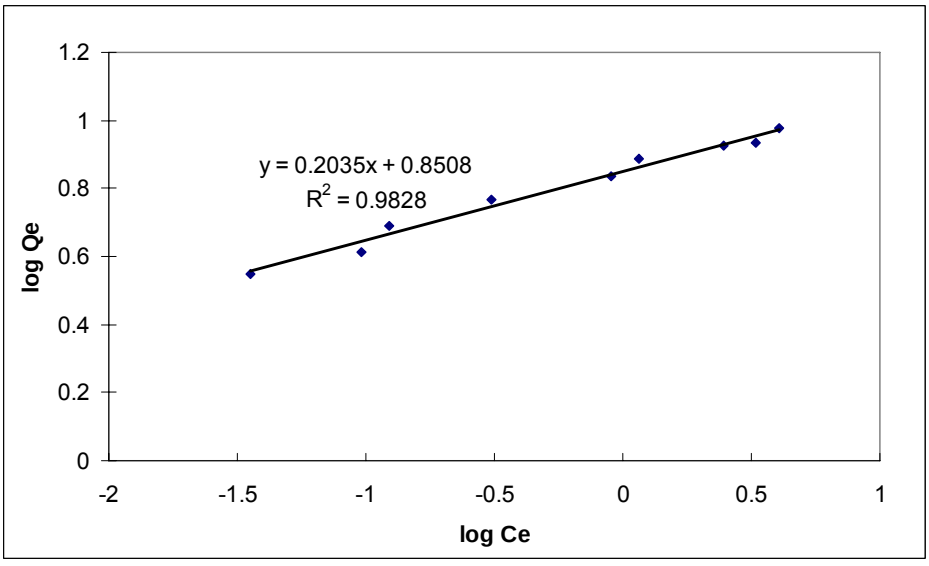


Figure 3.14 Linearized form of Freundlich isotherm for Diaion CRB 02 (45-75 μm).

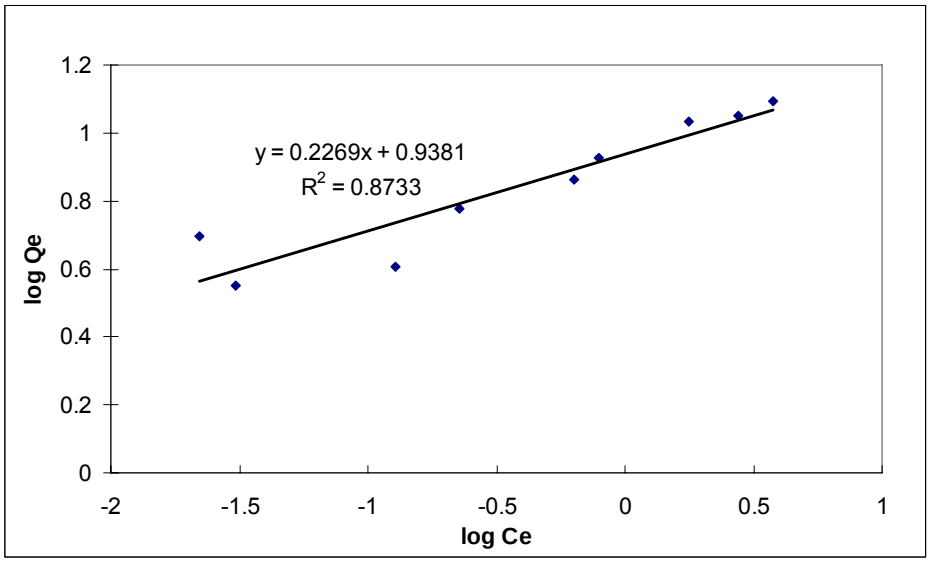


Figure 3.15 Linearized form of Freundlich isotherm for Dowex-XUS 43594.00 (45-75 μm).

The correlation coefficient for the linear regression fit of Freundlich isotherm equation was found to be 0.9673 for Diaion CRB 02 (0.355-0.500 mm). The resin showed better fit for Freundlich isotherm than Langmuir isotherm. The correlation coefficient for the linear regression fit of Langmuir isotherm equation was found to be 0.993 for Diaion CRB 02 (45-75 μm). The resin showed better fit for Langmuir isotherm than Freundlich isotherm when the particle size was decreased.

The correlation coefficient for the linear regression fit of Freundlich isotherm equation was found to be 0.9725 for Dowex-XUS 43594.00 (0.355-0.500 mm). The resin showed better fit for Freundlich isotherm than Langmuir isotherm. The correlation coefficient for the linear regression fit of Langmuir isotherm equation was found to be 0.9877 for Dowex-XUS 43594.00 (45-75 μm). The resin showed better fit for Langmuir isotherm than Freundlich isotherm when the particle size was decreased.

3.1.3 Kinetic performance of the resins in model seawater

Figures 3.16 and 3.17 shows the comparison of kinetic performances of the resins Diaion CRB 02 and Dowex-XUS 43594.00 with two different particle size ranges (0.355-0.500 mm and 45-75 μm) respectively. For comparison, effect of particle size on kinetic performance of both resins was given in Figure 3.18.

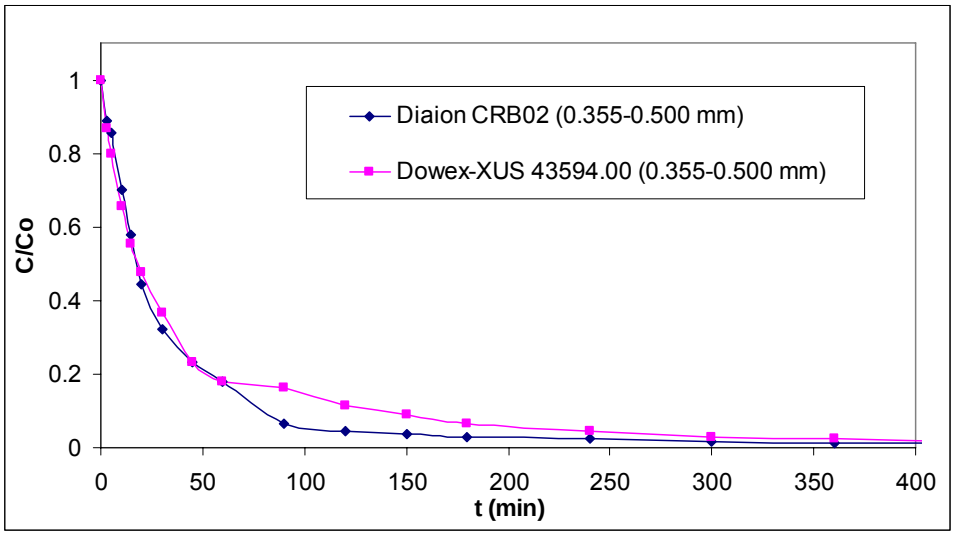


Figure 3.16 Comparison of kinetic performances of Diaion CRB 02 and Dowex-XUS 43594.00 (0.355-0.500 mm) for B removal**.**

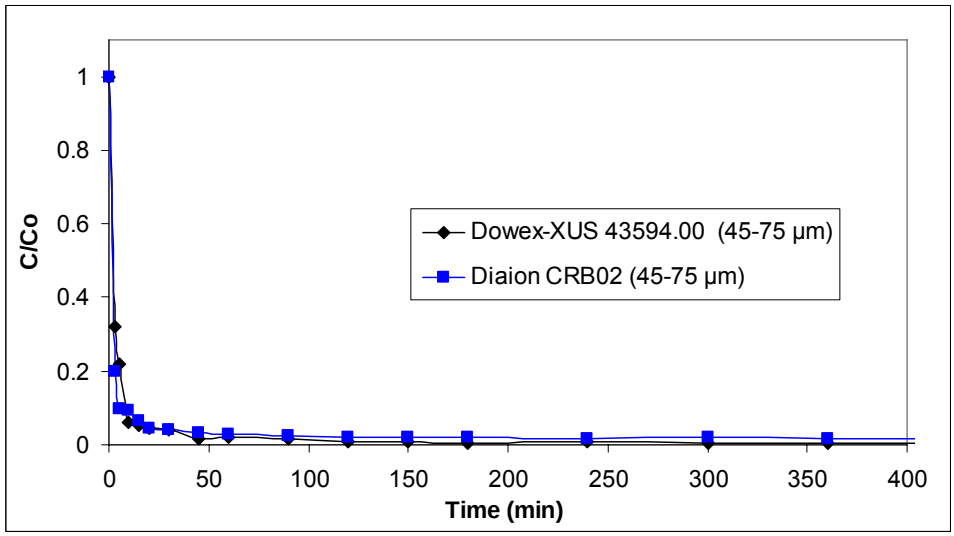


Figure 3.17 Comparison of kinetic performances of Diaion CRB 02 and Dowex-XUS 43594.00 (45-75 µm) for B removal**.**

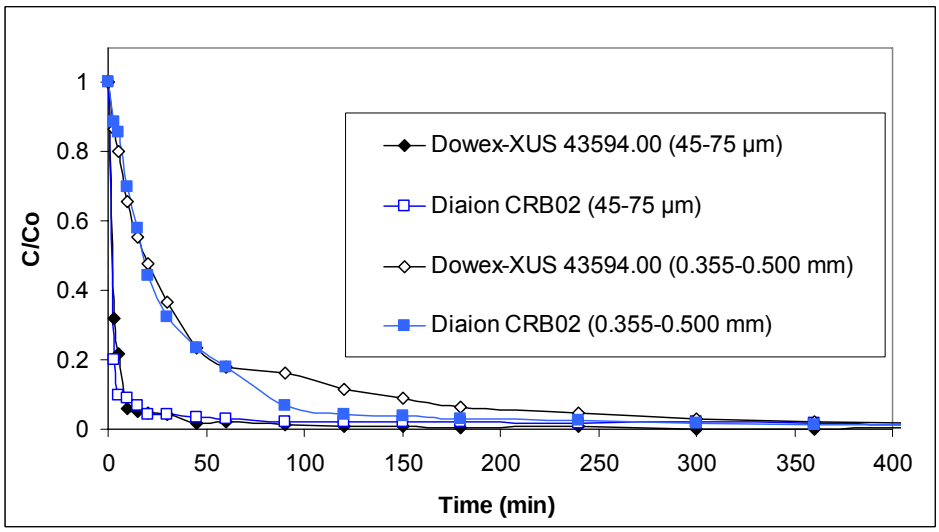


Figure 3.18 Effect of particle size on kinetic performance for B removal**.**

The equilibrium half-time for B removal were between 15-20 minutes with both Diaion CRB 02 and Dowex-XUS 43594.00 resin beads (0.355-0.500

mm). The corresponding values for powdered resins were less than 3 minutes for both resins.

Kinetic performance of the Dowex-XUS 43594.00 resin was relatively slower than that of Diaion CRB 02 resin with resin beads (0.355-0.500 mm). After reducing the particle sizes of the resins to 45-75 μm the kinetic performance became similar to each other. Kinetic performances of the resins improved effectively by decreasing the particle size.

The prediction of batch sorption kinetics is necessary for the design of industrial sorption columns. The nature of the sorption process will depend on physical or chemical characteristics of the adsorbent system and also on the system conditions. Previously several researchers used different kinetic models, such as Lagergren pseudo first order, pseudo second order, Elovich kinetic equation, and parabolic diffusion model, in order to predict the mechanism involved in the sorption process. From these models the sorption kinetics was usually described by the Lagergren pseudo-first-order model (Vadivelan and Kumar, 2005). Currently the pseudo-second-order model has been widely used for sorption systems due to its good representation of the experimental data for most of the adsorbent adsorbate systems (Vadivelan and Kumar, 2005).

Lagergren pseudo-first-order kinetics

The pseudo-first-order kinetic model has been widely used to predict the sorption kinetics. The sorption kinetics following the pseudo-first-order model is given by (Ho et al., 1998).

$$\frac{dq}{dt} = K_1(q_e - q_t) \qquad (3.1)$$

where q and q_e represent the amount of adsorbed (mg/g) at any time t and at equilibrium time, respectively, and K_1 represents the sorption rate constant (min^{-1}).

Eqn 3.1 with respect to boundary conditions

q = 0 at t = 0
and q = q at t = t ,

then Eqn 1.1 becomes

$$\log(q_e - q_t) = \log(q_e) - \frac{K_1 t}{2.303} \qquad (3.2)$$

Thus the rate constant K_1 (min^{-1}) can be calculated from the plot of $\log(q_e - q_t)$ versus time.

Ho pseudo-second-order kinetics

The kinetic data were further analyzed using Ho's pseudo second order kinetics, which is represented by (Ho, 2003)

$$\frac{dq}{dt} = K_2 (q_e - q_t)^2 \qquad (3.3)$$

where K_2 is the pseudo-second-order rate constant (g/ mg min), q_e and q represent the amount of the adsorbed (mg/g) at equilibrium and at any time t . Separating the variables in Eqn. 3.3 gives;

$$\frac{dq}{(q_e - q_t)^2} = K_2 dt \qquad (3.4)$$

Integrating Eqn. 3.4 for the boundary conditions

t = 0 to t = t
and q = 0 and q = q_e gives;

$$\frac{t}{q_t} = \frac{1}{K_2 q_e^2} + \frac{1}{q_e} t \qquad (3.5)$$

A plot between t/q versus t gives the value of the constants K_2 (g/mg h) and also q_e (mg/g) can be calculated. The constant K_2 is used to calculate the initial sorption rate h, at $t \rightarrow 0$, as follows:

$$h = K_2 q_e^2 \qquad (3.6)$$

Thus the rate constant K_2, initial sorption rate h, and predicted q_e can be calculated from the plot of t/q versus time t using Eqn. 3.5.

The optained kinetic data were fitted to sorption kinetics using the pseudo first order and pseudo second order kinetic model equations for Diaion CRB 02 and Dowex-XUS 43594.00. Diaion CRB 02 (0.355-0.500 mm) resin reached the equilibrium after 120 min (95.56% removal). Dowex-XUS 43594.00 (0.355-0.500 mm) resin reached the equilibrium after 240 min (95.45% removal). Diaion CRB 02 and Dowex-XUS 43594.00 (45-75 μm) resins reached the equilibrium after 10 min (90.84% and 94.03% removal respectively), the data obtained at contact time later minutes were neglected for first and second order reaction. Figures 3.19, 3.22, 3.25 and 3.28 were plotted in order to observe first order reactions by plotting $\log(q_e - q_t)$ versus time and Figures 3.20, 3.23, 3.26 and 3.29 were plotted in order to observe second order reactions by plotting t/q versus time. Predicted q_e values were also calculated from the graphs. Theoretical and experimental comparisons are given in the Figures 3.21, 3.24, 3.27 and 3.30 for Diaion CRB 02 and Dowex-XUS 43594.00 (0.355-0.500 mm and 45-75 μm) respectively. Related data wete tabulated in the Appendix-I section.

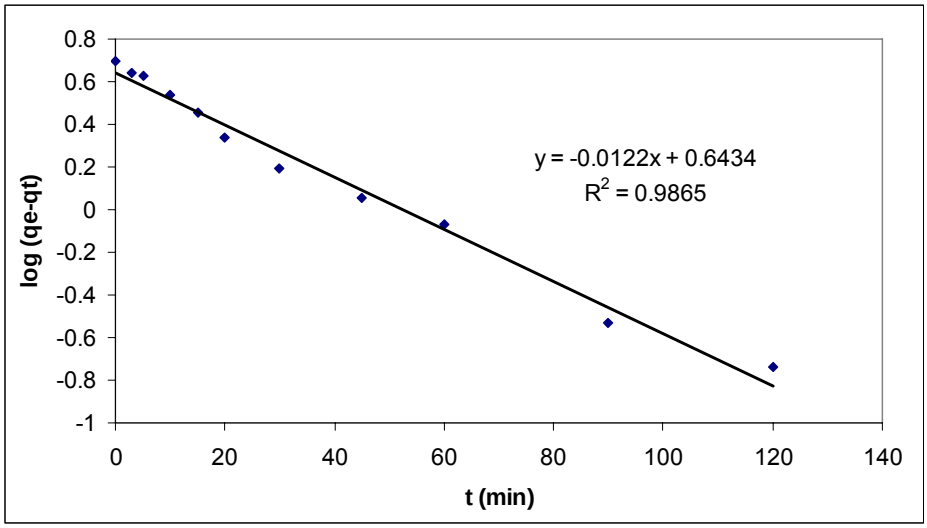


Figure 3.19 Lagergren pseudo-first-order kinetics for B adsorption on Diaion CRB 02 (0.355-0.500 mm).

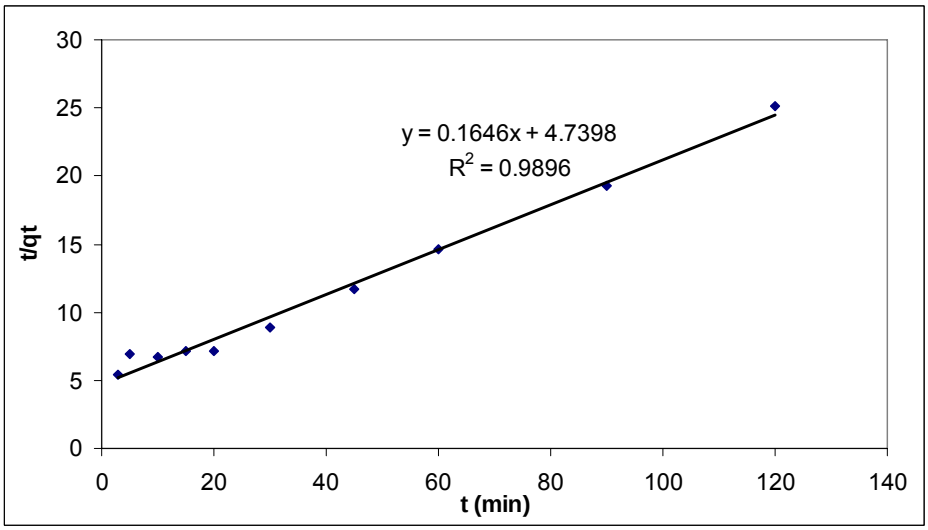


Figure 3.20 Ho pseudo-second-order kinetics for B adsorption on Diaion CRB 02 (0.355-0.500 mm).

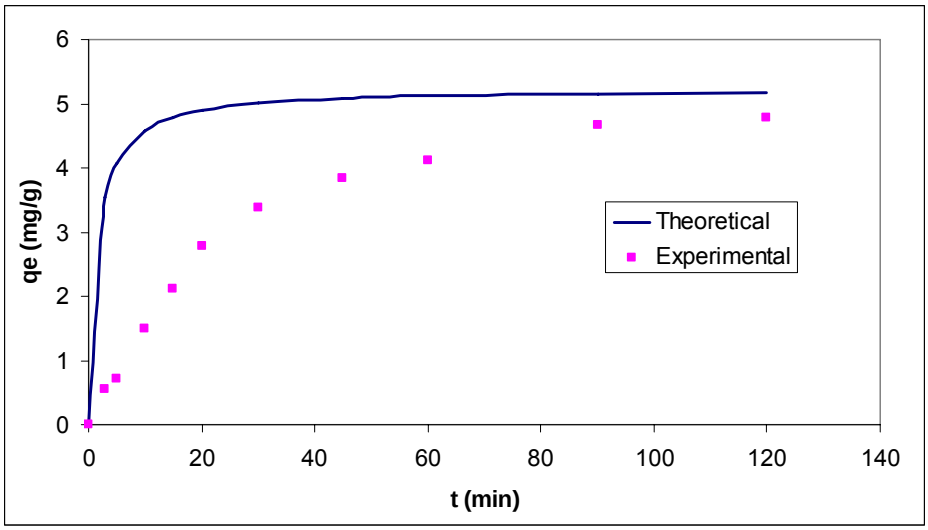


Figure 3.21 Comparison of second order kinetic models in predicting q_t for B adsorption on Diaion CRB 02 (0.355-0.500 mm).

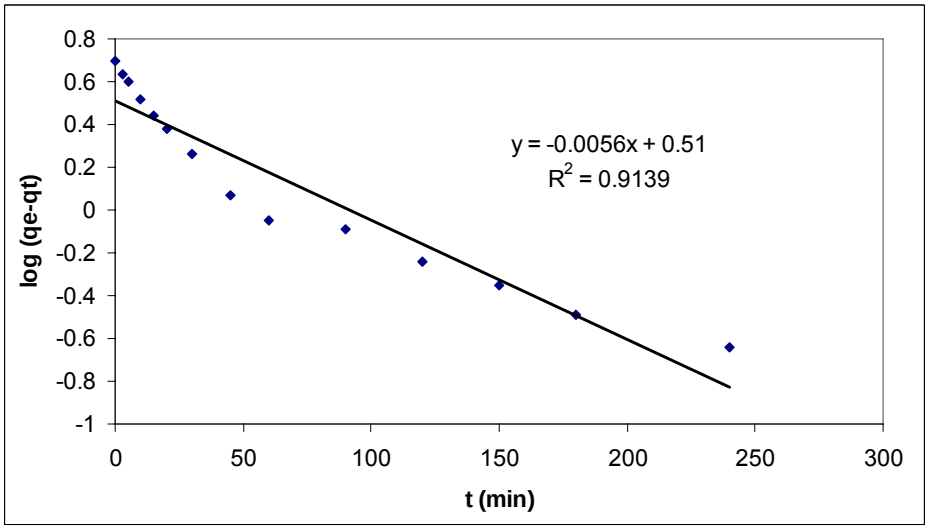


Figure 3.22 Lagergren pseudo-first-order kinetics for B adsorption on Dowex-XUS 43594.00 (0.355-0.500 mm).

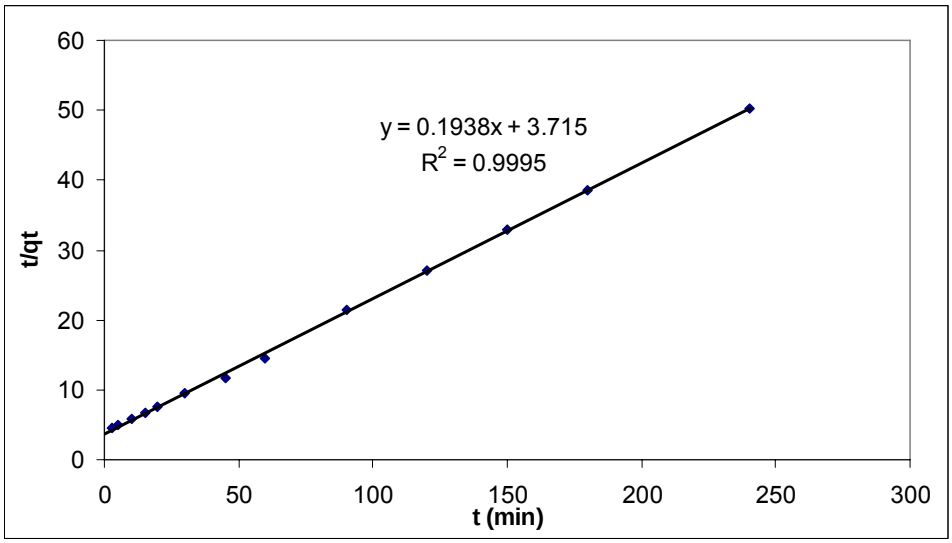


Figure 3.23 Ho pseudo-second-order kinetics for B adsorption on Dowex-XUS 43594.00 (0.355-0.500 mm).

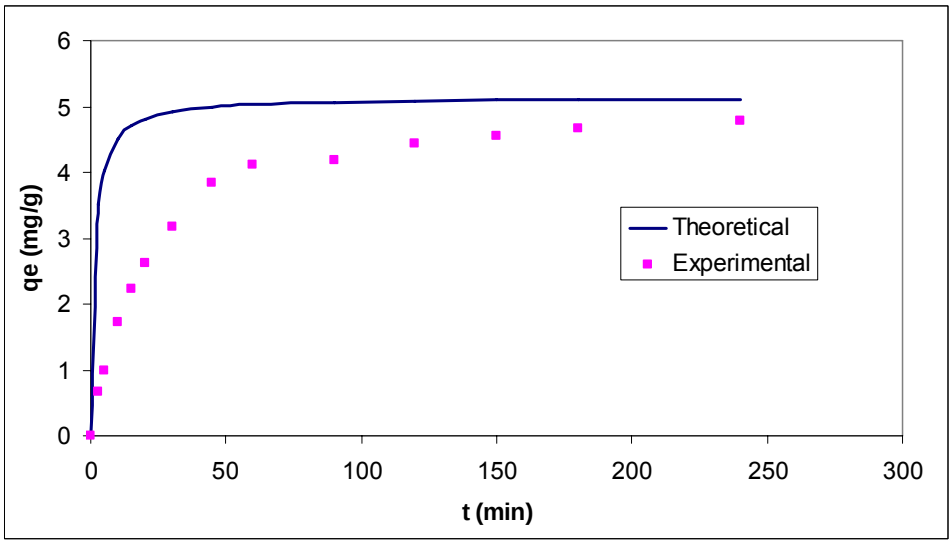


Figure 3.24 Comparison of second order kinetic models in predicting q_t for B adsorption on Dowex-XUS 43594.00 (0.355-0.500 mm).

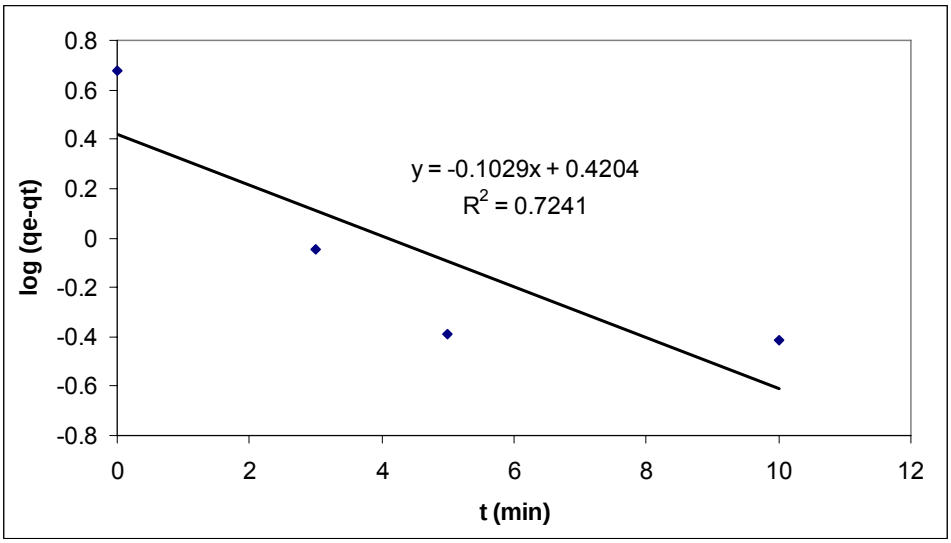


Figure 3.25 Lagergren pseudo-first-order kinetics for B adsorption on Diaion CRB 02 (45-75 μm).

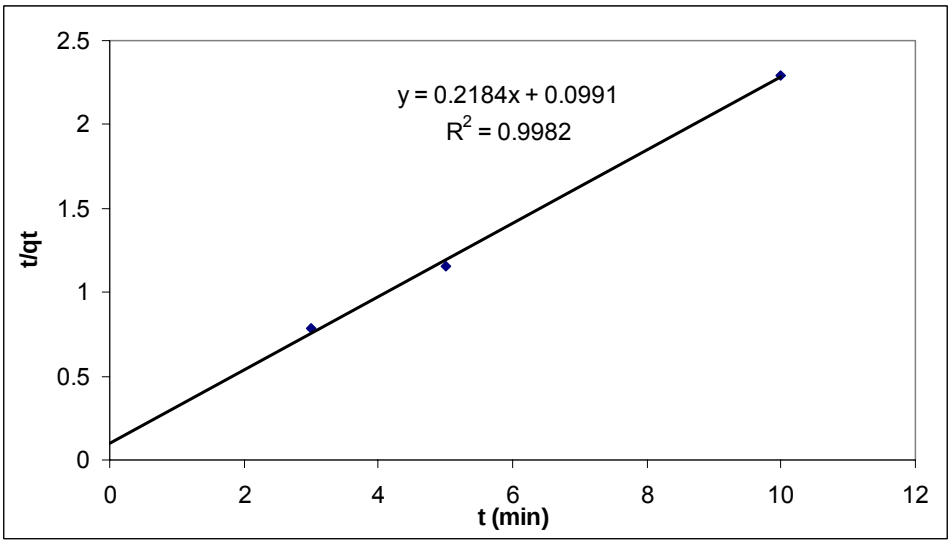


Figure 3.26 Ho pseudo-second-order kinetics for B adsorption on Diaion CRB 02 (45-75 μm).

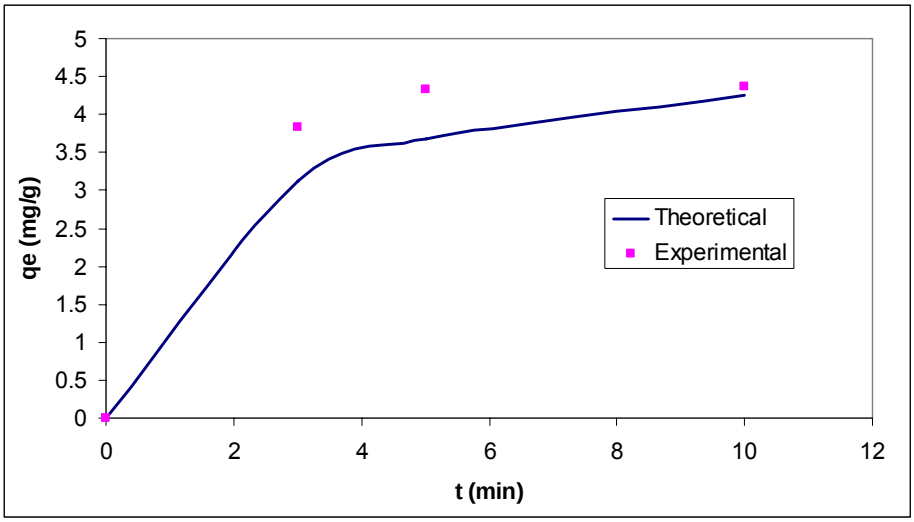


Figure 3.27 Comparison of second order kinetic models in predicting q_t for B adsorption on Diaion CRB 02 (45-75 μm).

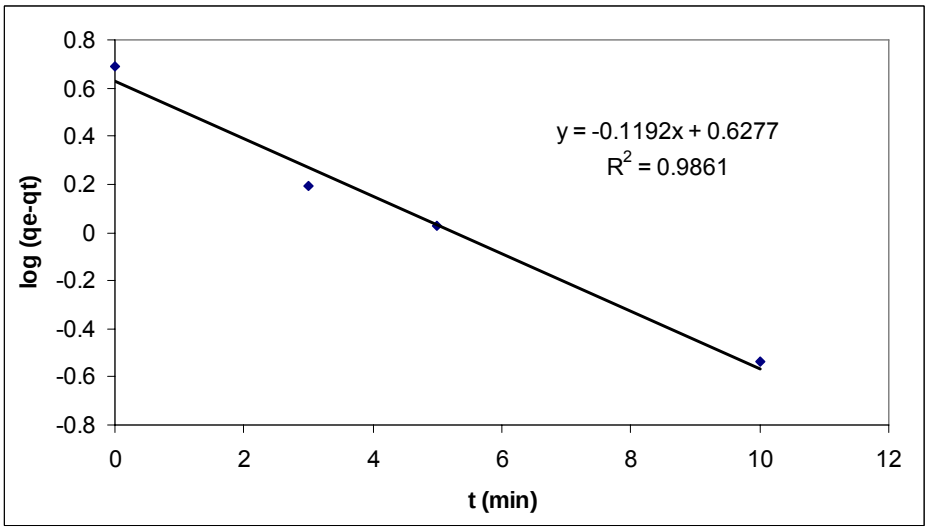


Figure 3.28 Lagergren pseudo-first-order kinetics for B adsorption on Dowex-XUS 43594.00 (45-75 μm).

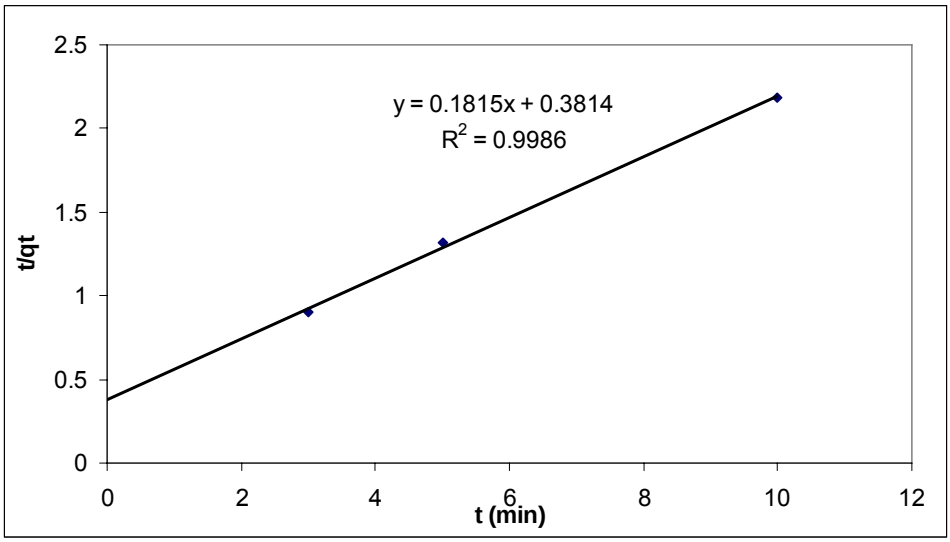


Figure 3.29 Ho pseudo-second-order kinetics for B adsorption on Dowex-XUS 43594.00 (45-75 μm).

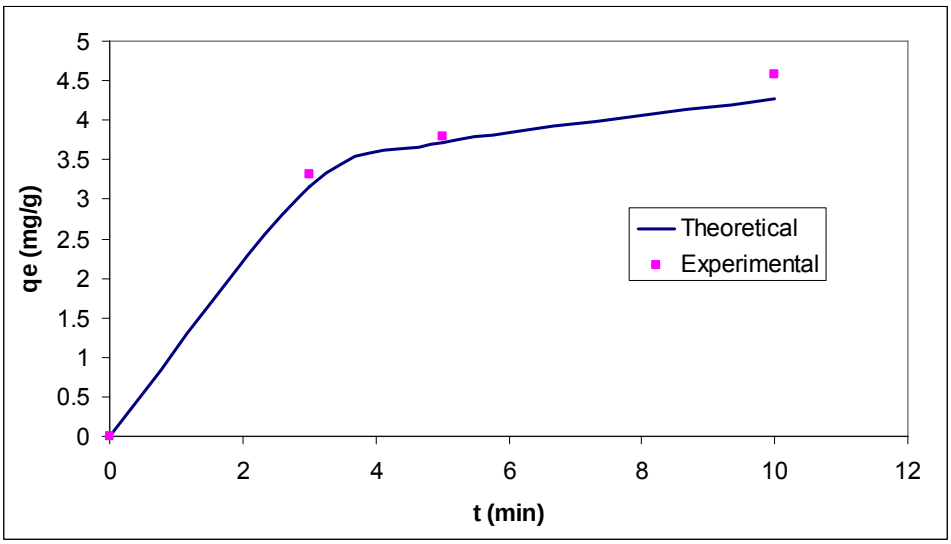


Figure 3.30 Comparison of second order kinetic models in predicting q_t for B adsorption on Dowex-XUS 43594.00 (45-75 μm).

Sorption kinetics reaction orders for Diaion CRB 02 and Dowex-XUS 43594.00 (0.355-0.500 mm and 45-75 μm) (r^2 = 0.9896 and 0.9982 for Diaion CRB 02 and r^2 = 0.9995 and 0.9986 for Dowex-XUS 43594.00 respectively) fit to Ho pseudo-second-order mechanism in each case. The comparison of the experimental and theoretical curves for second order kinetics showed similarity as a proof of the fitting to the Ho pseudo-second-order mechanism.

The kinetic data were also fitted to the following simplified kinetic models using equations given in Section 1.4.4 to evaluate the kinetic date and to find the rate determining steps.

A. Infinite Solution Volume Models (ISV)

A1. Particle Diffusion

Manipulating Vermeulen's approximation given by Eqn. (1.11), a simple expression can be obtained (Vermeulen, 1952):

$$-\ln(1-X^2) = 2kt \qquad (3.7)$$

where $k = \dfrac{D_r \pi^2}{r_o^2}$

If the particle diffusion is the rate controlling mechanism, a plot of $-\ln(1-X^2)$ versus time should result in a straight line. The value of diffusion coefficient can be found from the slope.

A2. Film Diffusion

If the film diffusion is the rate controlling mechanism, derivation of Eqn. (1.20) results in;

$$\ln(1-X) = k_{li}t \qquad (3.8)$$

where $k_{li} = \frac{3DC}{r_o \delta \overline{C}}$

B. Unreacted Core Model (UCM)

B1. Film Diffusion

When the fluid is the rate controlling layer, Eqn. (1.24) can be modified to represent the fractional attainment of equilibrium as a function of time.

$$X = \frac{3C_{Ao}K_{MA}}{ar_oC_{so}}t \qquad (3.9)$$

In the case of the film diffusion is in control of the ion exchange mechanism, the extent of the resin conversion X, plotted against t should produce a straight line and its slope is given by the expression $3\ C_{Ao}K_{MA}/ar_oC_{so}$.

B2. Reacted Layer Diffusion

If reacted layer diffusion controls the ion exchange process, Eqn. (3.19) can be used to find the mass transfer coefficient

$$\left[3-3(1-X)^{2/3}-2X\right]=\frac{6D_{e,r}C_{Ao}}{ar_o^2C_{so}}t \qquad (3.10)$$

A straight line should be obtained by plotting $\left[3-3(1-X)^{2/3}-2X\right]$ against time, t if reacted layer diffusion controls. The slope is given by the expression $6\overline{D_e}C_{Ao}/ar_o^2C_{so}$.

B3. Chemical Reaction

By manipulating the Eqn. (1.26) the following equation can be obtained to represent the rate controlling mechanism, in the case of the slowest step is the chemical reaction,

$$\left[1-(1-X)^{1/3}\right]=\frac{k_s C_{Ao}}{r_o} \qquad (3.11)$$

Then, a plot of $\left[1-(1-X)^{1/3}\right]$ versus time should produce a straight line. The slope is given by $C_{Ao}\, k_s / r_o$.

The summary of the models fitted to experimental results to find the rate control mechanism is given in Table 3.3. The various functions plotted to determine the rate controlling of Diaion CRB 02 (0.355-0.500 mm) and Dowex-XUS 43594.00 (0.355-0.500 mm and 45-75 μm) are shown Figures 3.31 – 3.36.

Table 3.3 Diffusional and reaction models (Samuelson, 1963)

Method	**Equation**	**Rate Controlling Step**
ISV	**-ln (1-X)**=kt, where $k=Dr\pi^2/r_o^2$	Film Diffusion
	-ln (1-X^2) $=k_{li}t$, where $k=3DC/r_o\delta Cr$	Particle Diffusion
UCM	**X**$=(3C_{Ao}K_{MA}/ar_oC_{So})t$	Liquid Film
	3-3(1-X)$^{2/3}$-2X $= (6D_{CR}C_{Ao}/ ar_o^2 C_{So})t$	Reacted Layer
	1-(1-X)$^{1/3}$ $= (k_sC_{Ao}/ r_o)t$	Chemical Reaction

The X values in the functions tabulated in Table 3.3 were calculated as (q_t/q_e) which means the fraction of boron adsorption in the resins at time (t) and in equilibrium. X=1 points were accepted as equilibrium. The functions were calculated to the point that X values reached 1. The time for Diaion CRB 02 (0.355-0.500 mm) for X=1 point was 60 minutes. The time for Dowex-XUS 43594.00 (0.355-0.500 mm) for X=1 point was 45 minutes. The time for Dowex-XUS 43594.00 (45-75 μm) for X=1 point was 10 minutes. The rate controlling of Diaion CRB 02 at 45-75 μm particle size was not determined because X=1 point was less than 10 minutes. The data obtained at contact time later minutes were neglected for film diffusion model described by Unreacted Core Model. The smaller particle sized resins showed faster kinetics as shown before (Figures 3.17 and 3.18). The equilibrium has been reached very early such as in 10 mins.

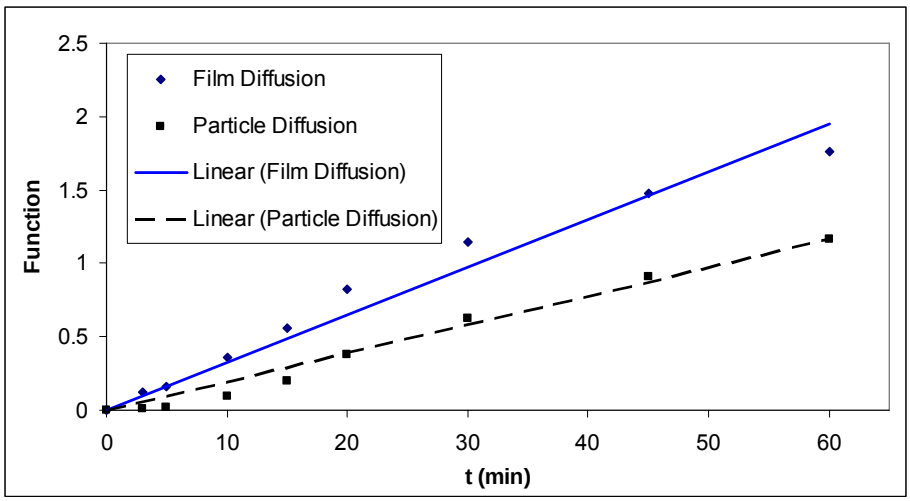


Figure 3.31 Kinetic behavior of Diaion CRB 02 (0.355-0.500 mm) based on Unreacted Core Models.

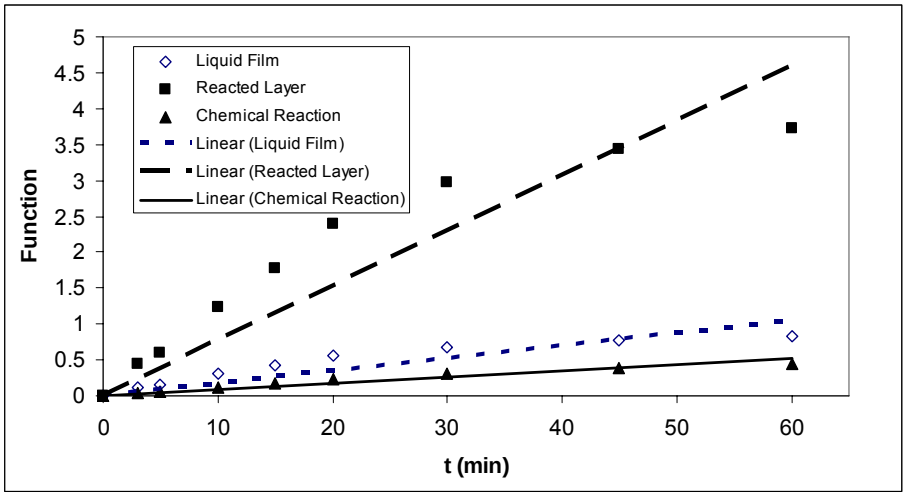


Figure 3.32 Kinetic behavior of Diaion CRB 02 (0.355-0.500 mm) based on Infinite Solution Models.

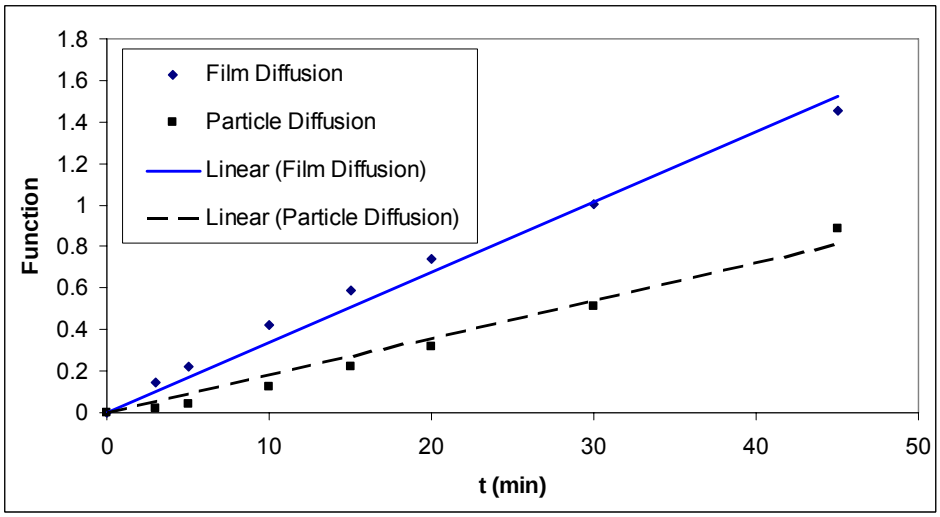


Figure 3.33 Kinetic behavior of Dowex-XUS 43594.00 (0.355-0.500 mm) based on Unreacted Core Models.

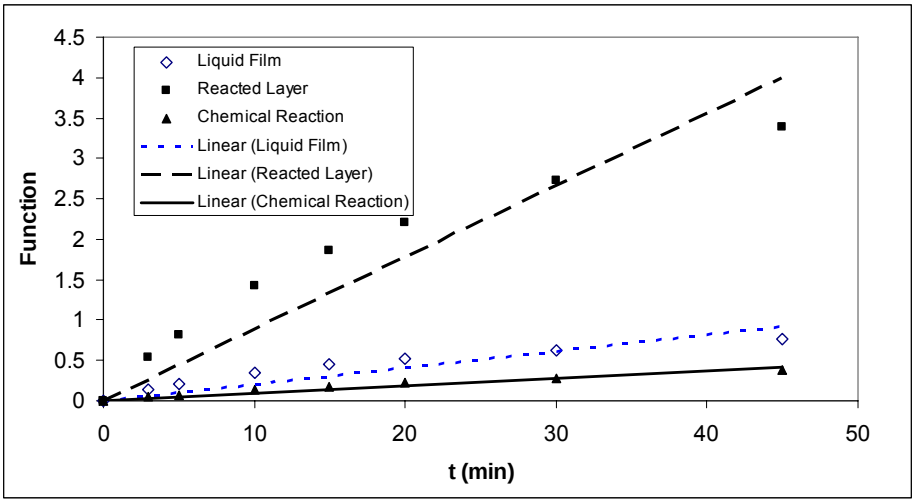


Figure 3.34 Kinetic behavior of Dowex-XUS 43594.00 (0.355-0.500 mm) based on Infinite Solution Models.

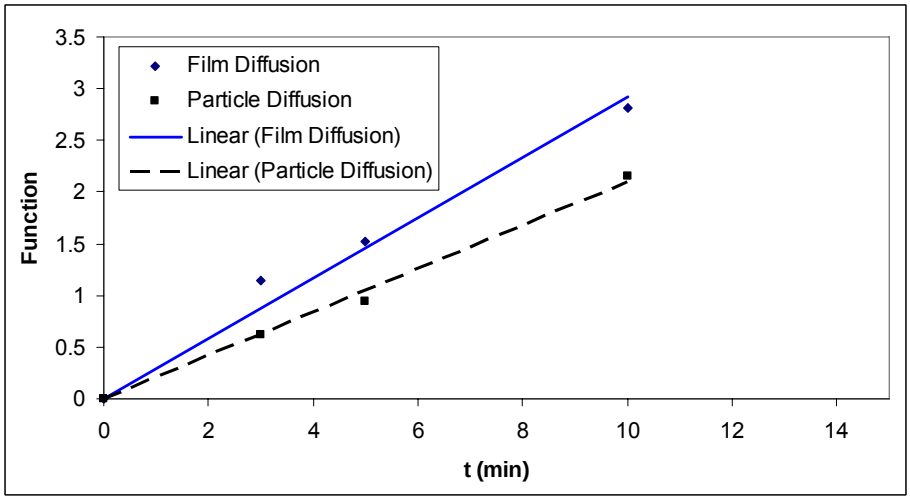


Figure 3.35 Kinetic behavior of Dowex-XUS 43594.00 (45-75 μm) based on Unreacted Core Models.

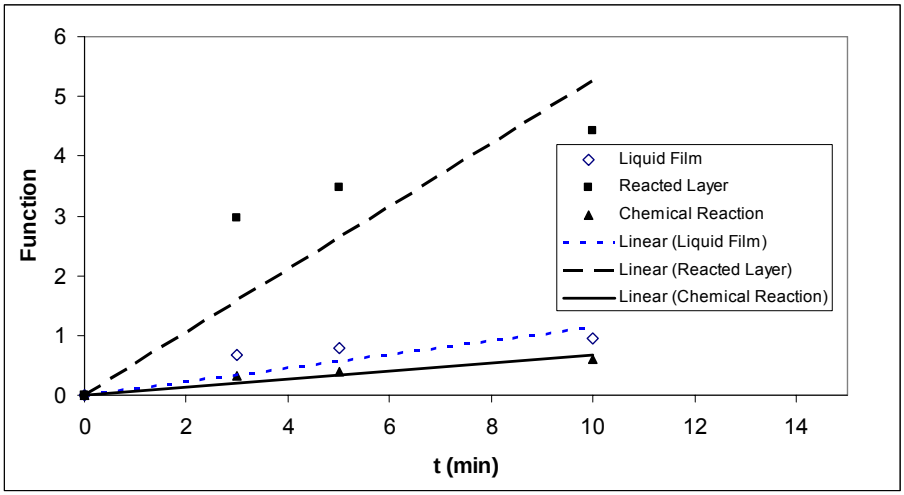


Figure 3.36 Kinetic behavior of Dowex-XUS 43594.00 (45-75 µm) based on Infinite Solution Models.

Table 3.4 gives the slope values and the linear correlation coefficients. As seen in the Table 3.4, the rate is controlled by chemical reaction for all resins and particle sizes according to Unreacted Core Model. For Dowex-XUS 43594.00 resin (0.355-0.500 mm) film diffusion was the rate determining step according to Infinite Solution Volume Model. But after powdering Dowex-XUS 43594.00 resin, rate determining step has changed to particle diffusion. Particle diffusion was the rate determining step for Diaion CRB 02 resin, according to Infinite Solution Volume Model.

Table 3.4 Evaluation of kinetic models for Diaion CRB 02 and Dowex-XUS 43594.00 (0.355-0.500 mm and 45-75 μm).

Model	Diaion CRB 02 (0.355-0.500 mm)		Dowex-XUS 43594.00 (0.355-0.500 mm)		Dowex-XUS 43594.00 (45-75 μm)	
	slope	r^2	*slope*	r^2	*slope*	r^2
-ln (1-X)	0.0325	0.9688	0.0339	**0.9839**	0.2928	0.9790
-ln (1-X^2)	0.0194	**0.9801**	0.0180	0.9734	0.2101	**0.9942**
X*	0.0147	0.7733	0.0205	0.8112	0.1146	0.6126
3-3(1-X)$^{2/3}$-2X	0.0767	0.8227	0.0887	0.8561	0.5261	0.6950
1-(1-X)$^{1/3}$	0.0086	**0.9240**	0.0094	**0.9475**	0.0674	**0.8902**

3.1.4 Column mode sorption-elution studies of the resins in model seawater

To compare the column performances of the resins Diaion CRB 02 and Dowex-XUS 43594.00, same conditions such as the particle size (0.355-0.500 mm), feed flow rate (SV 10, 15 and 20 h^{-1}) and column diameter (ID 0.7 cm) were employed. Breakthrough and elution curves of Diaion CRB 02 resin are given in Figures 3.37 and 3.38, respectively. Breakthrough and elution curves of Dowex-XUS 43594.00 resin are given in Figures 3.39 and 3.40, respectively. Related data were tabulated in the Appendix-I section.

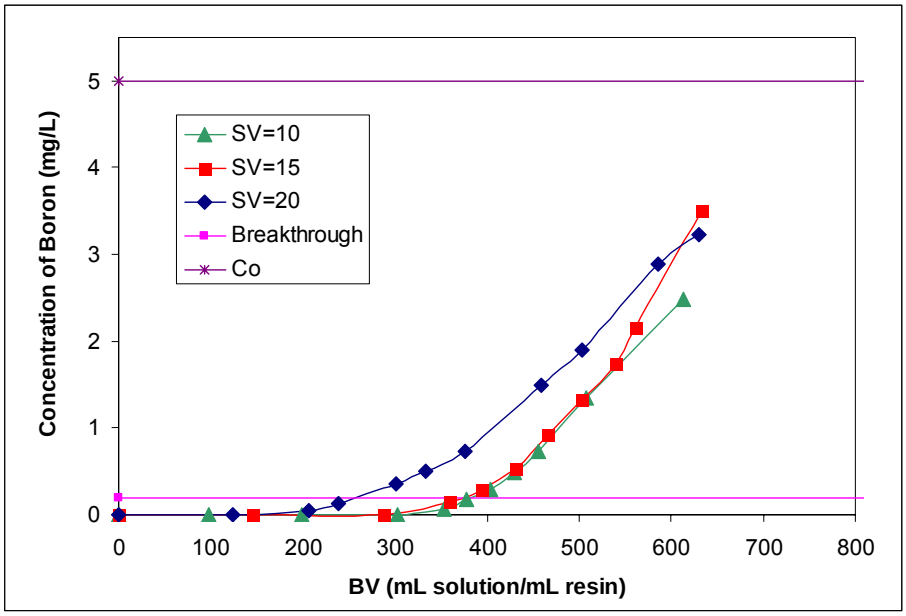


Figure 3.37 Breakthrough curves of boron selective resin (Diaion CRB02) for boron removal from model seawater solution as a function of SV.

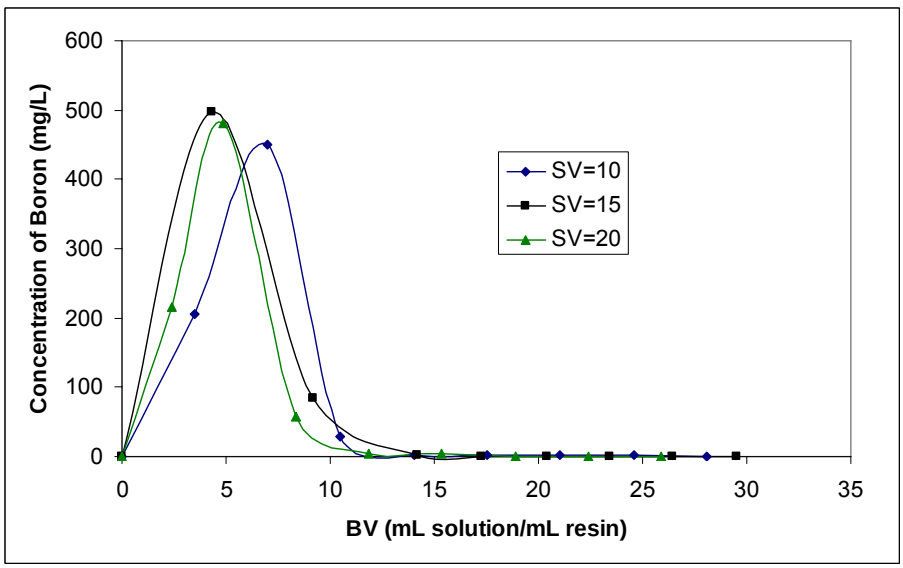


Figure 3.38 Elution curves of boron selective resin (Diaion CRB02) for boron removal from model seawater solution as a function of SV.

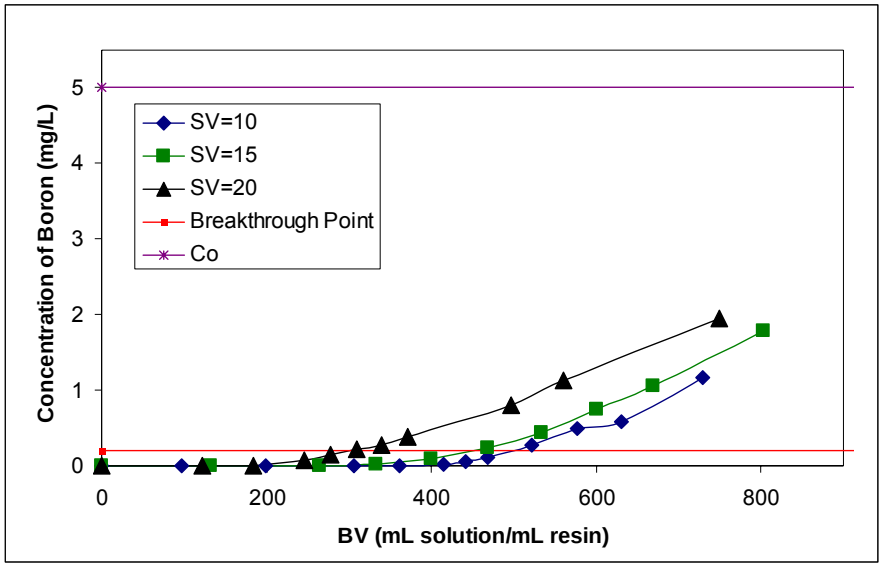


Figure 3.39 Breakthrough curves of boron selective resin (Dowex-XUS 43594.00) for boron removal from model seawater solution as a function of SV.

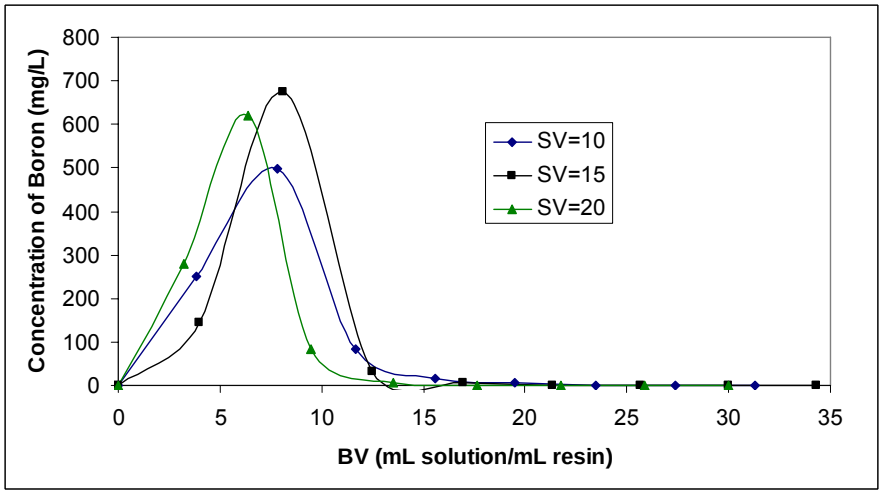


Figure 3.40 Elution curves of boron selective resin (Dowex-XUS 43594.00) for boron removal from model seawater solution as a function of SV.

The data obtained for Diaion CRB 02 and Dowex-XUS 43594.00 resins are given in Table 3.5. Breakthrough capacities of both resins increased with

decreasing SV. Figures 3.37 and 3.39 show the effect of SV on breakthrough point, which were especially remarkable when especially SV decreased from 20 from 15 h^{-1}. Similar breakthrough capacities were obtained for both resins when SV decreased from 10 and 15 h^{-1}. As shown in Table 3.5, Dowex-XUS 43594.00 has larger breakthrough capacities than Diaion CRB 02 regarding its volume capacity. When weight capacities were compared, it has been seen that both resins have similar breathrough capacities. This result shows that Dowex-XUS 43594.00 resin is denser than Diaion CRB 02 resin. Boron loaded onto the resin was eluted quantitatively from both resins using 5% H_2SO_4 solution.

Table 3.5 Column data for boron removal from model seawater solution.

Resin	SV (h^{-1})	Breakthrough Volume (BV)	Breakthrough capacity		Elution		Elution efficiency (%)
			(mg/mL)	(mg/g)	mg sorbed	mg eluted	
Diaion CRB02	20	263	1.29	4.22	1.386	0.967	69.8
	15	374	1.86	6.10	1.496	1.286	86.0
	10	383	1.91	6.27	1.478	1.214	82.1
Dowex-XUS 43594.00	20	303	1.52	4.08	2.180	1.574	72.2
	15	454	2.17	5.82	2.270	1.784	78.6
	10	500	2.49	6.69	1.749	1.665	95.2

3.2 Removal of Boron from NaCl + H_3BO_3 Solution

3.2.1 Kinetic performance of the resin in NaCl + H_3BO_3 Solution

Comparison of the kinetic performance of Diaion CRB02 resin with NaCl+H_3BO_3 and model seawater solutions was given in Figure 3.41. This comparison shows that the effect of the salts other than NaCl does not exist to change the kinetic performance of Diaion CRB 02 resin.

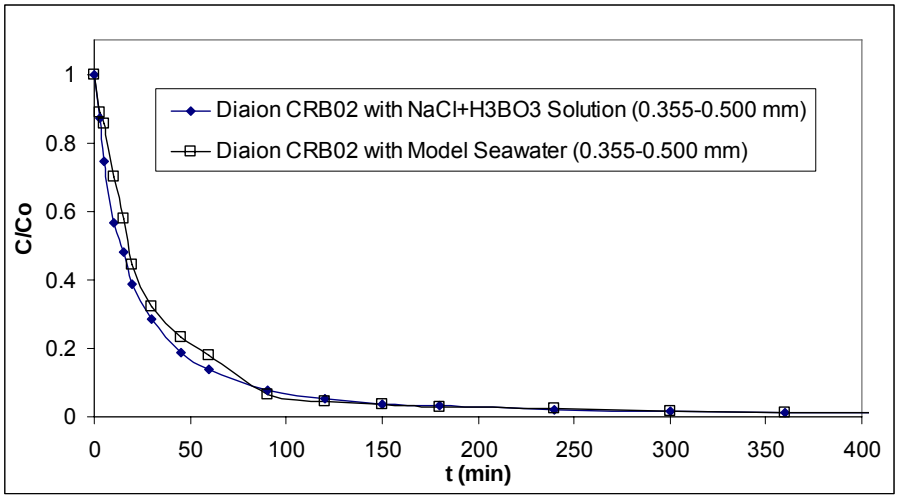


Figure 3.41 Comparison of the kinetic performance of boron selective resin (Diaion CRB02) with NaCl+H_3BO_3 and model seawater solutions.

The equilibrium half-time for B removal were between 10-15 minutes with Diaion CRB 02 resin (0.355-0.500 mm). Diaion CRB 02 resin shows similar kinetic performance in NaCl + H_3BO_3 and model seawater solutions.

The obtained kinetic data were fitted to sorption kinetics by means of first and second order reaction for Diaion CRB 02. Figure 3.42 was plotted in order to observe first order reactions by plotting $\log(q_e - q_t)$ versus time and Figure 3.43 was plotted in order to observe second order reactions by plotting t/q versus time. Predicted q_e values were also calculated from the graphs. Diaion CRB 02 (0.355-0.500 mm) resin reached the equilibrium after 180 min (96.86% removal). Theoretical and experimental comparison for second order reaction was given in the Figure 3.44 for Diaion CRB 02. Related data were tabulated in the Appendix-I section.

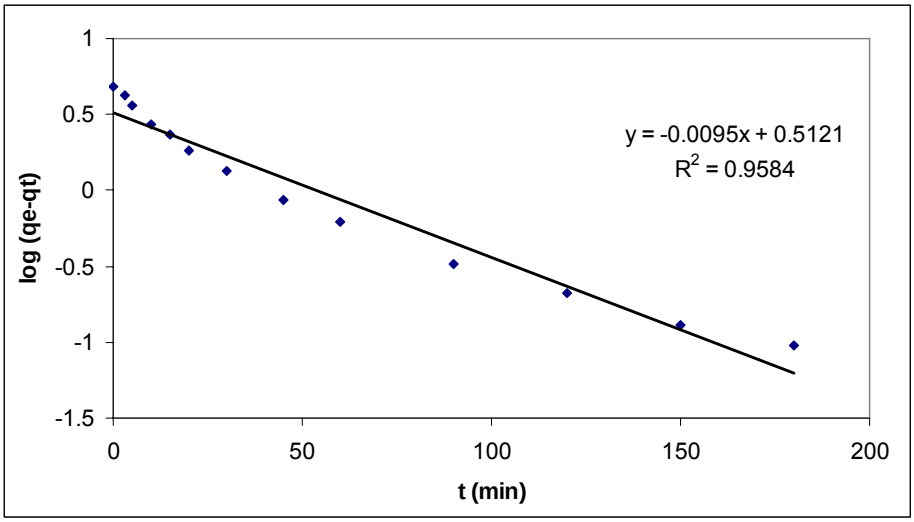


Figure 3.42 Lagergren pseudo-first-order kinetics for B adsorption on Diaion CRB 02 (0.355-0.500 mm) in NaCl + H_3BO_3 solution.

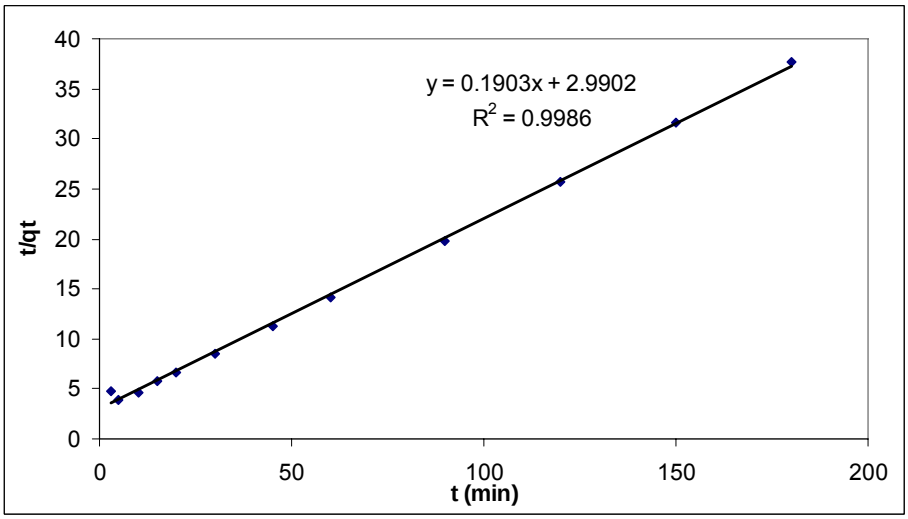


Figure 3.43 Ho pseudo-second-order kinetics for B adsorption on Diaion CRB 02 (0.355-0.500 mm) in NaCl + H_3BO_3 solution.

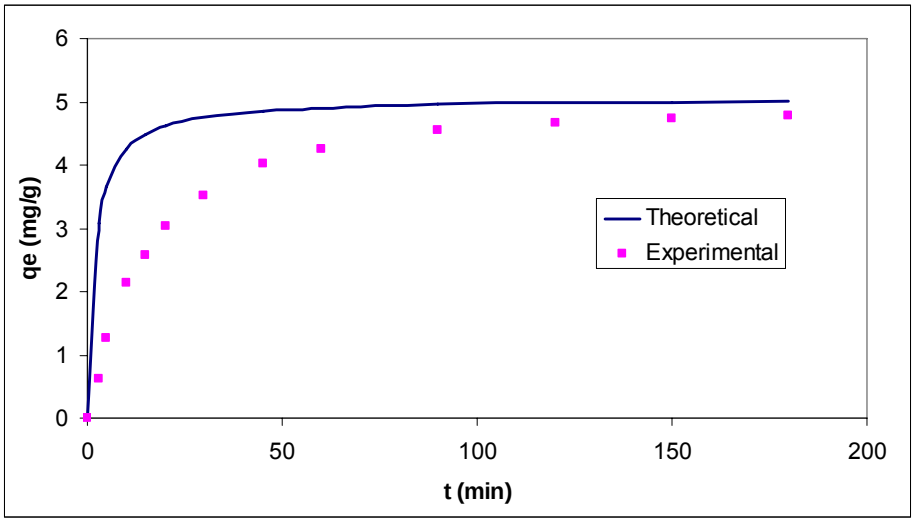


Figure 3.44 Comparison of second order kinetic models in predicting q_t for B adsorption on Diaion CRB 02 (0.355-0.500 mm) in NaCl + H_3BO_3 solution.

Sorption kinetics reaction orders for Diaion CRB 02 (0.355-0.500 mm) (r^2= 0.9986) fit to Ho pseudo-second-order mechanism. The comparison of the experimental and theoretical curves for second order kinetics showed similarity as a proof of the fitting to the Ho pseudo-second-order mechanism.

The time for Diaion CRB 02 (0.355-0.500 mm) for X=1 point was 60 min. The various functions plotted to determine the rate controlling of Diaion CRB 02 (0.355-0.500 mm) in NaCl + H_3BO_3 solution are shown Figures 3.45 and 3.46.

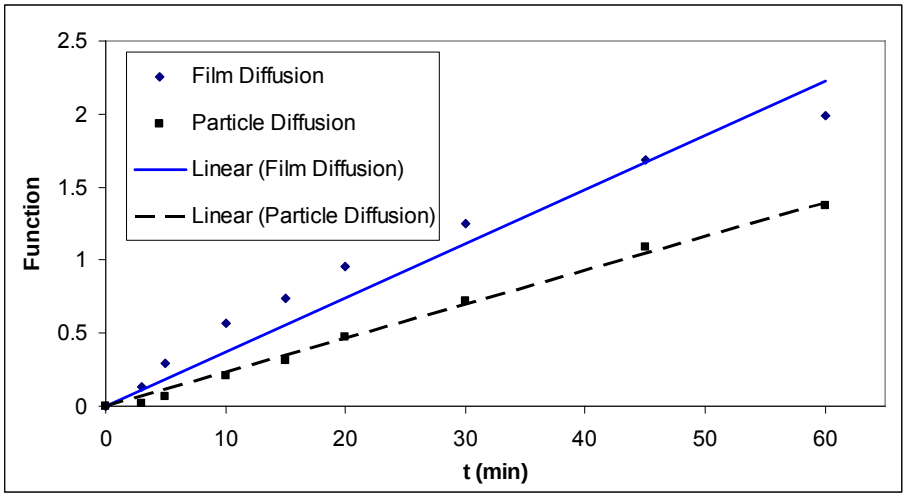


Figure 3.45 Kinetic behavior of Diaion CRB 02 (0.355-0.500 mm) in NaCl + H_3BO_3 solution based on Unreacted Core Models.

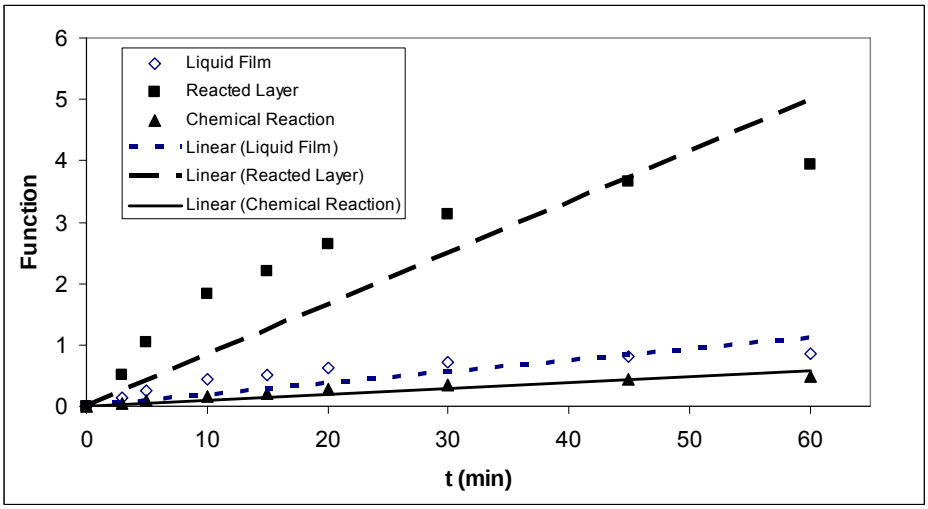


Figure 3.46 Kinetic behavior of Diaion CRB 02 (0.355-0.500 mm) in NaCl + H_3BO_3 solution based on Infinite Solution Models.

Table 3.6 gives the slope values and the linear correlation coefficients of Diaion CRB 02 in NaCl + H_3BO_3 and model seawater solution. As seen in the Table 3.6, the rate is controlled by chemical reaction for Daion CRB 02 in NaCl

+ H_3BO_3 solution for Unreacted Core Model. Particle diffusion was the rate determining step for Diaion CRB 02 resin 02 in NaCl + H_3BO_3 solution, according to Infinite Solution Volume Model.

Table 3.6 Evaluation of kinetic models for Diaion CRB 02 (0.355-0.500 mm) in NaCl + H_3BO_3 solution.

Model	**Diaion CRB 02 (0.355-0.500 mm) in model seawater**		**Diaion CRB 02 (0.355-0.500 mm) in NaCl + H_3BO_3 solution**	
	slope	r^2	*slope*	r^2
-ln (1-X)	0.0325	0.9688	0.0371	0.9467
-ln (1-X^2)	0.0194	**0.9801**	0.0232	**0.9951**
X*	0.0147	0.7733	0.0187	0.5961
3-3(1-X)$^{2/3}$-2X	0.0767	0.8227	0.0831	0.6826
1-(1-X)$^{1/3}$	0.0086	**0.9240**	0.0096	**0.8637**

3.2.2 Column mode sorption-elution studies of the resins in NaCl + H_3BO_3 solution

To compare the column performances of the resin Diaion CRB 0202 in NaCl + H_3BO_3 and model seawater solution, same conditions such as the particle size (0.355-0.500 mm), feed flow rate (SV 15 h^{-1}) and column diameter (ID 0.7 cm) were employed. Breakthrough and elution curves of Diaion CRB 02 resin are given in Figures 3.47 and 3.48, respectively. Related data were tabulated in the Appendix-I section.

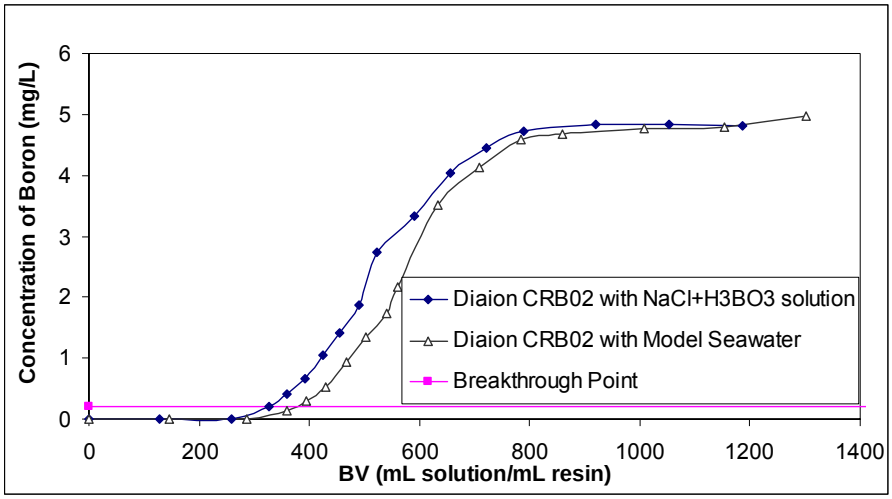


Figure 3.47 Breakthrough curves of boron selective resin (Diaion CRB02) for boron removal from NaCl + H_3BO_3 and model seawater solution.

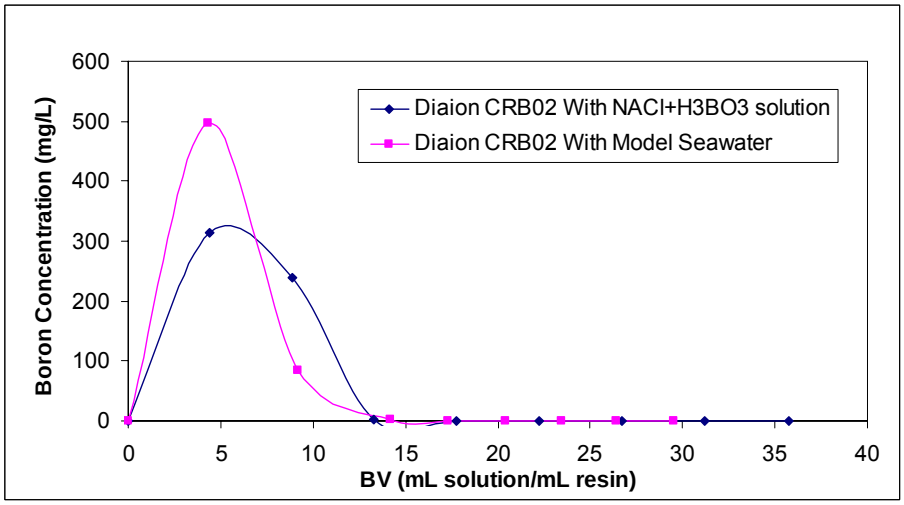


Figure 3.48 Breakthrough curves of boron selective resin (Diaion CRB02) for boron removal from NaCl + H_3BO_3 and model seawater solution.

The data obtained for Diaion CRB 02 resin in NaCl + H_3BO_3 and model seawater solution are given in Table 3.7. Column data (Figure 3.47 and Table 3.7) showed that the breakthrough capacity of the Diaion CRB 02 resin in model

seawater is relatively higher than that in NaCl + H_3BO_3 solution. Boron loaded onto the resin was eluted quantitatively from both resins using 5% H_2SO_4 solution.

Table 3.7 Column data for boron removal from model seawater solution.

Resin	SV (h^{-1})	Breakthrough Volume (BV)	Breakthrough capacity		Elution		Elution efficiency (%)
			(mg/mL)	(mg/g)	mg sorbed	mg eluted	
Diaion CRB02 in model seawater	15	374	1.86	6.10	1.496	1.286	86.0
Diaion CRB02 in NaCl + H_3BO_3 solution		326	1.57	5.15	1.277	1.235	96.7

3.3 Removal of Boron from H_3BO_3 Added Natural Seawater RO Permeate Solution

3.3.1 Effect of resin amount on removal of boron from H_3BO_3 added natural seawater RO permeate solution

Optimum resin amounts for boron removal from H_3BO_3 added natural seawater RO permeate solution were determined by using Diaion CRB02 and Dowex-XUS 43594.00 (0.355-0.500 mm) resins.

Table 3.8 and Figure 3.49 show that boron removal increases with increasing resin amounts from 0.010 g to 0.050 g/50 mL for both Diaion CRB 02 and Dowex-XUS 43594.00 (0.355-0.500 mm). But boron removal had a plateau for the resin amounts between 0.050 g to 0.070 g/50 mL for Diaion CRB 02 resin. According to these results, optimum resin amount was found as 1 g

resin/L for both Diaion CRB 02 and Dowex-XUS 43594.00 (0.355-0.500 mm) resins.

Table 3.8 Effect of Resin Amount on Removal of Boron from H_3BO_3 added natural seawater RO permeate solution by Diaion CRB 02 and Dowex-XUS 43594.00 (0.355-0.500 mm)

Resin	Resin Amount (g/50 mL)	Boron Removal (%)	Boron Removal (mg B)
Diaion CRB 02	0.01	56.77	0.042
	0.02	80.97	0.061
	0.03	90.00	0.068
	0.04	94.52	0.071
	0.05	97.42	0.073
	0.07	100.00	0.075
Dowex-XUS 43594.00	0.01	55.28	0.041
	0.02	75.78	0.057
	0.03	87.58	0.066
	0.04	90.06	0.068
	0.05	95.03	0.072

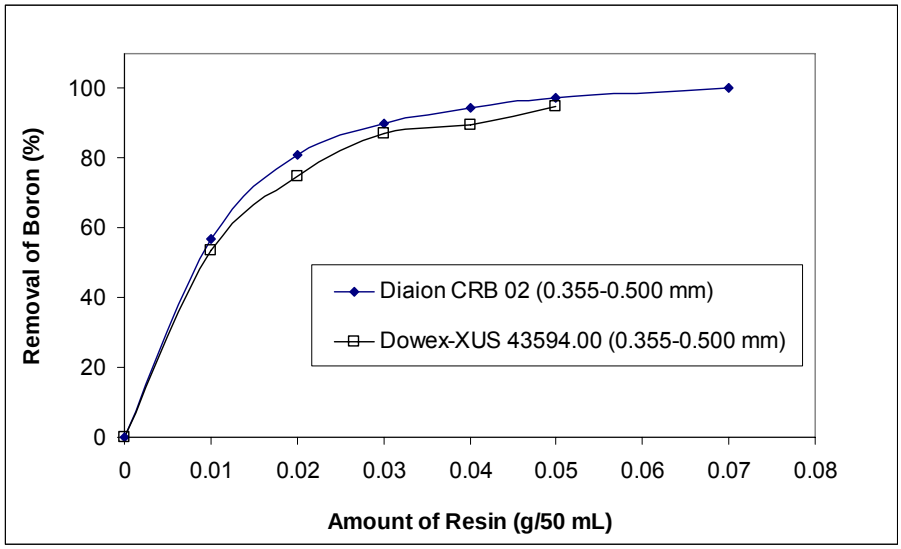


Figure 3.49 Removal of boron from H_3BO_3 added natural seawater RO permeate solution by boron selective resins (0.355-0.500 mm).

3.3.2 Sorption isotherms of removal of boron from H_3BO_3 added natural seawater RO permeate solution

Equilibrium data were obtained for B adsorption onto Diaion CRB 02 and Dowex-XUS 43594.00 resins (0.355-0.500 mm). Results were tabulated in Appendix-I section, respectively. The equilibrium relationships for Diaion CRB 02 and Dowex-XUS 43594.00 (0.355-0.500 mm) are also shown in Figures 3.50 and 3.51 respectively. The linearized fitting curves of for Diaion CRB 02 and Dowex-XUS 43594.00 (0.355-0.500 mm) are given for Langmuir isotherm in Figures 3.52 and 3.53 respectively. The linearized fitting curves of for Diaion CRB 02 and Dowex-XUS 43594.00 (0.355-0.500 mm) are given for Freundlich isotherm in Figures 3.54 and 3.55 respectively.

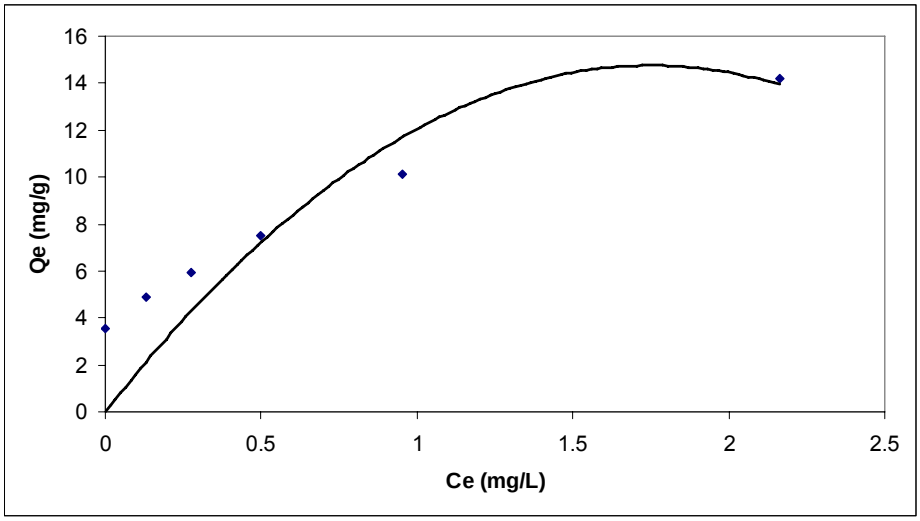


Figure 3.50 Equilibrium isotherm for loading B onto Diaion CRB 02 (0.355-0.500 mm) in H_3BO_3 added natural seawater RO permeate solution.

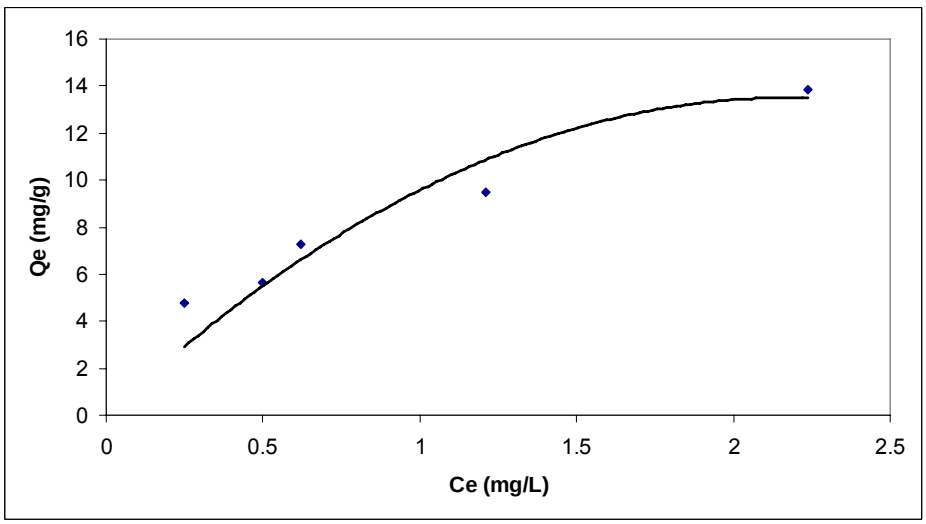


Figure 3.51 Equilibrium isotherm for loading B onto Dowex-XUS 43594.00 (0.355-0.500 mm) in H_3BO_3 added natural seawater RO permeate solution.

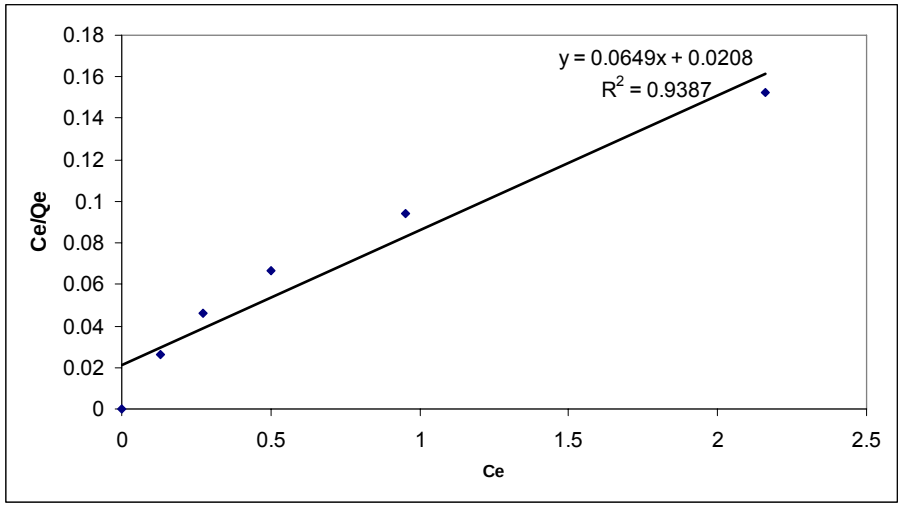


Figure 3.52 Linearized form of Langmuir isotherm for Diaion CRB 02 (0.355-0.500 mm) in H_3BO_3 added natural seawater RO permeate solution.

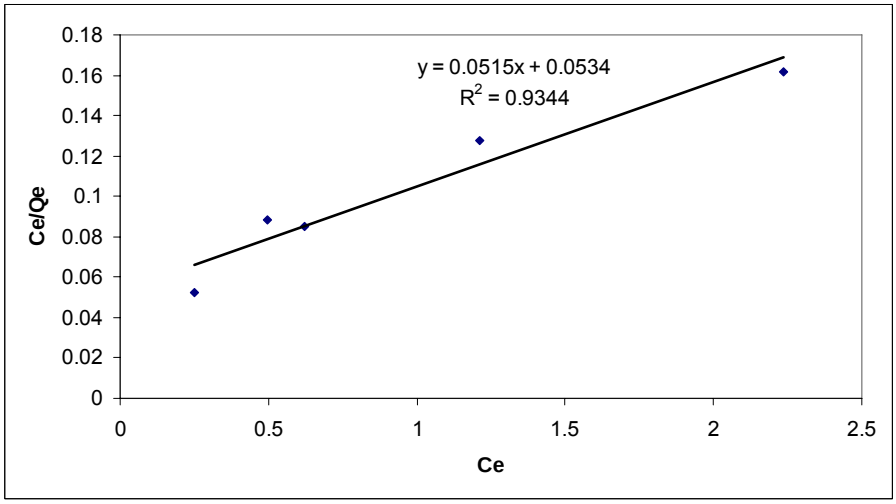


Figure 3.53 Linearized form of Langmuir isotherm for Dowex-XUS 43594.00 (0.355-0.500 mm) in H_3BO_3 added natural seawater RO permeate solution.

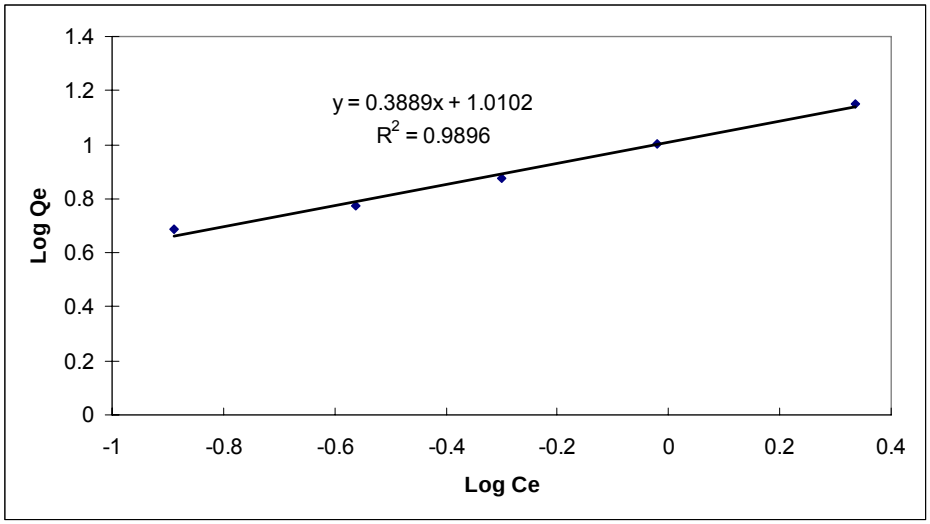


Figure 3.54 Linearized form of Freundlich isotherm for Diaion CRB 02 (0.355-0.500 mm) in H_3BO_3 added natural seawater RO permeate solution.

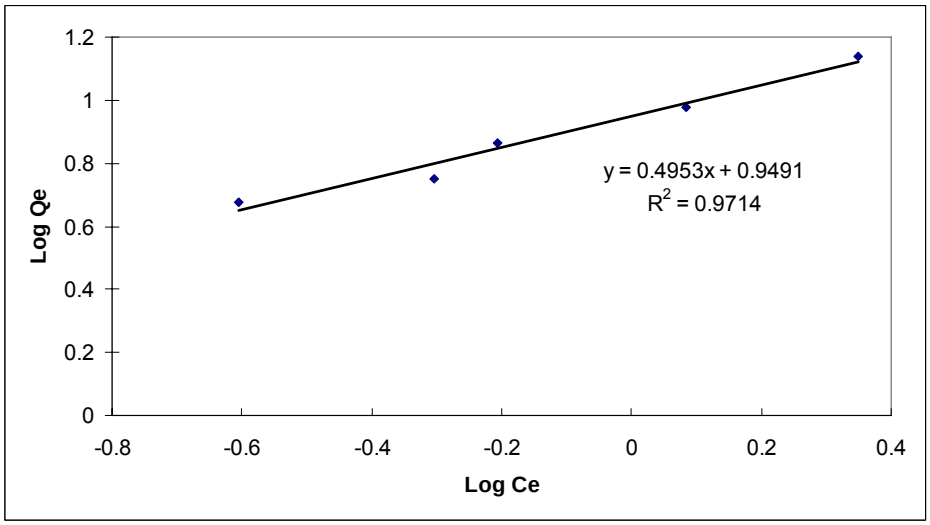


Figure 3.55 Linearized form of Freundlich isotherm for Dowex-XUS 43594.00 (0.355-0.500 mm) in H_3BO_3 added natural seawater RO permeate solution.

The correlation coefficient for the linear regression fit of Freundlich isotherm equation was found to be 0.9896 for Diaion CRB 02 (0.355-0.500

mm). The resin showed better fit for Freundlich isotherm than Langmuir isotherm. The correlation coefficient for the linear regression fit of Freundlich isotherm equation was found to be 0.9714 for Dowex-XUS 43594.00 (0.355-0.500 mm). The resin showed better fit for Freundlich isotherm than Langmuir isotherm.

3.3.3 Kinetic performance of the resins in H_3BO_3 added natural seawater RO permeate solution

Figure 3.56 shows the comparison of kinetic performances of the resins Diaion CRB 02 and Dowex-XUS 43594.00 (0.355-0.500 mm).

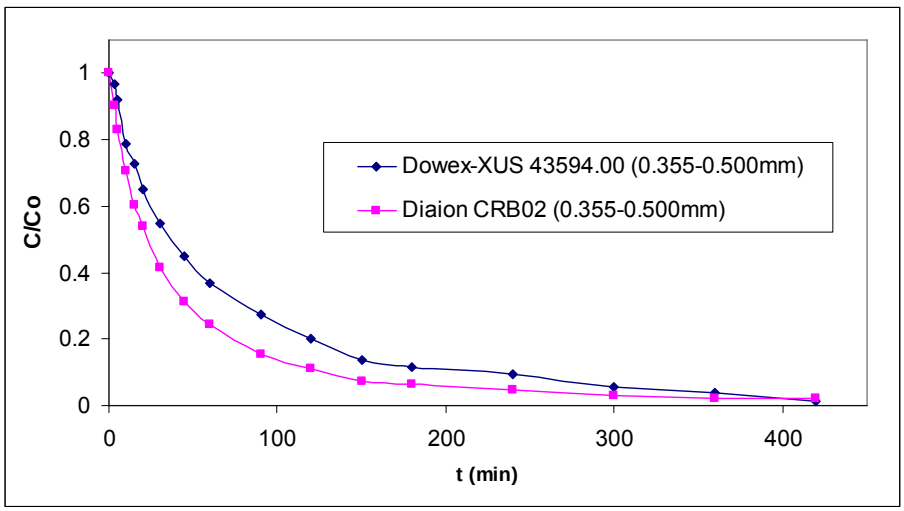


Figure 3.56 Comparison of kinetic performances of Diaion CRB 02 and Dowex-XUS 43594.00 (0.355-0.500 mm) for B removal with H_3BO_3 added natural seawater RO permeate solution**.**

The equilibrium half-time for B removal were between 30-45 minutes with Dowex-XUS 43594.00 and 20-30 minutes with Diaion CRB 02 resin

(0.355-0.500 mm). Kinetic performance of the Diaion CRB 02 resin was relatively faster than that of Dowex-XUS 43594.00 resin (0.355-0.500 mm).

The rate of removal the solute from the solution during batch mode of operation can be expressed as follows (Koltuniewics et al., 2004):

$$-\frac{dC}{dt} = \left[q^*(C_0) - q_0\right] X k e^{-kt} \tag{3.12}$$

As seen from the Eqn. 3.12 rate of removal the solute from the solution is directly proportional to initial concentration of the solute in the solution. Rate of removal the solute from the solution increases with increasing the initial concentration of the solute in the solution. Comparison of kinetic performances of the resin Diaion CRB 02 with model seawater and H_3BO_3 added natural seawater RO permeate solution is given in Figure 3.57.

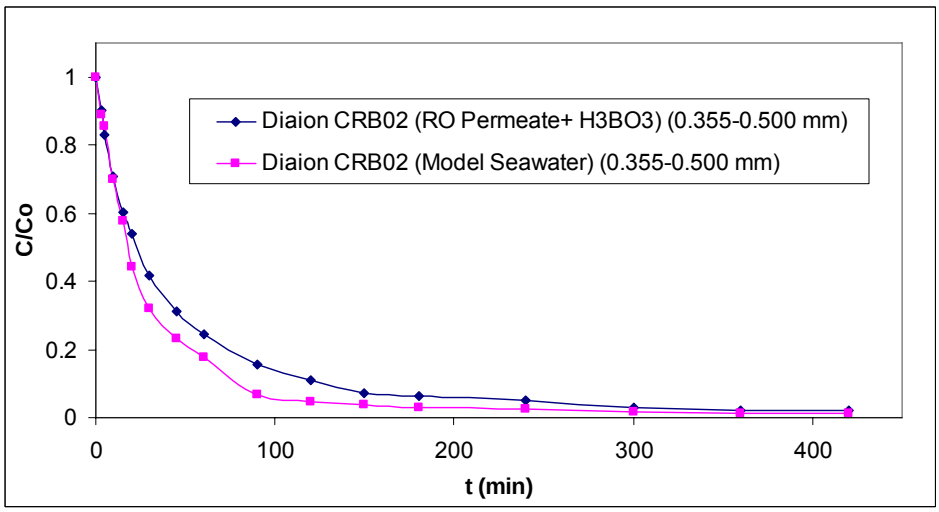


Figure 3.57 Comparison of kinetic performances of the resin Diaion CRB 02 (0.355-0.500 mm) with model seawater and H_3BO_3 added natural seawater RO permeate solution**.**

According to Eqn. 3.12, kinetic performance of the Diaion CRB 02 (0.355-0.500 mm) resin in model seawater was relatively faster than that of in H_3BO_3 added natural seawater RO permeate solution with respect to higher boron concentration in seawater (5 mgB/L) than H_3BO_3 added natural seawater RO permeate solution (1.5 mgB/L).

The optained kinetic data were fitted to sorption kinetics by means of first and second order reaction for Diaion CRB 02 and Dowex-XUS 43594.00 (0.355-0.500 mm) resins in H_3BO_3 added natural seawater RO permeate solution. . Diaion CRB 02 (0.355-0.500 mm) resin reached the equilibrium after 180 min (93.51% removal). Dowex-XUS 43594.00 (0.355-0.500 mm) resin reached the equilibrium after 240 min (90.79% removal). Figures 3.58 and 3.61 was plotted in order to observe first order reactions by plotting $\log(q_e - q_t)$ versus time and Figures 3.59 and 3.62 was plotted in order to observe second order reactions by plotting t/q versus time for Diaion CRB 02 and Dowex-XUS 43594.00 (0.355-0.500 mm) resins respectively. Predicted q_e values were also calculated from the graphs. Theoretical and experimental comparison is given in the Figures 3.60 and 3.63 for Diaion CRB 02 and Dowex-XUS 43594.00 (0.355-0.500 mm) resins respectively. Related data were tabulated in the Appendix-I section.

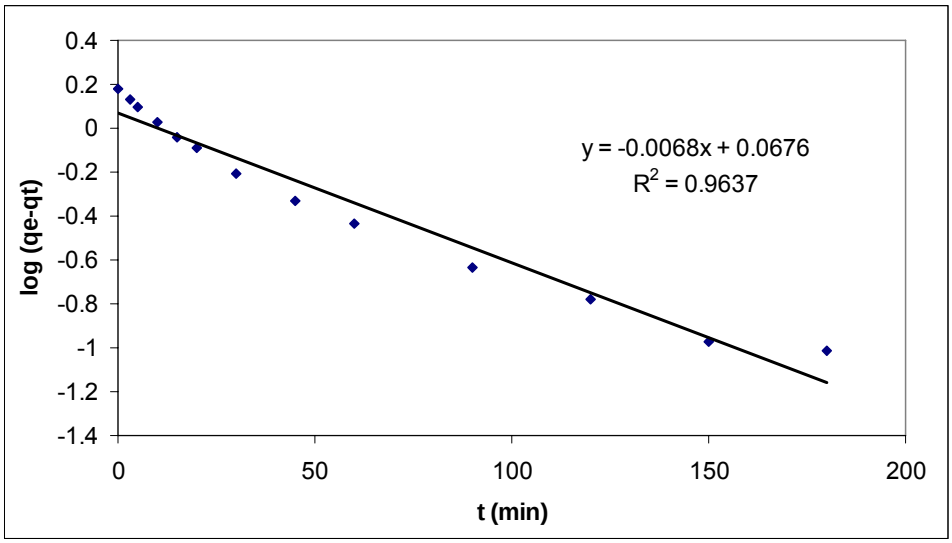


Figure 3.58 Lagergren pseudo-first-order kinetics for B adsorption on Diaion CRB 02 (0.355-0.500 mm) in H_3BO_3 added natural seawater RO permeate solution.

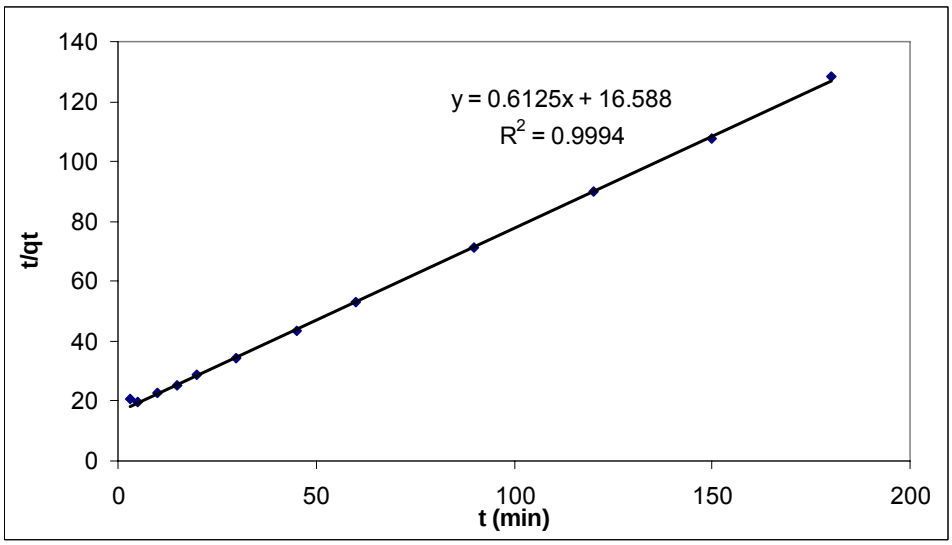


Figure 3.59 Ho pseudo-second-order kinetics for B adsorption on Diaion CRB 02 (0.355-0.500 mm) in H_3BO_3 added natural seawater RO permeate solution.

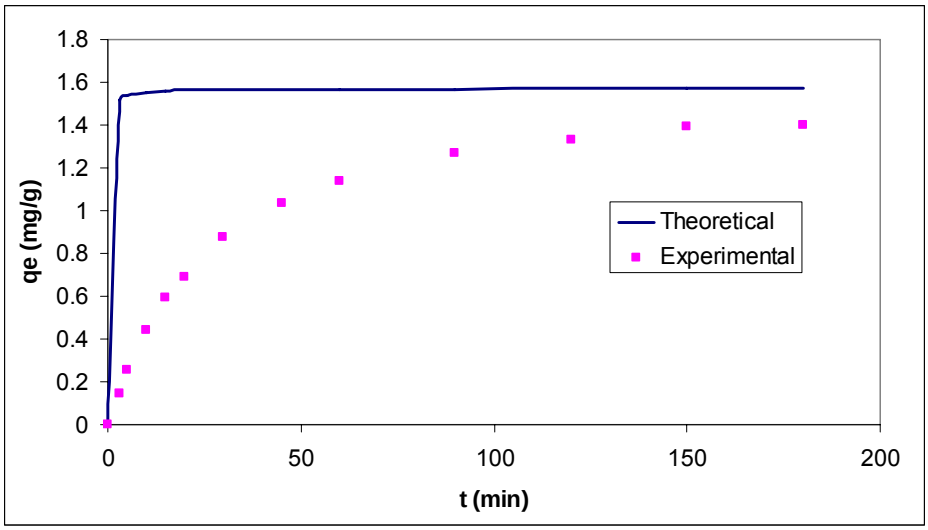


Figure 3.60 Comparison of second order kinetic models in predicting q_t for B adsorption on Diaion CRB 02 (0.355-0.500 mm) in H_3BO_3 added natural seawater RO permeate solution.

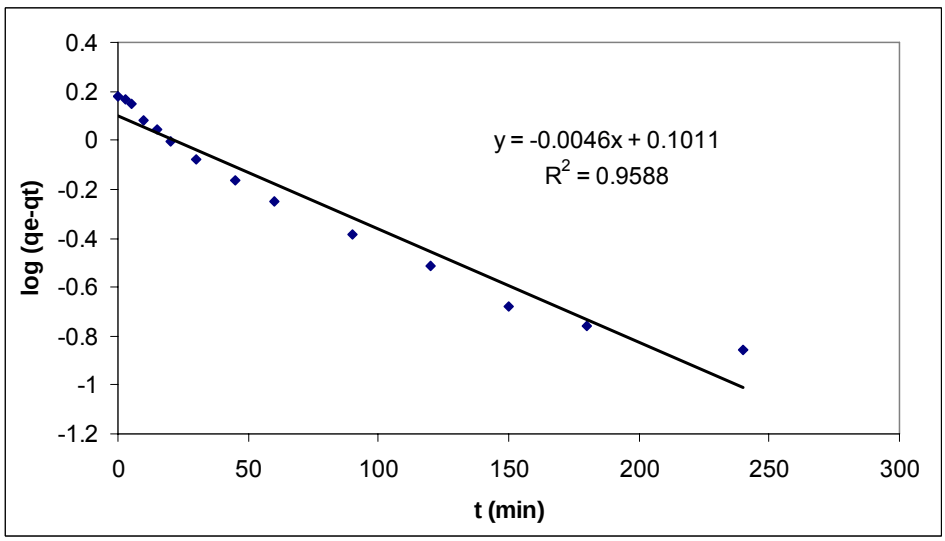


Figure 3.61 Lagergren pseudo-first-order kinetics for B adsorption on Dowex-XUS 43594.00 (0.355-0.500 mm) in H_3BO_3 added natural seawater RO permeate solution.

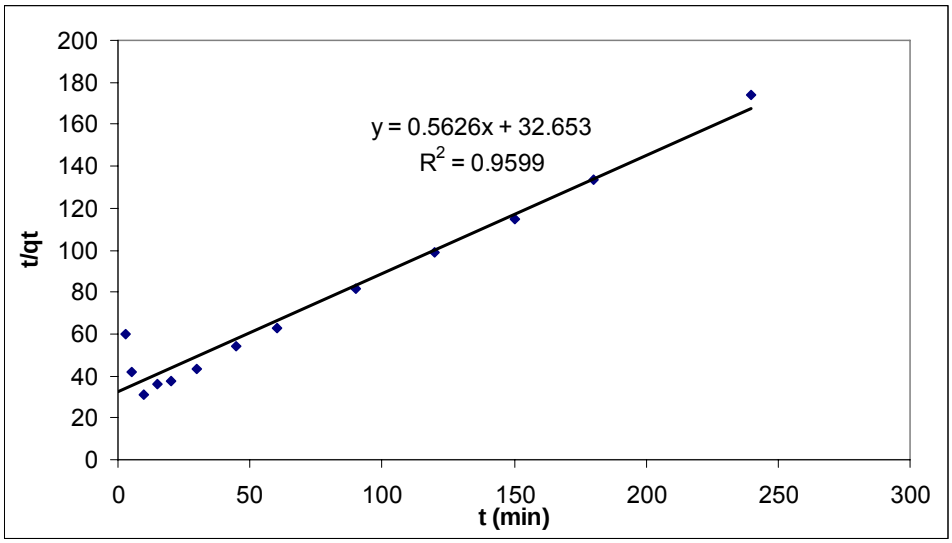


Figure 3.62 Ho pseudo-second-order kinetics for B adsorption on Dowex-XUS 43594.00 (0.355-0.500 mm) in H_3BO_3 added natural seawater RO permeate solution.

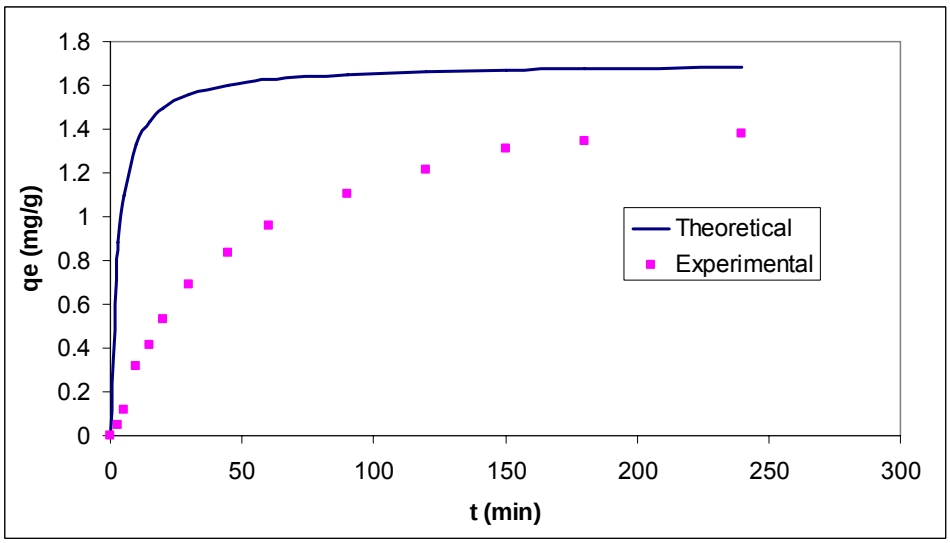


Figure 3.63 Comparison of second order kinetic models in predicting q_t for B adsorption on Dowex-XUS 43594.00 (0.355-0.500 mm) in H_3BO_3 added natural seawater RO permeate solution.

Sorption kinetics reaction orders for Diaion CRB 02 and Dowex-XUS 43594.00 (0.355-0.500 mm) (r^2 = 0.9994 for Diaion CRB 02 and r^2 = 0.9599 for Dowex-XUS 43594.00) resins in H_3BO_3 added natural seawater RO permeate solution fit to Ho pseudo-second-order mechanism. The comparison of the experimental and theoretical curves for second order kinetics showed similarity as a proof of the fitting to the Ho pseudo-second-order mechanism.

The kinetic data were also fitted to the following simplified linear models using equations given in Section 1.4.4 to evaluate the kinetic data and to find rate determining steps. The time for Diaion CRB 02 (0.355-0.500 mm) for X=1 point was 60 min. The time for Dowex-XUS 43594.00 (0.355-0.500 mm) for X=1 point was 60 min.

The various functions plotted to determine the rate controlling of Diaion CRB 02 and Dowex-XUS 43594.00 (0.355-0.500 mm) resins in H_3BO_3 added natural seawater RO permeate solution are shown Figures 3.64 – 3.67. Diaion CRB 02 and Dowex-XUS 43594.00 (0.355-0.500 mm) resins reaches equilibrium after a while, the data obtained at contact time later minutes were neglected for film diffusion model described by Unreacted Core Model.

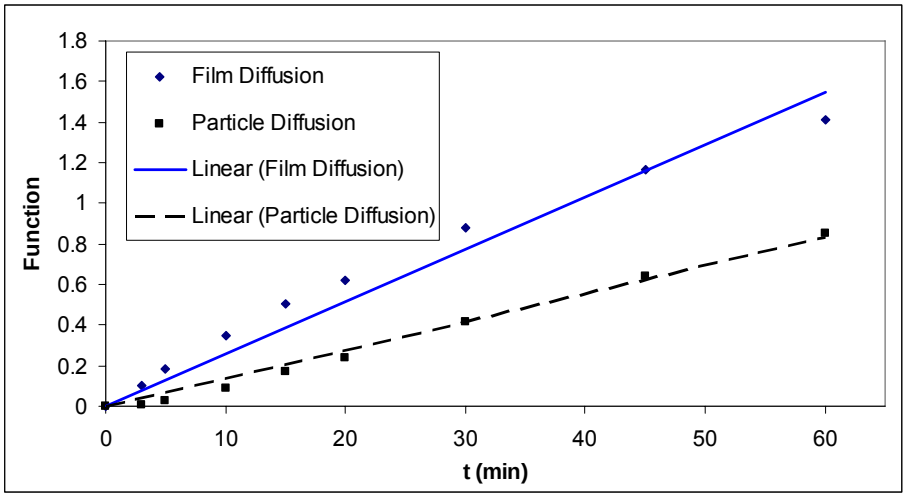


Figure 3.64 Kinetic behavior of Diaion CRB 02 (0.355-0.500 mm) in H_3BO_3 added natural seawater RO permeate solution based on Unreacted Core Models.

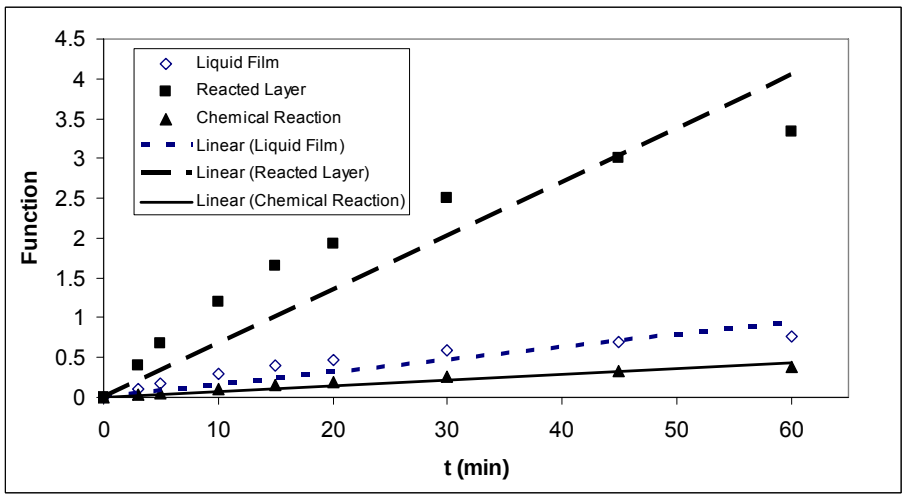


Figure 3.65 Kinetic behavior of Diaion CRB 02 (0.355-0.500 mm) in H_3BO_3 added natural seawater RO permeate solution based on Infinite Solution Models.

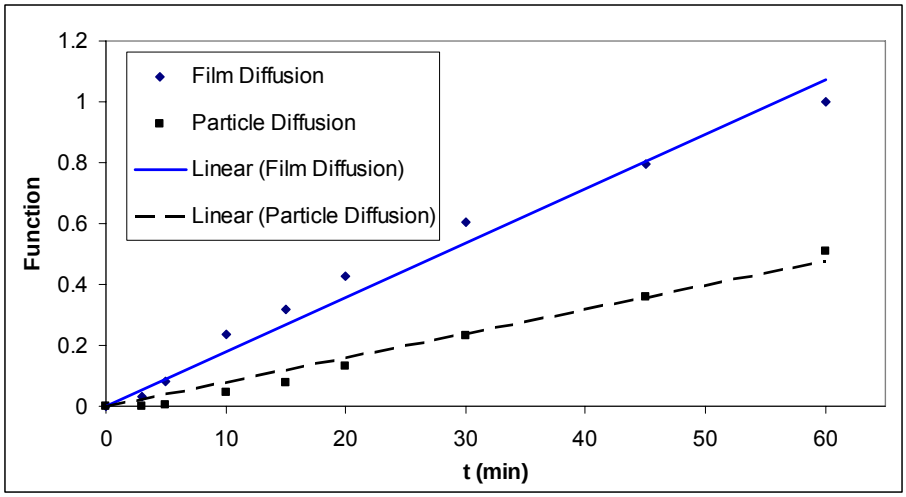


Figure 3.66 Kinetic behavior of Dowex-XUS 43594.00 (0.355-0.500 mm) in H_3BO_3 added natural seawater RO permeate solution based on Unreacted Core Models.

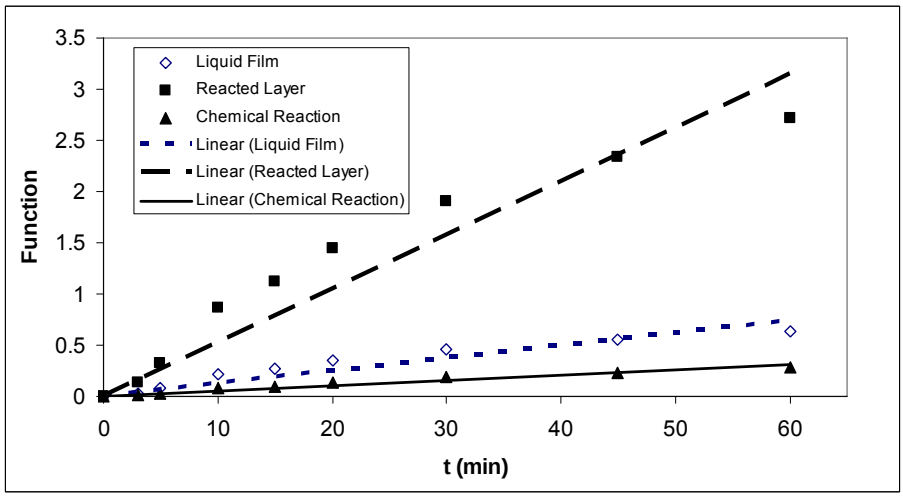


Figure 3.67 Kinetic behavior of Dowex-XUS 43594.00 (0.355-0.500 mm)) in H_3BO_3 added natural seawater RO permeate solution based on Infinite Solution Models.

Table 3.9 gives the slope values and the linear correlation coefficients. As seen in the Table 3.9, the rate is controlled by chemical reaction for both

resins for Unreacted Core Model. For Dowex-XUS 43594.00 resin (0.355-0.500 mm) film diffusion was the rate determining step according to Infinite Solution Volume Model. Particle diffusion was the rate determining step for Diaion CRB 02 resin, according to Infinite Solution Volume Model.

Table 3.9 Evaluation of kinetic models for Diaion CRB 02 and Dowex-XUS 43594.00 (0.355-0.500 mm) in H_3BO_3 added natural seawater RO permeate solution.

Model	**Diaion CRB 02 (0.355-0.500 mm)**		**Dowex-XUS 43594.00 (0.355-0.500 mm)**	
	slope	r^2	*slope*	r^2
-ln (1-X)	0.0258	0.9661	0.0179	**0.9780**
-ln (1-X^2)	0.0138	**0.9884**	0.0079	0.9751
X*	0.0155	0.7798	0.0123	0.8919
3-3(1-X)$^{2/3}$-2X	0.0673	0.8253	0.0524	0.9119
1-(1-X)$^{1/3}$	0.0072	**0.9219**	0.0052	**0.9566**

3.3.4 Column mode sorption-elution studies of the resins in H_3BO_3 added natural seawater RO permeate solution

To compare the column performances of the resins Diaion CRB 02 and Dowex-XUS 43594.00 for removal of boron from H_3BO_3 added natural seawater RO permeate solution, same conditions such as the particle size (0.355-0.500 mm), feed flow rate (SV 15 and 20 h^{-1}) and column diameter (ID 0.7 cm) were employed. Breakthrough and elution curves of Diaion CRB 02 resin are given in Figures 3.68 and 3.69, respectively. Breakthrough and elution curves of

Dowex-XUS 43594.00 resin are given in Figures 3.70 and 3.71, respectively. Related data were tabulated in the Appendix-I section.

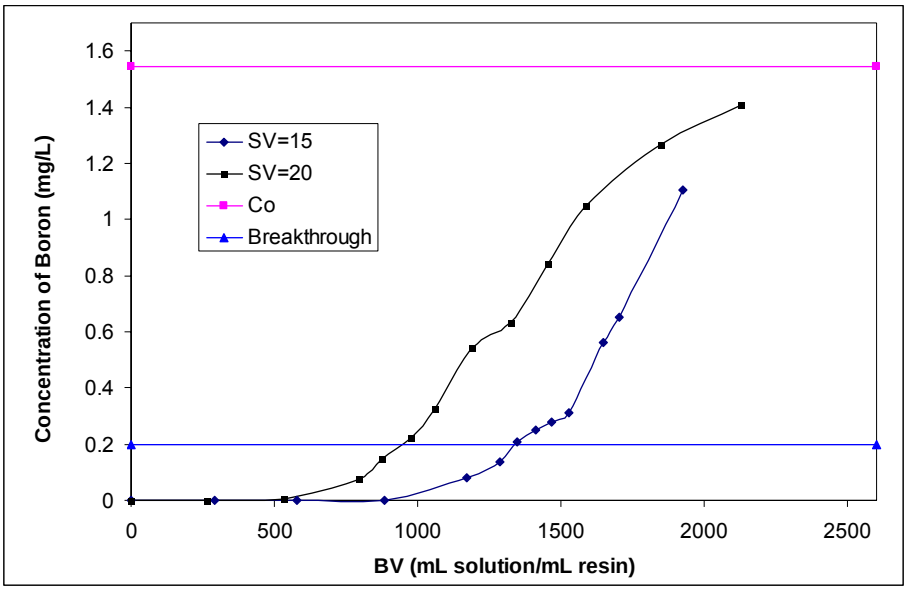


Figure 3.68 Breakthrough curves of boron selective resin (Diaion CRB02) for boron removal from H_3BO_3 added natural seawater RO permeate solution as a function of SV.

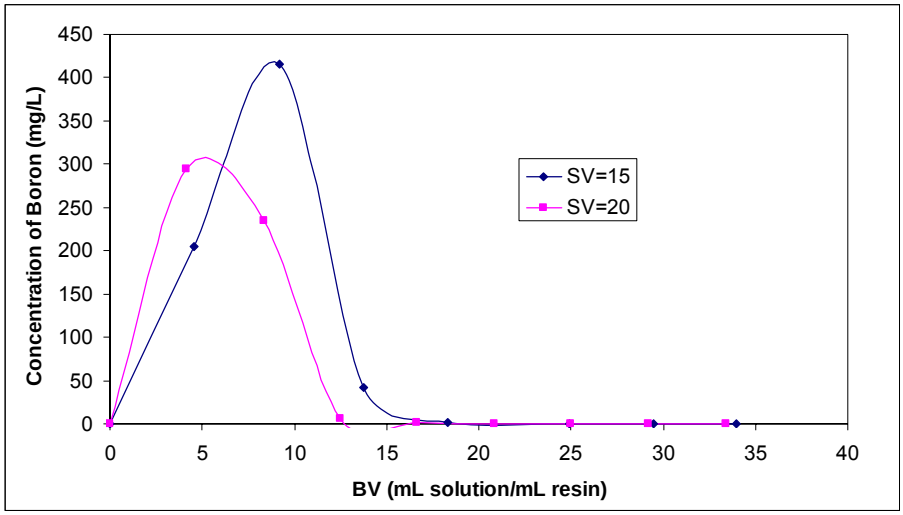


Figure 3.69 Elution curves of boron selective resin (Diaion CRB02) for boron removal from H_3BO_3 added natural seawater RO permeate solution as a function of SV.

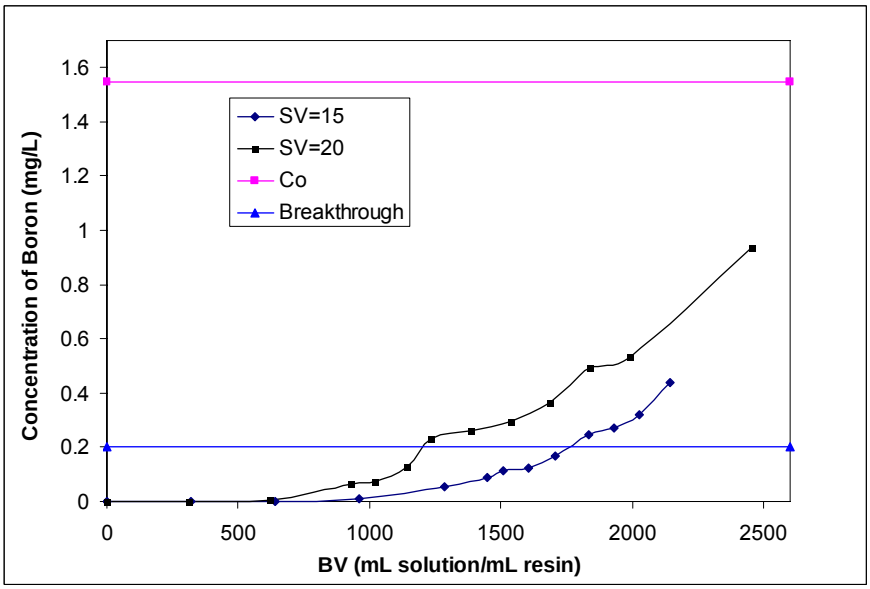


Figure 3.70 Breakthrough curves of boron selective resin (Dowex-XUS 43594.00) for boron removal from H_3BO_3 added natural seawater RO permeate solution as a function of SV.

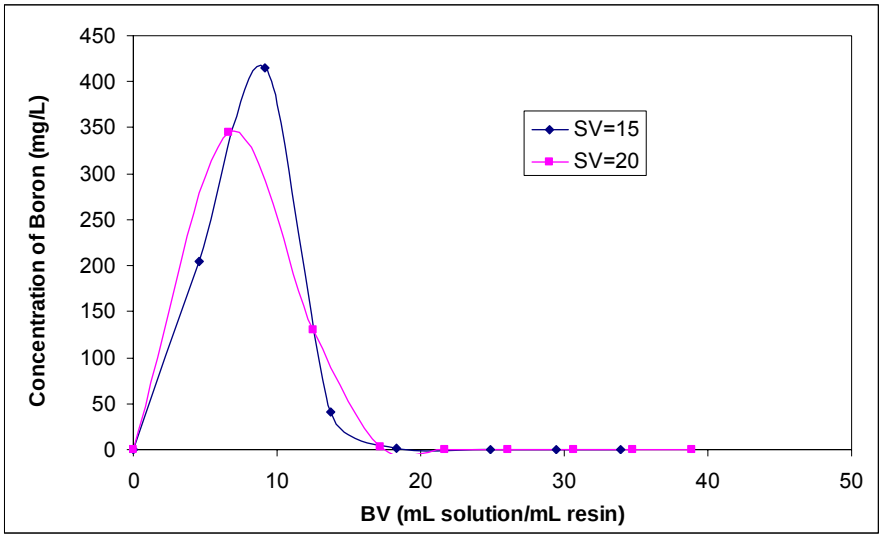


Figure 3.71 Elution curves of boron selective resin (Dowex-XUS 43594.00) for boron removal from H_3BO_3 added natural seawater RO permeate solution as a function of SV.

The data obtained for Diaion CRB 02 and Dowex-XUS 43594.00 resins are given in Table 3.10. Breakthrough capacities of both resins increased with decreasing SV. Figures 3.69 and 3.71 shows the effect of SV on breakthrough point, which were especially remarkable when SV decreased from 20 from 15 h^{-1}. As shown in Table 3.10, Dowex-XUS 43594.00 has larger breakthrough capacities than Diaion CRB 02 with respect to its volume capacity. Regarding their weight capacities, it has been seen that both resins have similar breathrough capacities. This result shows that Dowex-XUS 43594.00 resin is denser than Diaion CRB 02 resin. Boron loaded onto the resin was eluted quantitatively from both resins using 5% H_2SO_4 solution.

Table 3.10 Column data for boron removal from H_3BO_3 added natural seawater RO permeate solution.

Resin	SV (h^{-1})	Breakthrough Volume (BV)	Breakthrough capacity		Elution		Elution efficiency (%)
			(mg/mL)	(mg/g)	mg sorbed	mg eluted	
Diaion CRB02	15	1335	2.04	6.69	1.30	1.29	99.3
	20	952	1.50	4.92	1.18	1.12	94.9
Dowex-XUS 43594.00	15	1756	2.65	7.13	1.56	1.52	97.3
	20	1207	1.90	5.11	1.67	1.53	91.6

3.4 Removal of Boron by Sorption-Membrane Filtration Hybrid Method

3.4.1 Effect of resin amount on removal of boron from model solutions containing 1.5 mg B/L and 5 mg B/L

Optimum resin amounts for boron removal from 1.5 and 5 mg B/L solutions were determined by using Diaion CRB02 (45-125 μm) resin.

Table 3.11 and Figure 3.72 show that boron removal increased with increasing resin amounts from 0.005 g to 0.015 g/50 mL for 1.5 mg B/L solution with Diaion CRB 02 (45-125 μm) and 0.010 g to 0.050 g/50 mL for 5 mg B/L solution with Diaion CRB 02 (45-125 μm) But boron removal had a plateau for the resin amounts between 0.015 g to 0.025 g/50 mL in 1.5 mg B/L solution with Diaion CRB 02 (45-125 μm) and 0.050 g to 0.100 g/50 mL in 5 mg B/L solution with Diaion CRB 02 (45-125 μm). According to these results, optimum resin amounts were found as 0.3 g resin/L for 1.5 mg B/L solution and 1 g resin/L for 5 mg B/L solution with Diaion CRB 02 (45-125 μm) resin.

Table 3.11 Effect of resin amount on removal of boron from 1.5 and 5 mg B/L solutions by Diaion CRB 02 (45-125 μm).

Model Solution	Resin Amount (g/50 mL)	Boron Removal (%)	Boron Removal (mg B)
1.5 mgB/L	0.005	53.79	0.040
	0.010	86.55	0.065
	0.015	97.93	0.068
	0.020	98.97	0.074
	0.025	100.00	0.075
5 mgB/L	0.010	41.54	0.104
	0.025	85.64	0.214
	0.050	98.77	0.247
	0.075	99.79	0.249
	0.100	100.00	0.250

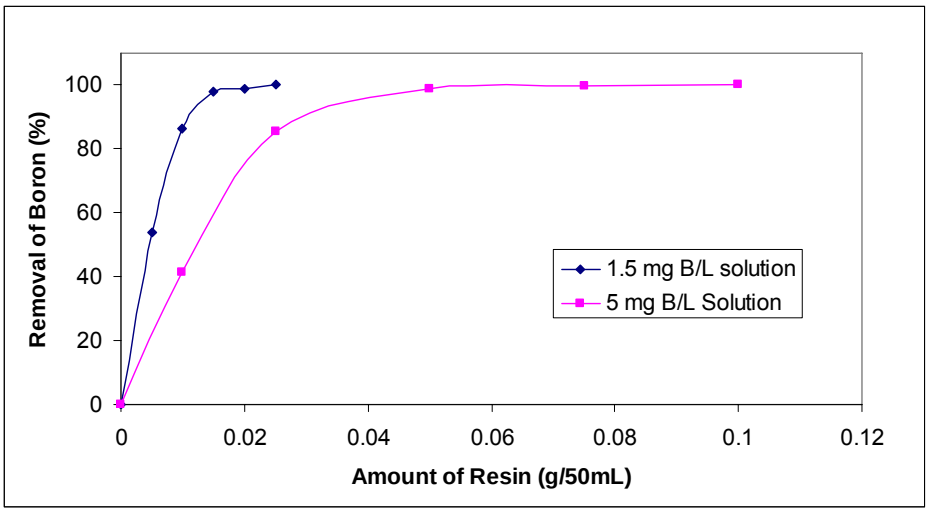


Figure 3.72 Removal of boron by Diaion CRB 02 (45-125 μm), as a function of B concentration.

3.4.2 Kinetic performance of the resins in 1.5 and 5 mg B/L solutions

Figure 3.73 shows the comparison of kinetic performances of the resin Diaion CRB 02 (45-125 µm) in 1.5 and 5 mg B/L solutions.

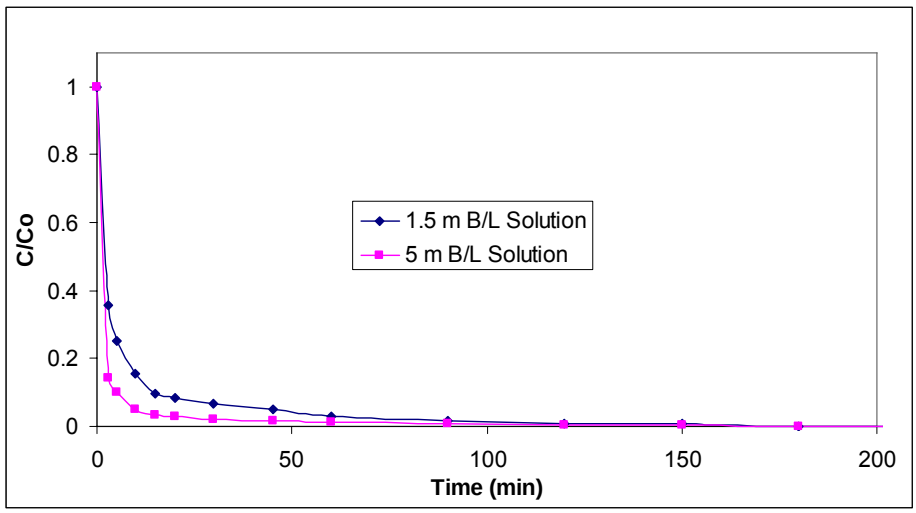


Figure 3.73 Comparison of kinetic performances of Diaion CRB 02 (45-125 µm) for B as a function of B concentration**.**

The equilibrium half-time for B removal was less than 3 minutes in 1.5 and 5 mg B/L solutions with Diaion CRB 02 resin (45-125 µm). Diaion CRB 02 (0.355-0.500 mm) resin reached the equilibrium for 1.5 mg B/L solution after 30 min (93.10% removal). Diaion CRB 02 (0.355-0.500 mm) resin reached the equilibrium for 5 mg B/L solution after 10 min (94.97% removal). According to Eqn. 3.12, Kinetic performance of the Diaion CRB 02 resin in 5 mg B/L solution was relatively faster than that of in 1.5 mg B/L solution.

3.4.3 Effect of pH on removal of boron from 5 mg B/L solution

Figure 3.74 shows the effect of pH on boron removal from 5 mg B/L solution with Diaion CRB 02 resin (0.355-0.500 mm).

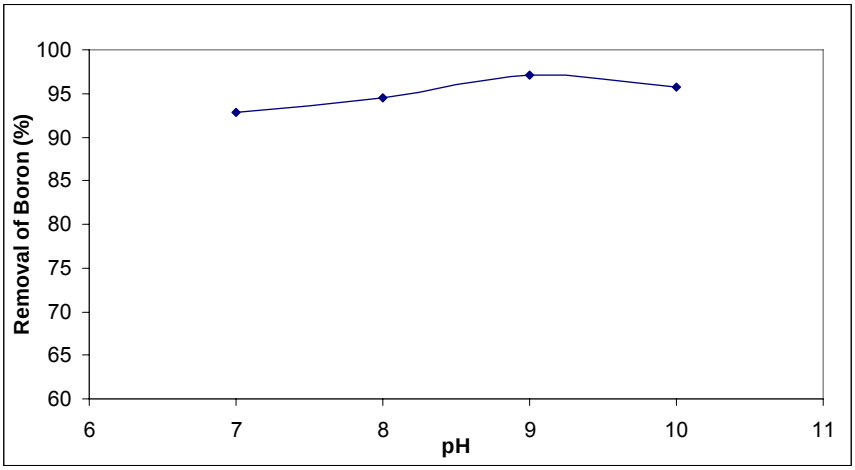


Figure 3.74 Efffect of pH on boron removal from 5 mg B/L solution with Diaion CRB 02 (0.355-0.500 mm).

As shown in Figure 3.75, pH is not very effective on boron removal by Diaon CRB 02 resin. The maximum boron removal was obtained at pH 9 with 97.1%.

3.4.4 Removal of boron by sorption-membrane filtration hybrid method using 1.5 mg B/L, 5 mg B/L and model RO permeate solutions

The main advantage of the membrane-sorption integrated system (in contrary to fixed bed) is the opportunity of using very fine particles of the sorbent, which increases a (specific surface) and result in higher uptakes and better kinetics (Koltuniewicz et al., 2004).

$$a = \frac{6}{d_p} \qquad (3.13)$$

The usage of the sorbent in form of “powder” is not possible in fixed bed adsorbers, because the pressure drop (and consequently the pumping costs of the

fluid through the sorbent), is very sensitive to particle size (d_p) according to Darcy law (Koltuniewicz et al., 2004):

$$\Delta P = u_0 \frac{\mu h}{K} \tag{3.14}$$

Where u_0 (m/s) is superficial velocity referred to the cross-section of the sorbent layer, μ (Pa.s) is velocity of the fluid, h (m) is the height of the layer and K (m^2) is the hydraulic permeability of the packed bed layer. The permeability of the layer formed with particles of various shapes is dependent on a surface area, a (m^2/m^3), the porosity, ε, and tortuosity, τ of the capillaries shaped between the sorbent particles (Koltuniewicz et al., 2004):

$$K = \frac{\varepsilon^3}{2a^2(1-\varepsilon)^2\tau} \tag{3.15}$$

According to eliminate the pressure drop and use very fine particles (Eqn. 3.13-3.15) membrane-sorption filtration hybrid process have been used.

Blank studies have been made for to evaluate the decrease of boron concentration by dilution and boron removal by the membrane system. The reason of the first peaks of the graphs in Figure 3.75 was the dilution came from the deionized water which, system was filled with before experiments. Blank curves of the permeate solutions taken from the membrane module in 1.5 mg B/L, 5 mg B/L and model RO permeate solutions are given in Figure 3.75. Boron removal rate and permeate concentration profiles with respect to time by using Diaion CRB 02 (45-125 μm) are given in Figures 3.76 and 3.77, respectively.

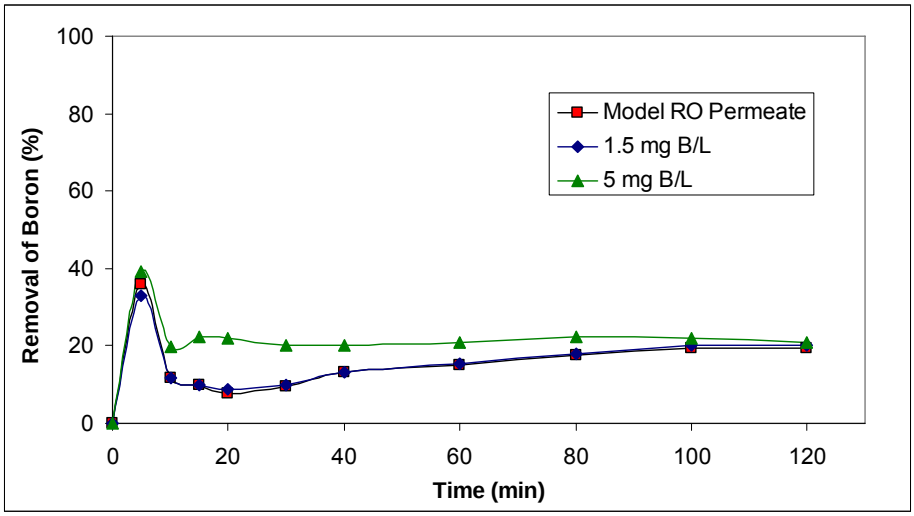


Figure 3.75 Blank curves of the permeate solutions in 1.5 mg B/L, 5 mg B/L and model RO permeate solutions**.**

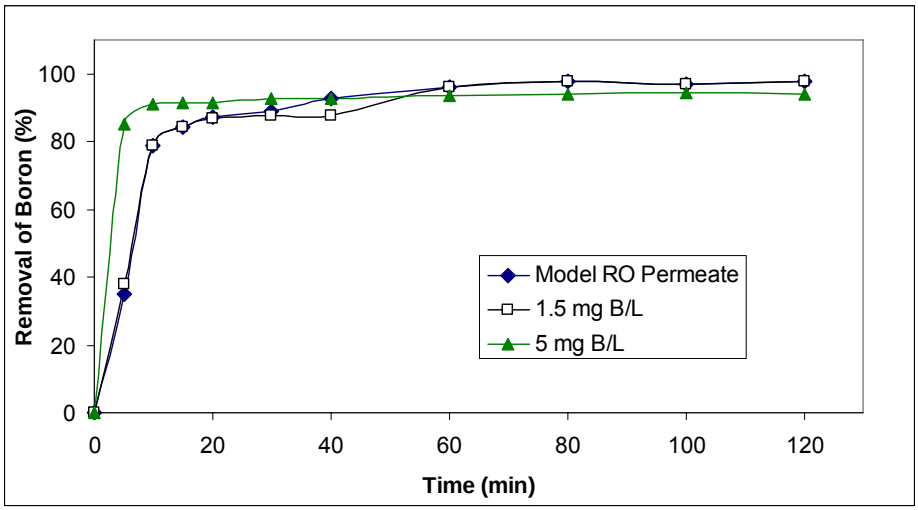


Figure 3.76 Boron removal by using sorption-membrane filtration hybrid method with Diaion CRB 02 (45-125 μm).

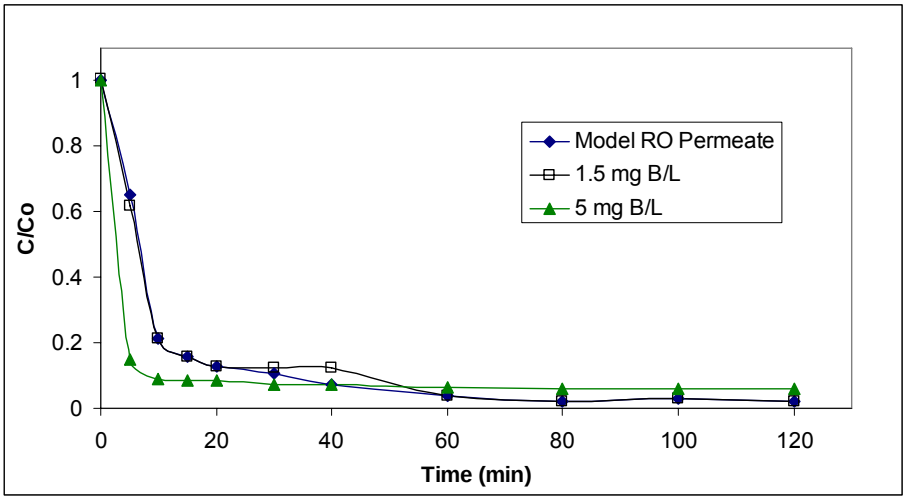


Figure 3.77 Boron removal by using sorption-membrane filtration hybrid method with Diaion CRB 02 (45-125 μm).

According to Eqn. 3.12, through the hybrid process, 5 mg B/L solution showed faster kinetic behaviour than the 1.5 mg B/L and model RO permeate solutions. The equilibrium half-time for B removal was less than 5 min. in 5 mg B/L solution in hybrid process. The equilibrium half-time for B removal was between 5 – 10 min. in 1.5 mg B/L and model RO permeate solutions. Optimum resin amounts were found as 0.3 g resin/L for model RO permeate and 1.5 mg B/L solution and 1 g resin/L for 5 mg B/L solution with Diaion CRB 02 (45-125 μm) resin. These amounts were used for hybrid processes.

Figure 3.78 shows the comparison graphs of boron removal from model RO permeate with sorption-membrane filtration hybrid (45-125 μm, Diaion CRB 02) and batch (0.355-0.500 mm, Diaion CRB 02) processes. Figure 3.79 shows the comparison of boron removal from 1.5 mg B/L solution with sorption-membrane filtration hybrid and batch (45-125 μm, Diaion CRB 02) processes.

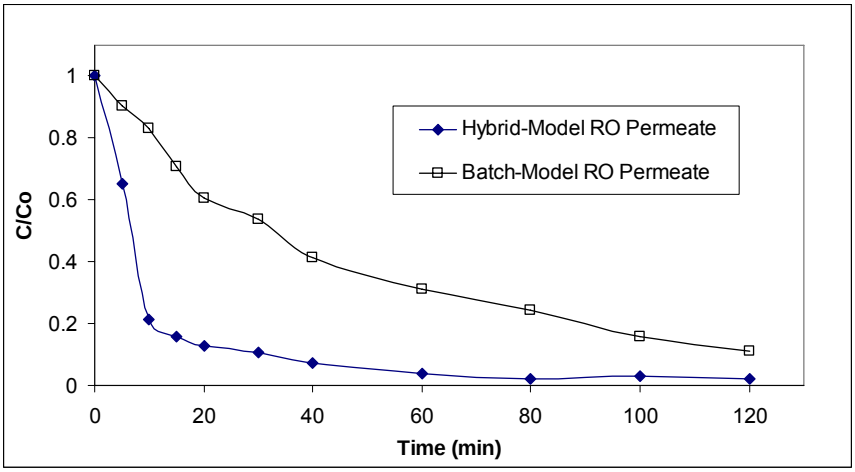


Figure 3.78 C/C_0 vs time plots obtained by using sorption-membrane filtration hybrid (45-125 μm, Diaion CRB 02) and batch (0.355-0.500 mm, Diaion CRB 02) methods.

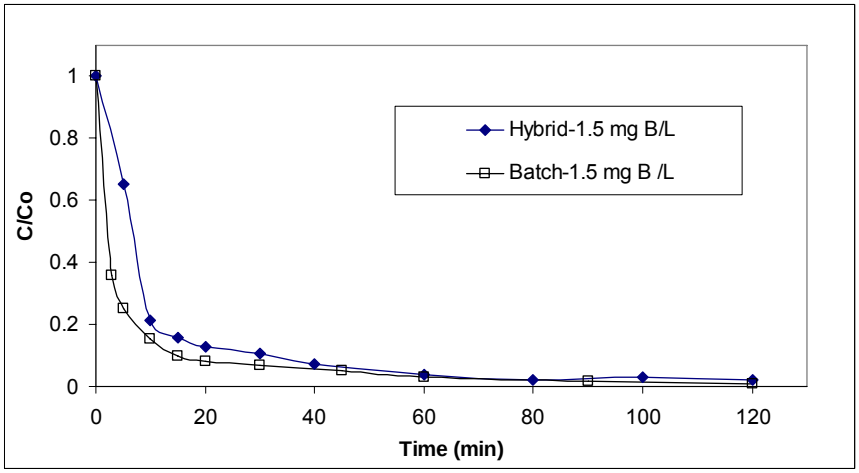


Figure 3.79 C/C_0 vs time plots obtained by using sorption-membrane filtration hybrid and batch methods with Diaion CRB 02 (45-125 μm).

As shown in Figures 3.80 and 3.81 sorption-membrane hybrid process showed faster kinetics than conventional batch process. This was most probably due to the increased kinetics of resin with smaller particle size. On the other

hand, as shown in Figure 3.79 the difference in kinetic performances of both process become less when resin with particle size of 45-125 μm is used in both processes. Due to the increasing pressure drop, the resin with a particle size of 45-125 μm cannot be used in a continuous ion exchange process. On the other hand, fast kinetics and high capacity could be obtained with a sorption-membrane filtration hybrid process using the resin with a particle size of 45-125 μm easily.

4. CONCLUSIONS

Requirement for fresh water increases worldwide, there is a need for more and more plants that are able to treat non-conventional water sources. Seawater has become an important source of fresh water in many arid regions. According to drinking water regulations and health effect of the boron against human and plants, removal of boron from seawater has become key subject for researchers.

In this study, removal of boron from seawater was investigated by using ion exchange and membrane processes. Four different solutions were used in this study, these are:

1. Model seawater
2. NaCl + H_3BO_3 solution
3. H_3BO_3 added natural seawater RO permeate
4. 1.5 and 5 mg B/L solutions

Two N-glucamine type chelating commercial resins (Diaion CRB 02 and Dowex-XUS 43594.00) were used for sorption studies. For sorption-membrane filtration hybrid studies polypropylene hollow fiber membranes were used.

Optimum resin amount for removal of boron from model seawater was determined using Diaion CRB 02 and Dowex-XUS 43594.00 resins with two different particle size (0.355-0.500 mm and 45-75 μm). By reducing the resin particle size, the optimum resin amounts decreased from 2 g resin/L to 1 g resin/L for both Diaion CRB 02 and Dowex-XUS 43594.00.

Better Freundlich fits are obtained for the equilibrium data than Langmuir fits for Diaion CRB 02 (0.355-0.500 mm and 45-75 μm) and Dowex-XUS 43594.00 (0.355-0.500 mm) for boron removal from model seawater. Better

Langmuir fits are obtained for the equilibrium data than Freundlich fits for Dowex-XUS 43594.00 (45-75 μm).

According to kinetic tests, the equilibrium half-times for B removal from model seawater were between 15-20 minutes with both Diaion CRB 02 and Dowex-XUS 43594.00 resin beads (0.355-0.500 mm). The corresponding values for powdered resins were less than 3 minutes for both resins. Kinetic performance of the Dowex-XUS 43594.00 resin was relatively slower than that of Diaion CRB 02 resin with resin beads (0.355-0.500 mm). After reducing the particle sizes of the resins to 45-75 μm the kinetic performance became similar to each other. Kinetic performances of the resins improved effectively by decreasing the particle size.

Sorption kinetics reaction orders for Diaion CRB 02 and Dowex-XUS 43594.00 (0.355-0.500 mm and 45-75 μm) (r^2 = 0.9896 and 0.9982 for Diaion CRB 02 and r^2 = 0.9995 and 0.9986 for Dowex-XUS 43594.00 respectively) in model seawater fit to Ho pseudo-second-order mechanism in each case. The comparison of the experimental and theoretical curves for second order kinetics showed similarity as a proof of the fitting to the Ho pseudo-second-order mechanism.

The data obtained from kinetic studies with model seawater were applied to the kinetic models known Infinite Solution Volume and Unreacted Core Models. The rate controlling of Diaion CRB 02 at 45-75 μm particle size was not determined because X=1 point was less than 10 minutes. As a result of this, the rate was controlled by chemical reaction for all resins and particle sizes for Unreacted Core Model. For Dowex-XUS 43594.00 resin (0.355-0.500 mm) film diffusion was the rate determining step according to Infinite Solution Volume Model. But after powdering the resins, rate determining step has changed to particle diffusion. Particle diffusion was the rate determining step for Diaion CRB 02 resin, according to Infinite Solution Volume Model.

Column mode sorption-elution studies for boron removal from model seawater showed that breakthrough capacities of both resins increased with decreasing the SV. The effect of SV on breakthrough point was especially remarkable when especially SV decreased from 20 from 15 h^{-1}. Similar breakthrough capacities were obtained for both resins when SV decreased from 10 and 15 h^{-1}. Dowex-XUS 43594.00 has larger breakthrough capacities than Diaion CRB 02 with respect to volume capacity. When the conversion of the resin amout from mL wet resin to mg dry resin, it has been seen that both resins have similar breathrough capacities as weight capacity. This result shows that Dowex-XUS 43594.00 resin is denser than Diaion CRB 02 resin. Boron loaded onto the resin was eluted quantitatively from both resins using 5% H_2SO_4 solution.

According to kinetic tests, the equilibrium half-time for B removal were between 10-15 minutes with Diaion CRB 02 resin (0.355-0.500 mm) in NaCl + H_3BO_3 solution. Diaion CRB 02 resin shows similar kinetic performance in NaCl + H_3BO_3 and model seawater solution. Sorption kinetics reaction orders for Diaion CRB 02 (0.355-0.500 mm) (r^2= 0.9986) fit to Ho pseudo-second-order mechanism. The rate is controlled by chemical reaction for Diaion CRB 02 in NaCl + H_3BO_3 solution for Unreacted Core Model. Particle diffusion was the rate determining step for Diaion CRB 02 resin in NaCl + H_3BO_3 solution, according to Infinite Solution Volume Model.

Column data showed that the breakthrough capacity of the Diaion CRB 02 resin in model seawater is relatively higher than that in NaCl + H_3BO_3 solution.

Optimum resin amounts for boron removal from H_3BO_3 added natural seawater RO permeate solution were determined by using Diaion CRB02 and Dowex-XUS 43594.00 (0.355-0.500 mm) resins. Optimum resin amount was found as 1 g resin/L for both Diaion CRB 02 and Dowex-XUS 43594.00 (0.355-0.500 mm) resins.

The correlation coefficient for the linear regression fit of Freundlich isotherm equation was found to be 0.9896 for Diaion CRB 02 (0.355-0.500 mm) in H_3BO_3 added natural seawater RO permeate solution. The resin showed better fit for Freundlich isotherm than Langmuir isotherm. The correlation coefficient for the linear regression fit of Freundlich isotherm equation was found to be 0.9714 for Dowex-XUS 43594.00 (0.355-0.500 mm). The resin showed better fit for Freundlich isotherm than Langmuir isotherm.

According to kinetic tests, the equilibrium half-times for B removal in H_3BO_3 added natural seawater RO permeate solution were between 30-45 minutes. with Dowex-XUS 43594.00 and 20-30 minutes. with Diaion CRB 02 resin (0.355-0.500 mm). Kinetic performance of the Diaion CRB 02 resin was relatively faster than that of Dowex-XUS 43594.00 resin (0.355-0.500 mm). Kinetic performance of the Diaion CRB 02 (0.355-0.500 mm) resin in model seawater was relatively faster than that of in H_3BO_3 added natural seawater RO permeate solution with respect to higher boron concentration in seawater (5 mgB/L) than H_3BO_3 added natural seawater RO permeate solution (1.5 mgB/L).

Sorption kinetics reaction orders for Diaion CRB 02 and Dowex-XUS 43594.00 (0.355-0.500 mm) ($r^2 = 0.9994$ for Diaion CRB 02 and $r^2 = 0.9599$ for Dowex-XUS 43594.00) resins in H_3BO_3 added natural seawater RO permeate solution fit to Ho pseudo-second-order mechanism. The rate is controlled by chemical reaction for both resins for Unreacted Core Model. For Dowex-XUS 43594.00 resin (0.355-0.500 mm) film diffusion was the rate determining step according to Infinite Solution Volume Model. Particle diffusion was the rate determining step for Diaion CRB 02 resin, according to Infinite Solution Volume Model.

Column mode sorption-elution studies for boron removal from model seawater showed that the breakthrough capacities of both resins in H_3BO_3 added natural seawater RO permeate solution, increased with decreasing SV. Dowex-

XUS 43594.00 has larger breakthrough capacities than Diaion CRB 02 with respect to its volume capacity.

Optimum resin amounts for boron removal from 1.5 and 5 mg B/L solutions were determined by using Diaion CRB02 (45-125 μm) resin. Optimum resin amounts were found as 0.3 g resin/L for 1.5 mg B/L solution and 1 g resin/L for 5 mg B/L solution with Diaion CRB 02 (45-125 μm) resin.

According to kinetic tests, the equilibrium half-time for B removal was less than 3 minutes. in 1.5 and 5 mg B/L solutions with Diaion CRB 02 resin (45-125 μm). Kinetic performance of the Diaion CRB 02 resin in 5 mg B/L solution was relatively faster than that of in 1.5 mg B/L solution.

Effect of pH on boron removal from 5 mg B/L solution was studied with Diaion CRB 02 resin (0.355-0.500 mm). It has been found that; pH is not very effective on boron removal by Diaon CRB 02 resin. The optimum boron removal was obtained at pH 9 with 97.1%.

According to sorption-membrane filtration hybrid process, 5 mg B/L solution showed faster kinetic behaviour than the 1.5 mg B/L and model RO permeate solutions. The equilibrium half-time for B removal was less than 5 min. in 5 mg B/L solution in hybrid process. The equilibrium half-time for B removal was between 5 – 10 min. in 1.5 mg B/L and model RO permeate solutions. Because of the high pressure drop in conventional continuous sytems, usage of small particle size such as 45-125 μm is not possible. With using sorption-membrane filtration hybrid process, continuous and efficient removal of boron was achieved.

APPENDIX-I

Batch-mode Studies:

Table A.1 Results of equilibrium studies for Diaion CRB 02 (0.355-0.500 mm) with model seawater.

Resin amount (g)	Removal of boron (%)	Q_e (mg / g-resin)	C_e/Q_e	log Q_e	log C_e
0.0125	40.24	8.048	0.371	0.906	0.475
0.0250	65.96	6.596	0.258	0.819	0.231
0.0500	85.12	4.256	0.175	0.629	-0.128
0.0750	90.00	3.000	0.167	0.477	-0.301
0.1000	94.88	2.372	0.108	0.375	-0.592
0.1250	97.87	1.957	0.054	0.292	-0.973

Table A.2 Results of equilibrium studies for Dowex-XUS 43594.00 (0.355-0.500 mm) with model seawater.

Resin amount (g)	Removal of boron (%)	Q_e (mg / g-resin)	C_e/Q_e	log Q_e	log C_e
0.0125	39.36	7.872	0.385	0.896	0.482
0.0250	65.85	6.585	0.259	0.819	0.232
0.0500	78.04	3.902	0.281	0.591	0.041
0.0750	89.14	2.971	0.183	0.473	-0.265
0.1000	93.29	2.332	0.144	0.368	-0.474
0.1250	95.85	1.917	0.108	0.283	-0.683

Table A.3 Results of equilibrium studies for Diaion CRB 02 (45-75 μm) with model seawater.

Resin amount (g)	Removal of boron (%)	Q_e (mg / g-resin)	C_e/Q_e	log Q_e	log C_e
0.0050	19.00	9.500	0.426	0.978	0.607
0.0100	34.34	8.585	0.382	0.934	0.516
0.0150	50.67	8.445	0.292	0.927	0.392
0.0250	77.00	7.700	0.149	0.886	0.061
0.0300	81.95	6.829	0.132	0.834	-0.045
0.0400	93.85	5.866	0.052	0.768	-0.512
0.0500	97.55	4.878	0.025	0.688	-0.912
0.0600	98.08	4.087	0.023	0.611	-1.018
0.0700	99.29	3.546	0.010	0.550	-1.450

Table A.4 Results of equilibrium studies for Dowex-XUS 43594.00 (45-75 μm) with model seawater.

Resin amount (g)	Removal of boron (%)	Q_e (mg / g-resin)	C_e/Q_e	log Q_e	log C_e
0.0050	24.67	12.335	0.305	1.091	0.576
0.0100	45.00	11.250	0.244	1.051	0.439
0.0150	64.67	10.778	0.164	1.033	0.247
0.0250	84.08	8.408	0.095	0.925	-0.099
0.0300	87.36	7.280	0.087	0.862	-0.199
0.0400	95.47	5.967	0.038	0.776	-0.645
0.0500	99.56	4.978	0.004	0.697	-1.658
0.0600	97.43	4.060	0.032	0.608	-0.891
0.0700	99.39	3.550	0.009	0.550	-1.516

Table A.5 Results of equilibrium studies for Diaion CRB 02 (0.355-0.500 mm) with H_3BO_3 added natural seawater RO permeate solution.

Resin amount (g)	Removal of boron (%)	Q_e (mg / g-resin)	C_e/Q_e	log Q_e	log C_e
0.010	56.77	14.194	0.152	1.152	0.335
0.020	80.97	10.121	0.094	1.005	-0.022
0.030	90.00	7.500	0.067	0.875	-0.301
0.040	94.52	5.907	0.046	0.771	-0.562
0.050	97.42	4.871	0.026	0.688	-0.889

Table A.6 Results of equilibrium studies for Dowex-XUS 43594.00 (0.355-0.500 mm) with H_3BO_3 added natural seawater RO permeate solution.

Resin amount (g)	Removal of boron (%)	Q_e (mg / g-resin)	C_e/Q_e	log Q_e	log C_e
0.0100	55.28	13.820	0.162	1.141	0.349
0.0200	75.78	9.472	0.128	0.976	0.083
0.0300	87.58	7.298	0.085	0.863	-0.207
0.0400	90.06	5.629	0.088	0.750	-0.304
0.0500	95.03	4.752	0.052	0.677	-0.605

Kinetic Studies:

Table A.7 Results of kinetic studies for for Diaion CRB 02 (0.355-0.500 mm) with model seawater.

Time (min)	q_t (mg / g-resin)	Log (q_e-q_t)	t/q_t	q_t predicted
3	0.56	0.644	5.40	3.55
5	0.72	0.627	6.93	4.07
10	1.50	0.539	6.67	4.58
15	2.11	0.455	7.11	4.78
20	2.78	0.339	7.20	4.89
30	3.39	0.196	8.85	5.00
45	3.83	0.052	11.74	5.08
60	4.11	-0.071	14.59	5.12
90	4.67	-0.532	19.29	5.16
120	4.78	-0.739	25.12	5.18
150	4.81	-0.827	31.18	5.19
180	4.86	-0.981	37.07	5.20
240	4.87	-1.056	49.26	5.21
300	4.92	-1.420	60.95	5.22
360	4.93	-1.569	72.98	5.22
420	4.94	-1.796	84.95	5.22

Table A.8 Results of kinetic studies for for Dowex-XUS 43594.00 (0.355-0.500 mm) with model seawater.

Time (min)	q_t (mg / g-resin)	Log (q_e-q_t)	t/q_t	q_t predicted
3	0.67	0.637	4.50	3.51
5	1.00	0.602	5.00	4.02
10	1.72	0.516	5.81	4.51
15	2.22	0.444	6.75	4.70
20	2.61	0.378	7.66	4.81
30	3.17	0.263	9.47	4.91
45	3.83	0.067	11.74	4.99
60	4.11	-0.051	14.59	5.03
90	4.18	-0.088	21.52	5.07
120	4.43	-0.242	27.10	5.08
150	4.56	-0.352	32.93	5.10
180	4.68	-0.491	38.48	5.10
240	4.77	-0.642	50.29	5.11
300	4.86	-0.840	61.79	5.12
360	4.88	-0.932	73.73	5.12
420	4.91	-1.051	85.52	5.13

Table A.9 Results of kinetic studies for for Diaion CRB 02 (45-75 μm) with model seawater.

Time (min)	q_t (mg / g-resin)	Log (q_e-q_t)	t/q_t	q_t predicted
3	3.84	-0.043	0.78	3.12
5	4.34	-0.388	1.15	3.68
10	4.36	-0.415	2.29	4.26
15	4.48	-0.577	3.35	4.49
20	4.59	-0.810	4.36	4.62
30	4.60	-0.839	6.52	4.75
45	4.64	-0.979	9.70	4.85
60	4.66	-1.046	12.89	4.89
90	4.69	-1.260	19.19	4.94
120	4.71	-1.398	25.50	4.97
150	4.70	-1.301	31.95	4.98
180	4.70	-1.301	38.34	4.99
240	4.72	-1.523	50.90	5.01
300	4.70	-1.347	63.83	5.01
360	4.72	-1.523	76.35	5.02
420	4.73	-1.824	88.79	5.02

Table A.10 Results of kinetic studies for for Dowex-XUS 43594.00 (45-75 μm) with model seawater.

Time (min)	q_t (mg / g-resin)	Log (q_e-q_t)	t/q_t	q_t predicted
3	3.31	0.190	0.91	3.16
5	3.80	0.025	1.32	3.71
10	4.57	-0.538	2.19	4.27
15	4.61	-0.602	3.25	4.49
20	4.64	-0.658	4.31	4.61
30	4.66	-0.699	6.44	4.74
45	4.79	-1.125	9.40	4.83
60	4.77	-1.022	12.59	4.88
90	4.79	-1.155	18.79	4.93
120	4.82	-1.347	24.92	4.95
150	4.83	-1.456	31.09	4.96
180	4.84	-1.602	37.23	4.97
240	4.83	-1.456	49.74	4.99
300	4.85	-2.000	61.86	4.99
360	4.85	-2.000	74.23	5.00
420	4.85	-1.824	86.69	5.00

Table A.11 Results of kinetic studies for for Diaion CRB 02 (0.355-0.500 mm) with $NaCl+H_3BO_3$ solution.

Time (min)	q_t (mg / g-resin)	Log (q_e-q_t)	t/q_t	q_t predicted
3	0.63	0.628	4.76	3.08
5	1.26	0.558	3.97	3.65
10	2.15	0.436	4.66	4.24
15	2.57	0.364	5.85	4.48
20	3.03	0.266	6.60	4.62
30	3.53	0.130	8.51	4.76
45	4.02	-0.066	11.21	4.85
60	4.26	-0.211	14.08	4.91
90	4.55	-0.481	19.80	4.96
120	4.67	-0.678	25.72	4.98
150	4.75	-0.886	31.61	5.00
180	4.78	-1.022	37.66	5.01
240	4.83	-1.301	49.74	5.02
300	4.85	-1.523	61.92	5.03

Table A.12 Results of kinetic studies for for Diaion CRB 02 (0.355-0.500 mm) with H_3BO_3 added natural seawater RO permeate solution.

Time (min)	q_t (mg / g-resin)	Log (q_e-q_t)	t/q_t	q_t predicted
3	0.15	0.13	20.53	1.52
5	0.25	0.10	19.75	1.54
10	0.44	0.03	22.82	1.55
15	0.59	-0.04	25.25	1.56
20	0.69	-0.09	28.92	1.56
30	0.88	-0.21	34.22	1.57
45	1.03	-0.33	43.59	1.57
60	1.13	-0.44	52.88	1.57
90	1.27	-0.63	71.07	1.57
120	1.33	-0.78	89.93	1.57
150	1.39	-0.97	107.69	1.57
180	1.40	-1.01	128.33	1.57
240	1.43	-1.14	168.19	1.57
300	1.46	-1.36	206.02	1.57
360	1.47	-1.53	244.77	1.57
420	1.47	-1.53	285.57	1.57

Table A.13 Results of kinetic studies for for Dowex-XUS 43594.00 (0.355-0.500 mm) with H_3BO_3 added natural seawater RO permeate solution.

Time (min)	q_t (mg / g-resin)	Log (q_e-q_t)	t/q_t	q_t predicted
3	0.05	0.167	60.00	0.89
5	0.12	0.146	41.67	1.10
10	0.32	0.079	31.25	1.33
15	0.42	0.043	36.14	1.44
20	0.53	-0.004	37.74	1.49
30	0.69	-0.081	43.48	1.56
45	0.84	-0.164	53.89	1.60
60	0.96	-0.252	62.50	1.62
90	1.11	-0.382	81.45	1.65
120	1.22	-0.516	98.77	1.66
150	1.31	-0.678	114.50	1.67
180	1.35	-0.757	133.83	1.67
240	1.38	-0.854	173.91	1.68
300	1.44	-1.071	209.06	1.68
360	1.46	-1.222	246.58	1.69
420	1.50	-1.699	280.00	1.69

Column Studies:

Table A.14 Results of column-mode sorption studies for Diaion CRB 02 (0.355-0.500 mm) with model seawater (SV=10 h^{-1}).

BV	C (mg B/L)	C/C_0	Sorbed Amount (mg B)
0.0	0.000	0.000	0.000
97.5	0.000	0.000	0.244
198.8	0.000	0.000	0.497
302.7	0.000	0.000	0.757
354.1	0.065	0.013	0.884
378.1	0.180	0.036	0.943
403.9	0.285	0.057	1.004
429.7	0.490	0.098	1.063
455.8	0.735	0.147	1.120
508.4	1.345	0.269	1.224
613.8	2.480	0.496	1.385
708.3	3.540	0.708	1.477

Table A.15 Results of column-mode elution studies for Diaion CRB 02 (0.355-0.500 mm) with model seawater (SV=10 h^{-1}).

BV	C(mg B/L)	Eluted Amount (mg B)
0.0	0.00	0.000
3.5	205.00	0.355
7.0	450.00	1.146
10.5	29.13	1.197
14.0	2.40	1.202
17.5	2.23	1.205
21.0	2.09	1.209
24.6	1.49	1.212
28.1	1.02	1.213

Table A.16 Results of column-mode sorption studies for Diaion CRB 02 (0.355-0.500 mm) with model seawater (SV=15 h^{-1}).

BV	C (mg B/L)	C/C_0	Sorbed Amount (mg B)
0.00	0.00	0.00	0.000
145.68	0.00	0.00	0.363
287.49	0.00	0.00	0.716
359.27	0.14	0.03	0.894
394.94	0.29	0.06	0.979
431.03	0.53	0.11	1.061
467.19	0.93	0.19	1.137
503.62	1.34	0.27	1.206
539.71	1.74	0.35	1.268
561.47	2.17	0.43	1.301
633.45	3.51	0.70	1.377
708.41	4.14	0.83	1.419
783.83	4.58	0.92	1.442
860.78	4.67	0.94	1.455
1008.65	4.77	0.96	1.475
1154.65	4.79	0.96	1.489
1300.91	4.98	1.00	1.496

Table A.17 Results of column-mode elution studies for Diaion CRB 02 (0.355-0.500 mm) with model seawater (SV=15 h^{-1}).

BV	C(mg B/L)	Eluted Amount (mg B)
0	0	0.000
4.3	497.5	1.073
9.2	85.0	1.281
14.2	2.1	1.286
17.3	0.1	1.286
20.4	0.0	1.286
23.4	0.0	1.286
26.4	0.0	1.286
29.5	0.0	1.286

Table A.18 Results of column-mode sorption studies for Diaion CRB 02 (0.355-0.500 mm) with model seawater (SV=20 h^{-1}).

BV	C (mg B/L)	C/C_0	Sorbed Amount (mg B)
0.00	0.000	0.00	0.000
124.57	0.000	0.00	0.307
206.47	0.050	0.01	0.507
238.06	0.130	0.03	0.584
301.05	0.350	0.07	0.731
332.82	0.500	0.10	0.802
376.82	0.730	0.15	0.896
459.45	1.490	0.30	1.053
503.92	1.900	0.39	1.124
585.95	2.880	0.59	1.226
629.90	3.225	0.66	1.268
756.04	4.150	0.85	1.345
883.34	4.925	1.01	1.368
1010.44	4.900	1.00	1.368
1137.57	4.900	1.00	1.370

Table A.19 Results of column-mode elution studies for Diaion CRB 02 (0.355-0.500 mm) with model seawater (SV=20 h^{-1}).

BV	C(mg B/L)	Eluted Amount (mg B)
0.0	0.0	0.000
2.4	215.0	0.261
4.9	480.0	0.849
8.4	57.0	0.949
11.9	5.0	0.958
15.4	5.0	0.966
18.9	0.2	0.967
22.4	0.1	0.967
25.9	0.0	0.967

Table A.20 Results of column-mode sorption studies for Dowex-XUS 43594.00 (0.355-0.500 mm) with model seawater (SV=10 h^{-1}).

BV	C (mg B/L)	C/C_0	Sorbed Amount (mg B)
0.0	0.00	0.00	0.000
97.5	0.00	0.00	0.244
199.6	0.00	0.00	0.499
306.8	0.00	0.00	0.767
360.6	0.00	0.00	0.901
414.1	0.01	0.00	1.035
440.9	0.06	0.01	1.102
467.9	0.11	0.02	1.168
522.6	0.27	0.05	1.299
576.9	0.49	0.10	1.424
631.1	0.58	0.12	1.545
730.0	1.17	0.23	1.749

Table A.21 Results of column-mode elution studies for Dowex-XUS 43594.00 (0.355-0.500 mm) with model seawater (SV=10 h^{-1}).

BV	C(mg B/L)	Eluted Amount (mg B)
0.0	0.00	0.000
3.9	250.00	0.484
7.8	497.00	1.458
11.7	82.50	1.619
15.6	16.63	1.652
19.5	6.50	1.665
23.4	0.01	1.665
27.4	0.00	1.665
31.3	0.00	1.665

Table A.22 Results of column-mode sorption studies for Dowex-XUS 43594.00 (0.355-0.500 mm) with model seawater (SV=15 h^{-1}).

BV	C (mg B/L)	C/C_0	Sorbed Amount (mg B)
0.0	0.00	0.00	0.000
328.4	0.05	0.01	0.800
361.0	0.09	0.02	0.879
393.7	0.13	0.03	0.956
426.6	0.20	0.04	1.034
459.5	0.28	0.06	1.110
492.5	0.39	0.08	1.185
525.3	0.49	0.10	1.257
589.6	0.77	0.16	1.393
654.1	0.90	0.18	1.524
717.5	1.26	0.26	1.644
783.0	1.66	0.34	1.755
915.9	2.56	0.53	1.937
1040.7	3.31	0.68	2.058
1307.9	4.08	0.84	2.233

Table A.23 Results of column-mode elution studies for Dowex-XUS 43594.00 (0.355-0.500 mm) with model seawater (SV=15 h^{-1}).

BV	C(mg B/L)	Eluted Amount (mg B)
0.0	0.0	0.000
4.2	205.0	0.433
9.2	457.5	1.571
14.5	69.5	1.756
19.9	27.1	1.829
25.2	10.9	1.858
30.6	2.4	1.865
36.0	0.0	1.865
41.4	0.0	1.865

Table A.24 Results of column-mode sorption studies for Dowex-XUS 43594.00 (0.355-0.500 mm) with model seawater (SV=20 h^{-1}).

BV	C (mg B/L)	C/C_0	Sorbed Amount (mg B)
0.0	0.00	0.00	0.000
122.9	0.00	0.00	0.310
184.7	0.01	0.00	0.466
246.7	0.07	0.01	0.622
277.8	0.15	0.03	0.698
309.1	0.22	0.04	0.774
340.3	0.28	0.06	0.849
371.9	0.39	0.08	0.924
497.5	0.80	0.16	1.202
560.3	1.13	0.22	1.330
749.1	1.95	0.39	1.670
876.6	2.50	0.50	1.849
1005.1	3.20	0.63	1.990
1134.1	3.70	0.73	2.092

Table A.25 Results of column-mode elution studies for Dowex-XUS 43594.00 (0.355-0.500 mm) with model seawater (SV=20 h^{-1}).

BV	C(mg B/L)	Eluted Amount (mg B)
0.0	0.0	0.000
3.2	280.0	0.451
6.4	620.0	1.434
9.4	82.5	1.559
13.6	6.0	1.572
17.7	0.8	1.573
21.8	0.1	1.574
25.9	0.0	1.574
30.0	0.0	1.574

Table A.27 Results of column-mode sorption studies for Diaion CRB 02 (0.355-0.500 mm) with NaCl+H_3BO_3 solution (SV=15 h^{-1}).

BV	C (mg B/L)	C/C_0	Sorbed Amount (mg B)
0.0	0.00	0.00	0.000
129.4	0.00	0.00	0.313
260.1	0.00	0.00	0.630
326.1	0.21	0.04	0.786
359.2	0.41	0.08	0.861
392.3	0.67	0.13	0.932
425.2	1.04	0.21	0.997
455.6	1.41	0.28	1.051
491.3	1.86	0.37	1.108
524.1	2.73	0.55	1.148
589.7	3.33	0.67	1.207
655.4	4.04	0.81	1.244
721.9	4.44	0.89	1.264
788.0	4.72	0.95	1.272
920.8	4.85	0.97	1.276
1053.5	4.85	0.97	1.276
1185.3	4.81	0.97	1.277

Table A.28 Results of column-mode elution studies for Diaion CRB 02 (0.355-0.500 mm) with NaCl+H_3BO_3 solution (SV=15 h^{-1}).

BV	C(mg B/L)	Eluted Amount (mg B)
0.0	0.0	0.000
4.4	315.0	0.695
8.9	240.0	1.228
13.3	2.1	1.233
17.8	0.5	1.234
22.2	0.3	1.235
26.7	0.2	1.235
31.2	0.0	1.235
35.7	0.0	1.235

Table A.29 Results of column-mode sorption studies for Diaion CRB 02 (0.355-0.500 mm) with with H_3BO_3 added natural seawater RO permeate solution (SV=15 h^{-1}).

BV	C (mg B/L)	C/C_0	Sorbed Amount (mg B)
0.0	0.00	0.00	0.000
289.8	0.00	0.00	0.224
580.5	0.00	0.00	0.448
881.6	0.00	0.00	0.681
1171.9	0.08	0.05	0.899
1288.1	0.14	0.09	0.983
1346.4	0.21	0.14	1.023
1410.1	0.25	0.16	1.065
1468.5	0.28	0.18	1.102
1527.1	0.31	0.20	1.138
1644.7	0.56	0.36	1.203
1702.7	0.65	0.42	1.231
1925.5	1.11	0.72	1.304

Table A.30 Results of column-mode elution studies for Diaion CRB 02 (0.355-0.500 mm) with with H_3BO_3 added natural seawater RO permeate solution (SV=15 h^{-1}).

BV	C(mg B/L)	Eluted Amount (mg B)
0.0	0.0	0.000
4.9	287.5	0.706
9.1	260.0	1.255
13.4	14.5	1.286
17.6	2.5	1.291
21.9	1.1	1.293
26.1	0.6	1.295
30.4	0.0	1.295
34.7	0.0	1.295

Table A.31 Results of column-mode sorption studies for Diaion CRB 02 (0.355-0.500 mm) with with H_3BO_3 added natural seawater RO permeate solution (SV=20 h^{-1}).

BV	C (mg B/L)	C/C_0	Sorbed Amount (mg B)
0.0	0.00	0.00	0.000
265.6	0.00	0.00	0.214
530.6	0.01	0.00	0.427
794.6	0.08	0.05	0.634
872.7	0.15	0.09	0.692
978.4	0.22	0.14	0.768
1057.9	0.33	0.20	0.821
1190.2	0.55	0.34	0.898
1321.2	0.64	0.39	0.965
1452.8	0.84	0.52	1.022
1584.8	1.05	0.65	1.066
1848.2	1.27	0.79	1.125
2130.1	1.41	0.87	1.163

Table A.32 Results of column-mode elution studies for Diaion CRB 02 (0.355-0.500 mm) with with H_3BO_3 added natural seawater RO permeate solution (SV=20 h^{-1}).

BV	C(mg B/L)	Eluted Amount (mg B)
0.0	0.0	0.000
4.1	295.0	0.612
8.3	235.0	1.102
12.5	6.0	1.114
16.7	1.5	1.117
20.8	0.3	1.118
25.0	0.2	1.118
29.2	0.0	1.118
33.4	0.0	1.118

Table A.33 Results of column-mode sorption studies for Dowex-XUS 43594.00 (0.355-0.500 mm) with with H_3BO_3 added natural seawater RO permeate solution (SV=15 h^{-1}).

BV	C (mg B/L)	C/C_0	Sorbed Amount (mg B)
0.0	0.00	0.00	0.000
319.6	0.00	0.00	0.247
639.6	0.00	0.00	0.494
961.8	0.01	0.01	0.742
1284.1	0.06	0.04	0.986
1445.6	0.09	0.06	1.105
1510.1	0.12	0.07	1.151
1606.7	0.13	0.08	1.220
1704.1	0.17	0.11	1.288
1834.0	0.24	0.16	1.375
1931.2	0.27	0.17	1.437
2027.7	0.32	0.21	1.497
2143.6	0.44	0.28	1.565

Table A.34 Results of column-mode elution studies for Dowex-XUS 43594.00 (0.355-0.500 mm) with with H_3BO_3 added natural seawater RO permeate solution (SV=15 h^{-1}).

BV	C(mg B/L)	Eluted Amount (mg B)
0.0	0.0	0.000
4.6	205.0	0.469
9.2	415.0	1.424
13.7	41.5	1.518
18.3	1.3	1.521
24.9	0.5	1.523
29.5	0.1	1.523
34.0	0.0	1.523
38.6	0.0	1.523

Table A.35 Results of column-mode sorption studies for Dowex-XUS 43594.00 (0.355-0.500 mm) with with H_3BO_3 added natural seawater RO permeate solution (SV=20 h^{-1}).

BV	C (mg B/L)	C/C_0	Sorbed Amount (mg B)
0.0	0.00	0.00	0.000
311.2	0.00	0.00	0.251
620.1	0.01	0.00	0.499
929.7	0.07	0.04	0.742
1019.8	0.08	0.05	0.812
1140.7	0.13	0.08	0.903
1233.2	0.23	0.14	0.969
1385.2	0.26	0.16	1.072
1536.3	0.30	0.18	1.173
1685.9	0.37	0.23	1.269
1838.7	0.49	0.31	1.359
1991.4	0.53	0.33	1.442
2452.1	0.93	0.58	1.644

Table A.36 Results of column-mode elution studies for Dowex-XUS 43594.00 (0.355-0.500 mm) with with H_3BO_3 added natural seawater RO permeate solution (SV=20 h^{-1}).

BV	C(mg B/L)	Eluted Amount (mg B)
0.0	0.0	0.000
6.6	345.0	1.140
12.5	130.0	1.522
17.2	2.5	1.528
21.7	0.4	1.529
26.1	0.4	1.530
30.6	0.1	1.530
34.8	0.0	1.530
38.9	0.0	1.530

APPENDIX-II

In this section, the studies that have been done in Gwangju Institude of Science and Technology (GIST) in South Korea during the internship study between August – December 2005, are given.

Solute Concentration Effect on Removal of Ibuprofen and TCEP by Using UF Membranes

Sarper Sarp[1, 2)], Noeon Park [1)], Jaeweon Cho[1, 4)], Sungyun Lee[1)], Shane A. Snyder[3)] and Nalan Kabay[2)]

1) Department of Environmental Science and Engineering, Gwanju Institute of Scinence and Technology (GIST), Gwangju 500-712, Korea

2) Department of Chemical Engineering, Ege University, 35040, Bornova, Izmir, Turkey

3) Southern Nevada Water Authority, 243 Lakeshore Road, Boulder City, Nevada 89005

4) Corresponding author: e-mail: jwcho@gist.ac.kr

Abstract

The organophosphorus esters such as tris-(2-chloroethyl)-phosphate (TCEP) have been widely used as flame retardants and fire preventing agents. Ibuprofen is one of the most popular anti-inflammatory drugs. Therefore, removal efficiencies of these micropollutants which are existed in surface and ground waters were investigated by using UF membranes. At the same time the solute concentration effects of these micropollutants were also investigated. To improve the research abilities, membrane characterizations of three membranes were done before membrane selection. With respect to use same MWCO, PBTK and PLTK membranes were selected. As the name of hydrophobic interaction, membrane-micropollutant couples which have similar hydrophobicity characteristics showed relatively high removal efficiency in high concentrations.

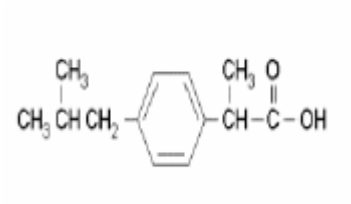
Introduction

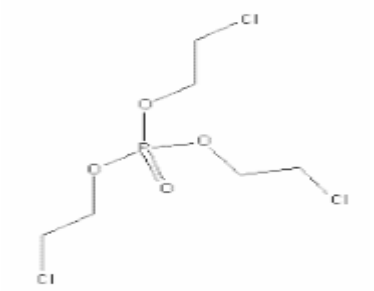
Presence of micropollutants in the aquatic environment has been become an important subject for researchers. Therefore, removal of micropollutants such as Ibuprofen and TCEP should be considered seriously.

TCEP is a colorless to pale yellow liquid, which is used as a flame retardant mainly in the production of liquid unsaturated polyester resins. It is also used in textile back-coating formulations, PVC compounds, cellulose ester compounds and coatings. It is not volatile and its solubility in water is 8 g/liter. It is soluble in most organic solvents. Its log octanol/water partition coefficient is 1.7. Even tough there are no drinking water regulations about TCEP in WHO, EU and EPA standards, the adverse effects of TCEP to rats and mice were been proved by researchers.[2, 3, 4, 7]

Ibuprofen belongs to a class of drugs called non-steroidal anti-inflammatory drugs (NSAIDs). It is relatively insoluble in water. Ibuprofen inhibits the synthesis of prostaglandins; this may be responsible for its effects. It is used in treating chronic symptomatic rheumatoid arthritis and osteoarthritis, dysmenorrhea, athletic injuries, and many other diseases and conditions. Ibuprofen can be found in wastewater treatment effluents easily as a result of it's widely usage. Removal of Ibuprofen is a promising subject for researchers, for these reasons several reports about residues of Ibuprofen and other pharmaceuticals (PhACs) in surface and drinking waters have increased in scientific publications. There are also no drinking water regulations about Ibuprofen in WHO, EU and EPA standards. Recent studies are shown that EC_{50} values of Ibuprofen from biotests with *Lemna minor* algae are in the harmful concentration range to aquatic organisms.[4. 5, 6, 8, 11]

Chemical structures and molecular weights of these chemicals are given in Figure 1. Ibuprofen is relatively hydrophobic than TCEP with respect to $LogK_{OW}$ values.





(a) (b)

Figure 1. Chemical structures of (a) Ibuprofen (MW: 206.1, $LogK_{OW}$: 3.97), (b) TCEP (MW: 285.5, $LogK_{OW}$: 1.44)

Several removal methods were applied for removal of TCEP and Ibuprofen from drinking and waste waters such as; Coagulation and Softening, Powdered Activated Carbon (PAC), Magnetic Ion-Exchange (MIEX), UV, Chlorine, Ozone, UV+Peroxide and MBR. In several studies it has been seen that the lowest removal rate was observed for TCEP. Also Ibuprofen has the lowest removal rate in comparing with the other PhACs. Some removal rates of these micropollutants are given in Table 1.[6, 9, 10, 12]

Removal of TCEP is insufficient even tough using high oxidative chemicals such as ozone and peroxide, because TCEP has an aliphatic structure and it is very hard to oxidize this compound. In the case of Ibuprofen, using high oxidative chemicals are very effective to remove this micropollutant.[9]

Main objective of this study is to observe removal efficiency of Ibuprofen and TCEP by using UF with respect to solute concentration. Some previous works has been showed that the removal efficiencies of micropollutants are decreasing in very low concentrations such as 200 ng/L[13]. In this study, it was focused on that phenomenon. The removal efficiencies of membrane systems depend on three removal mechanisms, these are; size exclusion, electrostatic repulsion and hydrophobic interaction.

Table 1. Removal rates of Ibuprofen and TCEP with respect to several removal methods.

	TCEP	**Ibuprofen**		**TCEP**	**Ibuprofen**
Coagulation & Softening	<10%	<10%	**Chlorine (3.5 mg/l 24 hr)**	<30%	30-70%
PAC (5mg/l)	~50%	<50%	**Ozone(2.5 mg/l)**	<30%	>70%
MIEX (20ml-10min)	**-**	~20%	**UV + 8 ppm Peroxide**	<30%	>80%
UV (40 mJ)	<30%	<30%	**MBR**	**-**	≤90%

Materials and Methods

Membrane Characterization:

In order to investigate the solute concentration effect on UF membrane, first two membranes were selected which have same MWCO (30000 Da). These are;

1. PBTK (Polyether-Sulphone) membrane (Millipore, USA)
2. PLTK (Regenerated Cellulose) membrane (Millipore, USA).

Molecular weights of the selected micropollutants were much less than MWCO of the membranes. The objective of these selection was to eliminate fouling effect on removal efficiency.

The membrane characterizations were done for four parameters:

1. Zeta Potential
2. Contact Angle
3. Roughness
4. Pore Size distribution

The zeta potential values of the membranes were determined from electrophoretic mobility measurements using ELS-8000 apparatus produced by Otsuka Electronics, Japan. Contact Angle values of the membranes were determined by using Sessile Drop Method and Captive Bubble Method. Roughnesses of the membranes were determined by using AFM. In the pore size distribution experiments 2 ppm PEG solution is prepared from PEG which has 35000 g/mol molecular weight. The calibration was made by different PEG solutions which concentrations were same but the molecular weights of the PEGs were different. Initial pressure and retentate flux were adjusted to 20 psi and 500 ml/min respectively. Samples were analyzed in HPLC-RI apparatus.

Membrane Filtration

Concentration range is one of the most important parameter for this study, so four concentrations were selected; 0.2, 0.5, 1 and 5 ppb. In membrane filtrations cross-flow membrane unit was used**.** Retentate flux was adjusted to 500 ml/min and all filtration tests were conducted at same permeate flux (23-25 ml/min). To eliminate the temperature effect on filtration, temperature controller was used and temperatures of the solutions were adjusted to 25^{o}C. Membrane filtrations were conducted for 2 hours and three samples were collected for initial, 1 hour and two hours time periods for both feed and permeate flux. Membrane filtration data were classified for two time intervals, these were: 0-20 min and 110-130 min.

Sample Analysis

Ibuprofen samples were analyzed with LC/MS/MS apparatus which is supported by IERC. The detection limit of the Ibuprofen was 10 ppb. TCEP samples were analyzed with GC/MS and the detection limit of the GC/MS apparatus was observed as 400 ppb.

To achieve available concentration for both LC/MS/MS and GC/MS apparatus SPE and following Nitrogen evaporation were conducted. Various volumes of samples were concentrated to 10 ml with using proper SPE cartridge. Following SPE, Nitrogen evaporation was done for each sample to obtain 1 ml solution which is the lower sampling limit of the apparatus.

Results and Discussion

Membrane Characterization

Zeta Potential

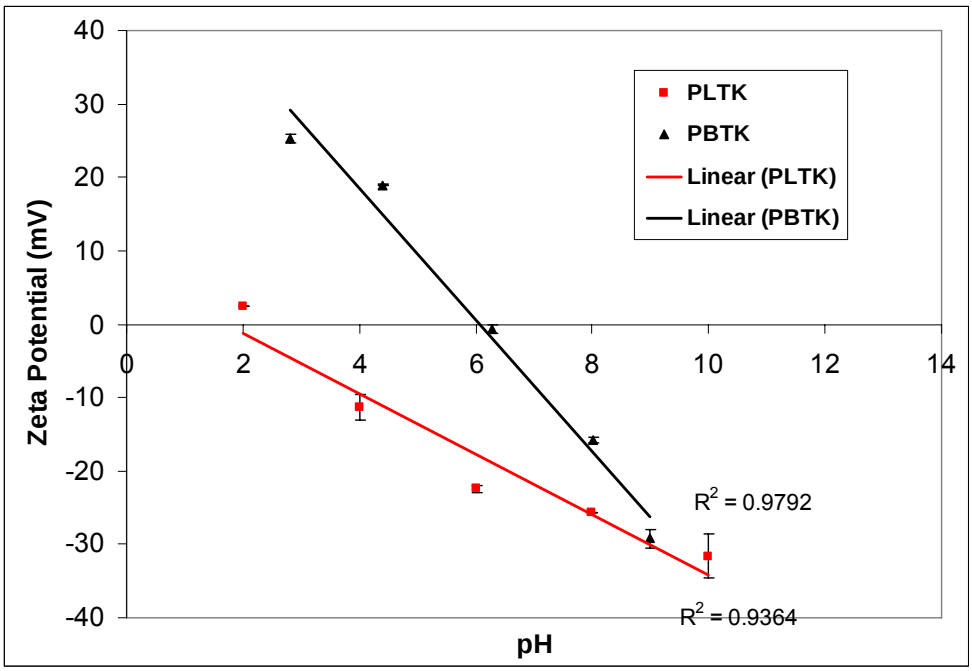


Figure 1. Zeta Potential of the selected membranes with respect to pH.

PLTK membrane has a relatively high charge in the name of neutral pH. The solutions pH values that were prepared with DI water were between pH 6-7 (Figure 1).

Contact Angle

Table 1. Contact angle of selected membranes with two different methods.

Sessile Drop Method		**Captive Bubble Method**	
PBTK	**PLTK**	**PBTK**	**PLTK**
44°	20°	40.6°	-

For contact angle tests PBTK has a more hydrophobic characteristic than PLTK. Because of the highly hydrophilic properties of PLTK Captive Bubble Method couldn't be applied to this membrane.

Roughness

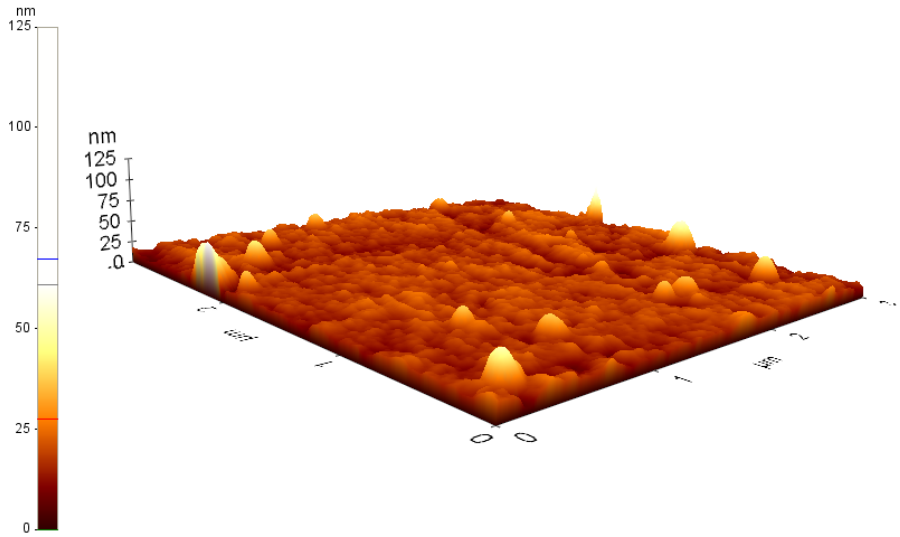


Figure 2. AFM image of the PBTK membrane (Rq=3.280 nm)

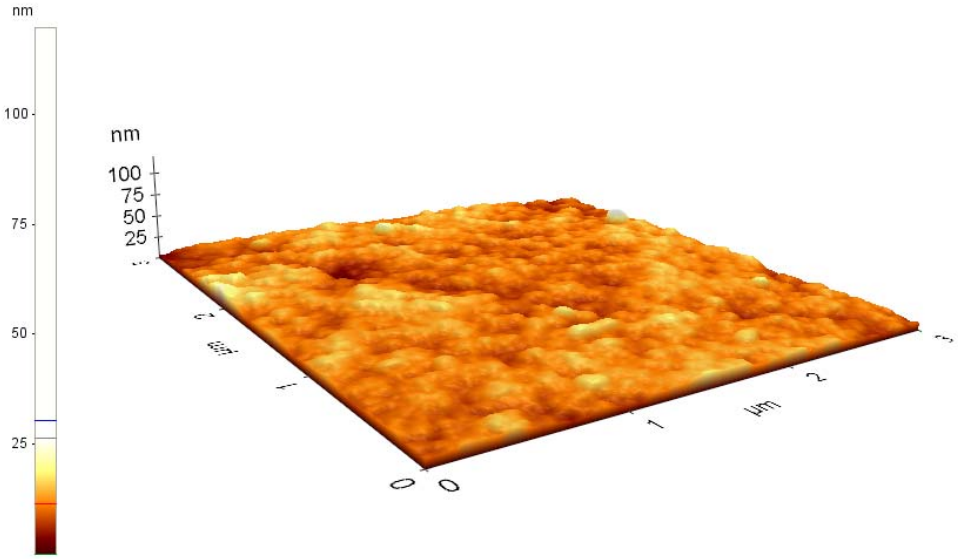


Figure 3. AFM image of the PLTK membrane (Rq=2.979 nm)

Roughness of PBTK membrane was measured as more higher than PLTK regarding to AFM and SEM measurements (Figures 2 to 5). PBTK membrane may be fouled by micropollutants, but in this study, concentrations of the solutions, filtration time and pore size distribution effects were small enough to prevent fouling.

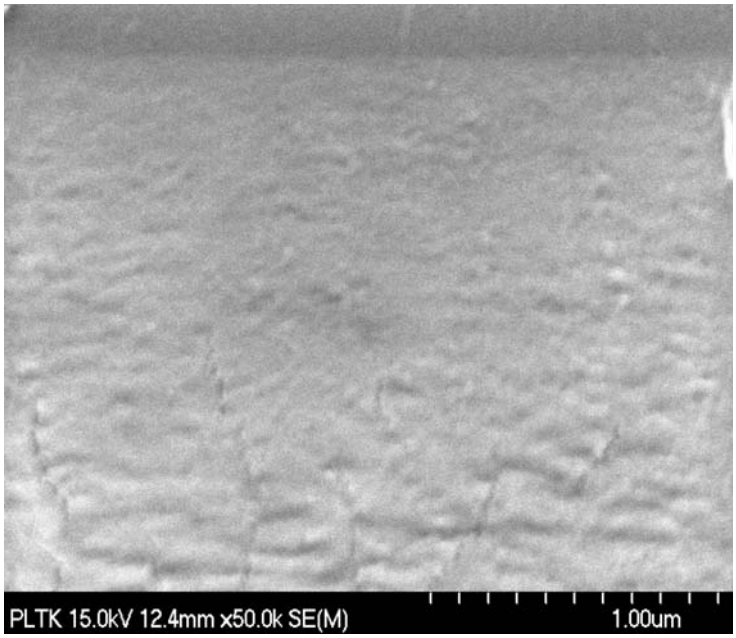


Figure 4. SEM image of the PLTK membrane

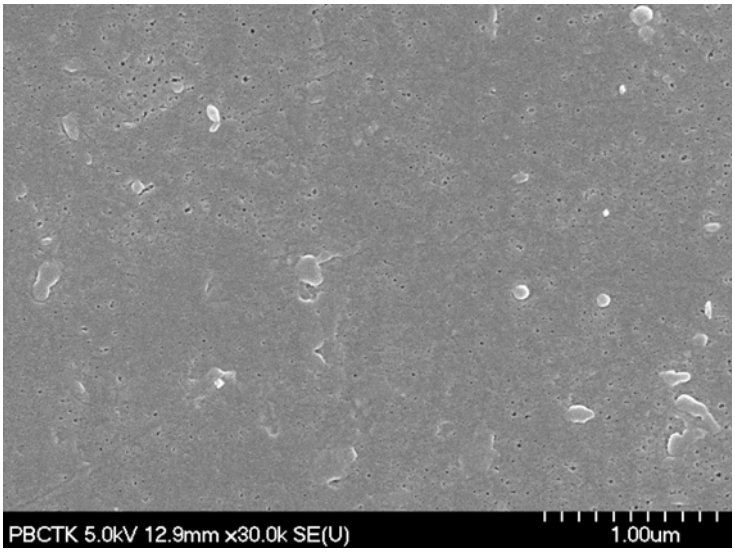


Figure 5. SEM image of the PBTK membrane

Pore Size Distribution

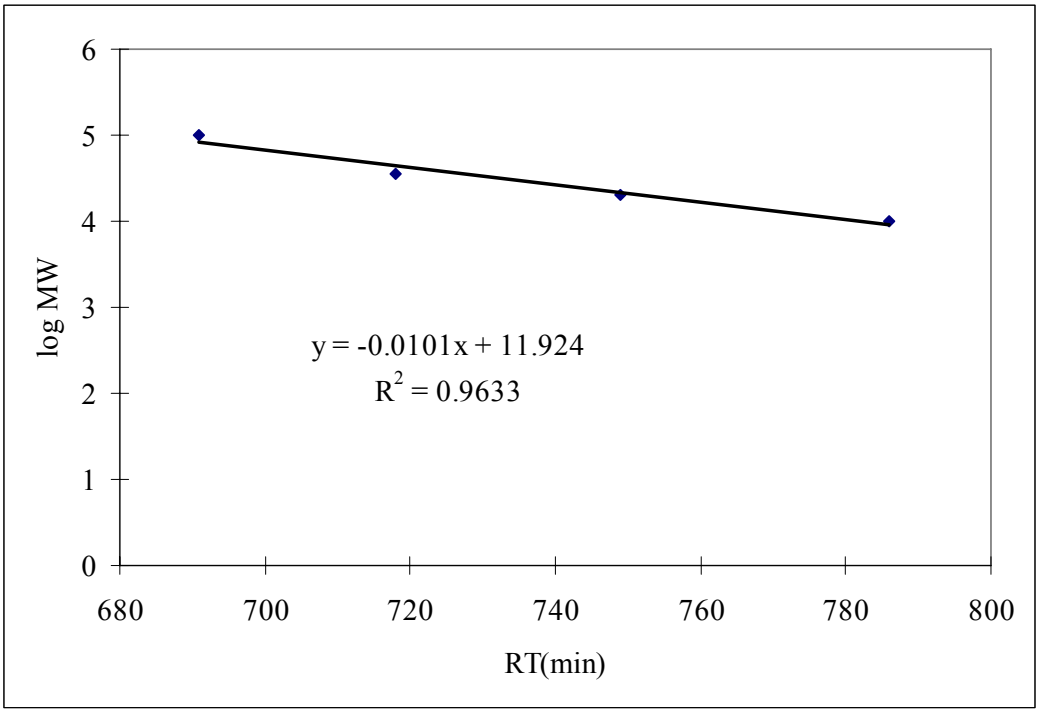


Figure 6. Calibration curve for Pore Size Distribution experiments.

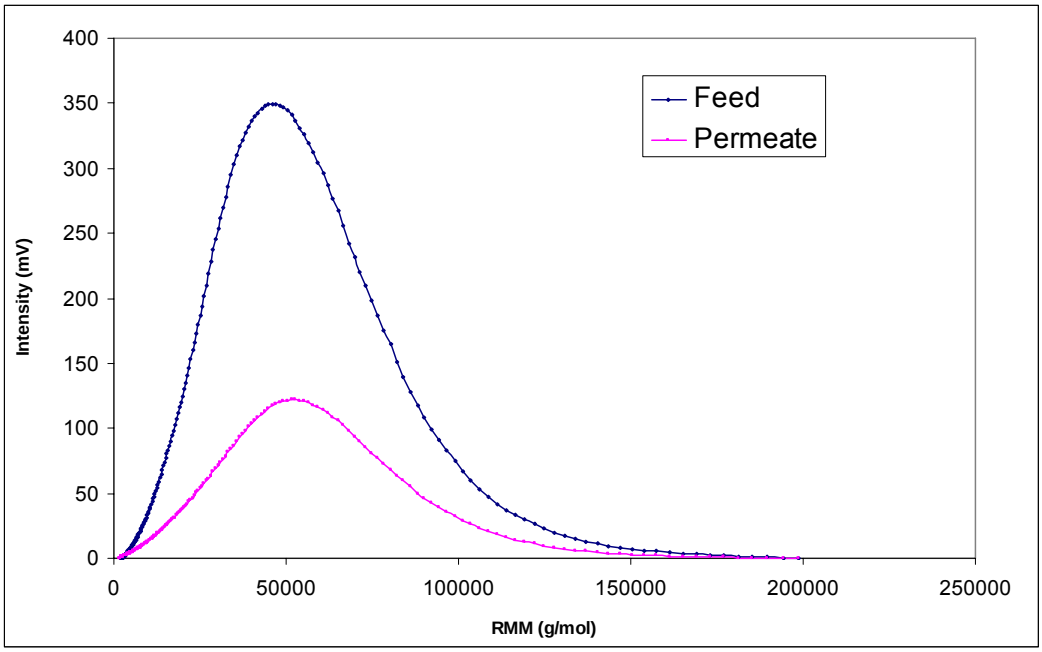


Figure 7. Pore Size Distribution curve of PLTK membrane

PLTK : Initial permeate flux and the final permeate flux were measured as 1.05 ml/min and 4.04 ml/min respectively. Final pressure was measured as 22 psi. The removal rate of PEG was calculated as %65.7. MWCO was calculated as 27282 Da for %72 fractional rejection (Figure 7).

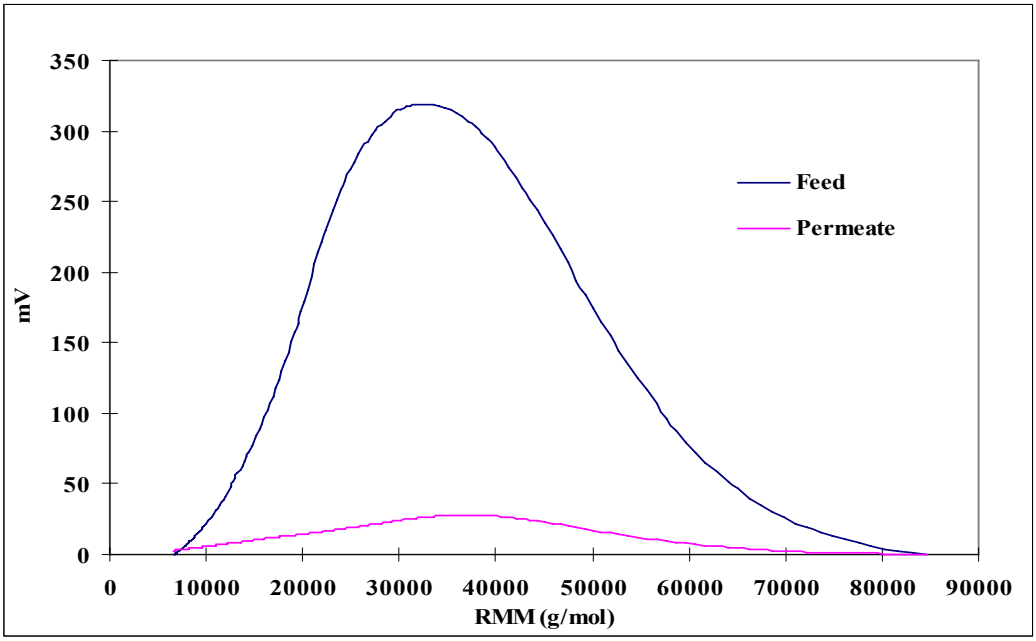


Figure 8. Pore Size Distribution curve of PBTK membrane

PBTK : Initial permeate flux and the final permeate flux were measured as 31.5 ml/min and 2.13 ml/min respectively. Final pressure was measured as 23 psi. The removal rate of PEG was calculated as %90. MWCO was calculated as 26199 Da for %92 fractional rejection (Figure 8).

Membrane Filtration

Ibuprofen Removal:

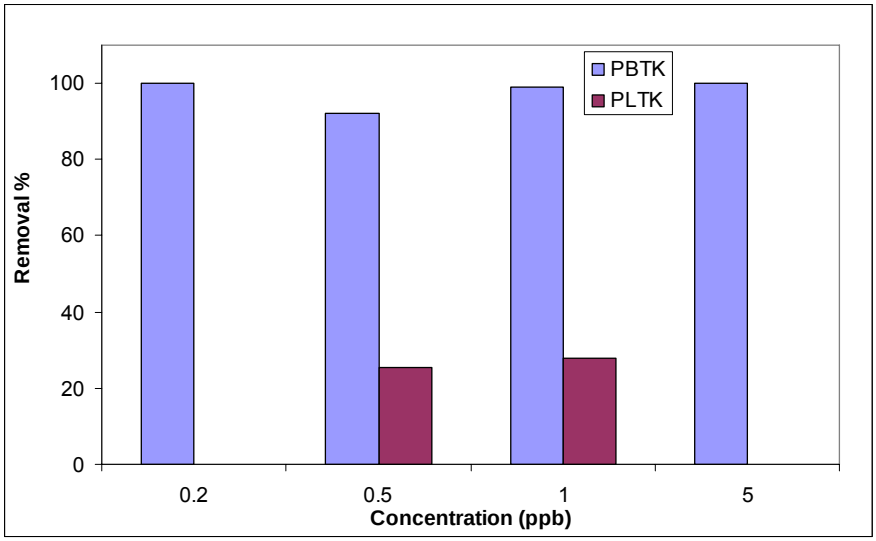


Figure 9. Comparison of the removal rates of Ibuprofen by PBTK and PLTK membranes with respect to first time interval (0-20 min).

Removal rate of the first time interval mainly depends on adsorption through the membrane surface. Because of similar hydrophobic characteristic of PBTK-Ibuprofen couple removal rate of Ibuprofen by PBTK membrane at the first time interval was very high in all concentrations (Figure 9).

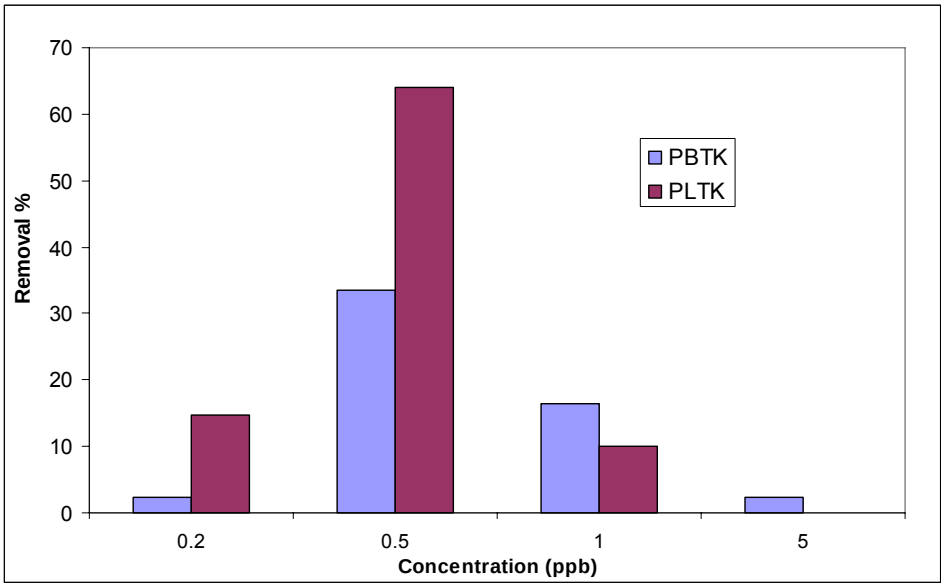


Figure 10. Comparison of the removal rates of Ibuprofen by PBTK and PLTK membranes with respect to second time interval (110-130 min).

Removal rate of the second time interval mainly depends on hydrophobic interaction and electrostatic repulsion. It was expected that removal rate of the Ibuprofen should be higher with using PBTK membrane. But for 0.5 and 0.2 ppb concentrations it has been seen that removal rate of Ibuprofen with PLTK was higher than removal by PBTK. This unexpected result led further investigations as contact angle measurement for used membranes. As can be seen from Table 2, at these concentrations PLTK membrane surface properties turned from hydrophilic to hydrophobic. These might came from fouling by external pollutants such as dust. It has been decided to repeat these experiments as soon as possible.

For 0.2 ppb experiments it has seen that removal efficiency of both membranes was decreased. Some of the previous studies shown that removal efficiency somehow affected by very low concentrations. Further studies on this subject should be done.

Table 2. Contact angle results for PLTK membrane after filtration by using 0.2 and 0.5 ppb Ibuprofen solutions (Sessile Drop Method)

Non-used PLTK	After 0.2 ppb Ibuprofen filtration	After 0.5 ppb Ibuprofen filtration
20^o	55.5^o	72^o

TCEP Removal:

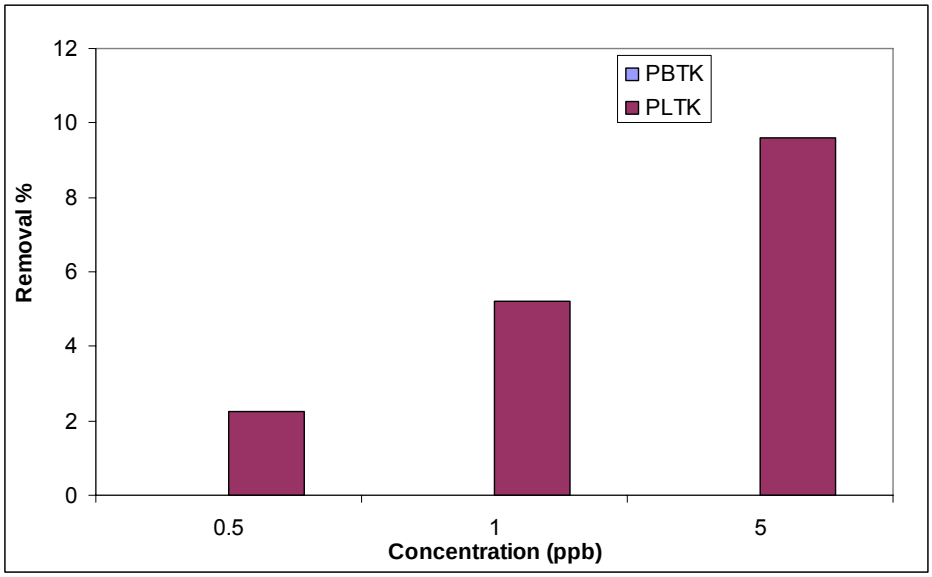


Figure 11. Comparison of the removal rates of TCEP by PBTK and PLTK membranes with respect to first time interval (0-20 min).

Removal rate of the first time interval mainly depends on adsorption through the membrane surface. Because of similar hydrophobic characteristic of PLTK-TCEP couple removal rate of TCEP by PLTK membrane was increased with increasing concentration (Figure 11). The adsorption of TCEP to PLTK membrane is increased with increasing concentration in short time interval and below adsorption capacity. TCEP removal with PBTK membrane could not be observed for the reason of high detection limit of GC/MS equipment.

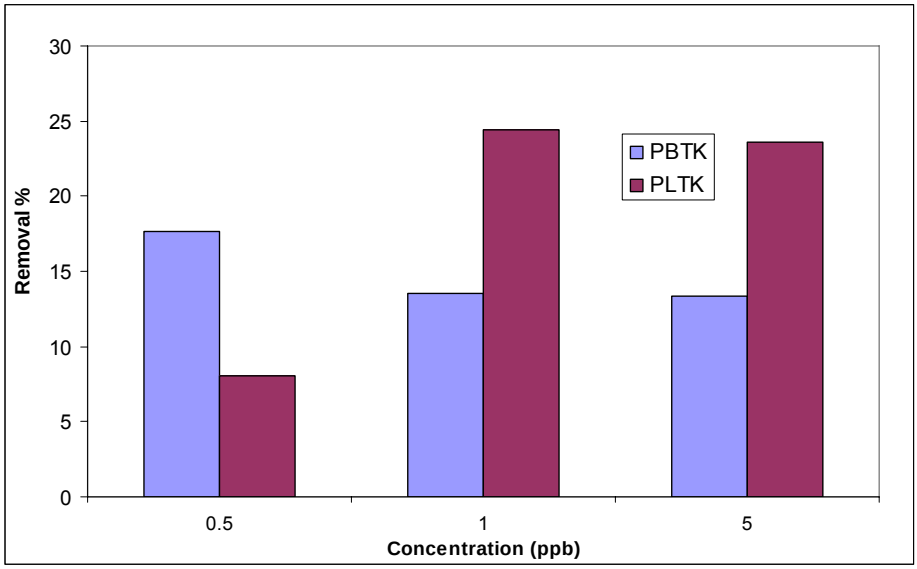


Figure 12. Comparison of the removal rates of TCEP by PBTK and PLTK membranes with respect to second time interval (110-130 min).

Removal rate of the second time interval mainly depends on hydrophobic interaction and electrostatic repulsion. It was expected that removal rate of the TCEP should be higher with using PLTK membrane than PBTK membrane due to hydrophobic similarity of TCEP-PLTK membrane couple. At 0.5 ppb removal efficiency of the TCEP with PLTK membrane decreased unexpectedly with respect to higher concentrations. This result was similar with the results of Ibuprofen filtration. In this manner further studies should be conducted through this observation. For 1 and 5 ppb TCEP solutions removal efficiency with PLTK membrane showed regular trends as expected. Removal efficiency of TCEP with using PBTK membrane showed expected trend with respect to concentration.

Conclusion

Solute concentration effects on removal of TCEP and Ibuprofen by using two different UF membranes were investigated. At 0.2 ppb concentration unexpected results occurred during Ibuprofen filtration. This might because of the other factors such as diffusion and partitioning behavior of solute-membrane couples that affect filtration processes. Further studies should be focused on observing of these factors. Similar result was taken from TCEP filtration experiments with using PLTK membrane at 0.5 ppb concentration. For TCEP measurements GC/MS was used and some samples couldn't be observed even though SPE and following nitrogen evaporation were done. This was because of the relatively high detection limit of the apparatus. With using more sensitive GC/MS or tandem mass equipment more accurate result may be observed.

References (for Appendix II)

1. **NoHwa Lee , Gary Amya, Jean-Philippe Crou´e, Herve Buisson,** "Morphological analyses of natural organic matter (NOM) fouling of low-pressure membranes (MF/UF)" Journal of Membrane Science 261 (2005) 7–16.
2. **Elke Fries, Wilhelm Puttmann**, "Occurrence of organophosphate esters in surface water and ground water in Germany", J. Environ. Monit., 2001, 3, 621–626.
3. **Yasunori Kawagoshi, Isao Fukunaga, Hisao Itoh,** "Distribution of organophosphoric acid triesters between water and sediment at a sea-based solid waste disposal site", J Mater Cycles Waste Manag (1999) 1:53–61.
4. **Brett J. Vanderford,* Rebecca A. Pearson, David J. Rexing, Shane A. Snyder,** "Analysis of Endocrine Disruptors, Pharmaceuticals, and Personal Care Products in Water Using Liquid Chromatography/Tandem Mass Spectrometry", Anal. Chem.2003, 75,6265-6274.
5. **A. Tauxe-Wuersch□, L.F. De Alencastro, D. Grandjean, J. Tarradellas,** "Occurrence of several acidic drugs in sewage treatment plants in Switzerland and risk assessment", Water Research 39 (2005) 1761–1772.

6. **Adriano Joss,□, Elvira Keller, Alfredo C. Alder, Anke Gobel, Christa S. McArdell, Thomas Ternes, Hansruedi Siegrist,** "Removal of pharmaceuticals and fragrances in biological wastewater treatment", Water Research 39 (2005) 3139–3152.
7. **W. F¨ollmann, J. Wober,** "Investigation of cytotoxic, genotoxic, mutagenic, and estrogenic effects of the flame retardants tris-(2-chloroethyl)-phosphate (TCEP) and tris-(2-chloropropyl)-phosphate (TCPP) in vitro", Article in Press.
8. **Michael Cleuvers,** "Aquatic ecotoxicity of pharmaceuticals including the assessment of combination effects", Toxicology Letters 142 (2003) 185/194.
9. **Paul Westerhoff , Yeomin Yoon, Shane Snyder , Anderic Wert,** "Fate of Endocrine-Disruptor,Pharmaceutical, and Personal Care Product Chemicals during Simulated Drinking Water Treatment Processes", Environ. Sci. Technol.2005, 39,6649-6663
10. **Shane A. Snyder, Paul Westerhoff, Yeomin Yoon, David L. Sedlak,** "Pharmaceuticals, Personal Care Products, and Endocrine Disruptors in Water: Implications for the Water Industry", ENVIRONMENTAL ENGINEERING SCIENCE Volume 20, Number 5, 2003.
11. **Shane A. Snyder, Erin Snyder, Daniel Villeneuve, Kannan Kurunthachalam, Alex Villalobos, Alan Blankenship, and John Giesy,** "Instrumental and Bioanalytical Measures of Endocrine Disruptors in Water", American Chemical Society: Washington, DC, 2000, pp 73-95.
12. **Katsuki Kimura, Hiroe Hara, Yoshimasa Watanabe,** "Removal of pharmaceutical compounds by submerged membrane bioreactors (MBRs)", Desalination 178 (2005) 135-140.
13. **Katsuki Kimura, Gary Amy, Jorg E. Drewes, Thomas Heberer, Tae-Uk Kim, Yoshimasa Watanabe,** "Rejection of organic micropollutants (disinfection by-products, endocrine disturbing compounds and pharmaceutically active compounds) by NF/RO membranes", Journal of Membrane Science 227 (2003) 113-121.

REFERENCES

ABC News., 2001. Clean fuel from soap? http://www.abcnews.go.com, accessed March 2003.

Abou-Shakra, F.R., Havercroft, J.M., et al., 1989, Lithium and boron in biological tissues and fluids, Trace Elem. Med. 6, 142.

Anderson JL, Eyring EM, Whittaker MP., 1964, Temperature jump rate studies of polyborate formation in aqueous boric acid. J Phys Chem 68:1128-1132.

Ando M., Iwahori H., Nakahara R. and Tawada S., 2001, Design operation and environmental aspects of 40,000 m^3/day seawater RO plant in Okinawa, Japan. Development of high boron rejection membrane technology, Proc. 4th Annual IDS Conference, Haifa, Israel.

Avril, T. n.d. Turning tide: Fuel-cell cars that make soap. http://www.energreen.org, accessed August 2002.

Badruk M., Kabay N., Demircioğlu M., Mordoğan H., İpekoğlu U., 1999, Sep. Sci. Technol., 34(15); 2981.

Banerji, S.K., May 1969, Boron adsorption on soils and biological sludges and its effects on endogenous respiration. 24th Industrial Waste Conference, Purdue University.

Banerji, S.K. Bracken, B.D. et al., May 1968, Effect of boron on aerobic biological waste treatment. 23rd Industrial Waste Conference, Purdue University.

REFERENCES (Continued)

Bolto, B. A. and Pawlowski, L., 1987, Wastewater Treatment by Ion exchange, McGraw-Hill Publishing, London, 57-62 pp.

Bringmann, G., and Kuhn, R., 1980, Comparison of the toxicity thresholds of water pollutants to bacteria, algae, and protozoa in the cell multiplication inhibition test, Water Res. 14, 231–241.

Bruggen B. V., 2003, Desalination by distillation and by reverse osmosis – trends towards the future, Membrane Technology, February.

Busch M., Mickols W. E., Jons S., Redondo J., Witte J. D., 2003, Boron Removal In Sea Water Desalination, Presented at International Desalination Association World Congress on Desalination and Water Reuse September 28 – October 3, 2003, Paradise Island, Bahamas.

Busch M., Mickols W. E., Prabhakaran S., Lomax I., Tonner J., 2005, Boron removal at the lowest cost, International Desalination Association SP05-024.

Butterwick, L., Oude, N.D., et al., 1989, Safety assessment of boron in aquatic and terrestrial environments. Ecotoxicol. Environ. Safety 17, 339–371.

Council of the European Union., 1998, Council Directive 98/83/EC, November 3, 1998, on the quality of water intended for human consumption.

Dean, J.A.,1987, ed. Lange's handbook of chemistry. New York: McGraw-Hill.

Desilva, J., 1999, Essentials of Ion Exchange, Presented at 25th W.Q.A. Annual Conference.

REFERENCES (Continued)

Draize, J.H., and Kelley, E.A., 1959, The urinary excretion of boric acid preparations following oral administration and topical applications to intact and damaged skin of rabbits, Toxicol. Appl. Pharmacol. 1, 267.

Fail, P.A., George, J.D., et al., 1990, Final report on the reproductive toxicity of boric acid (CAS No. 10043-35-3) in CD-1 Swiss mice. National Toxicology Program, National Institute of Environmental Health and Safety, Research Triangle Park, NC.

Fail, P.A., George, J.D., et al., 1991, Reproductive toxicity of boric acid in Swiss (CD-1) mice: Assessment using the continuous breeding protocol, Fundam. Appl. Toxicol. 17, 225–239.

Forbes, R.M., Cooper, A.R., et al., 1954, On the occurrence of beryllium, boron, cobalt, and mercury in human tissues, J. Biol. Chem. 209, 857–865.

Glueckstem P., Priel M., 2003, Optimization of boron removal in old and new SWFCO systems, Desalination 156, 219-228.

Harchelroad, F., and Peskind, R., 1993, Boric acid ingestion during the second trimester pregnancy, 1993 Int. Congr. Clin. Toxicol. 1993, 105.

Harland, C.E., 1994, Ion Exchange: Theory and Practise, The Permutit Company Limited, UK.

Hawthorne, M.F., 1993, The role of chemistry in the development of boron neutron capture therapy of cancer, Angew. Chem. Int. Ed. Engl. 32, 950–984.

Health Canada., 2002, Summary of Guidelines for Canadian Drinking Water Quality. 2003. Ottawa: Health Canada.

REFERENCES (Continued)

Hegsted, M., Keenan, M.J., et al., 1991, Effect of boron on vitamin D deficient rats, Biol. Trace Elem. Res. 28, 243–255.

Helfferich, F., 1962, Ion Exchange, Dover Publications, Inc., New York.

Ho Y.S., McKay G., 1998, Sorption of dye from aqueous solution by peat, Chem. Eng. J. 70 (2), 115–124.

Ho Y.S., 2003, Water Res. 37: 2323.

Holleman, A.F., and Wiberg, E., 2001, Inorganic chemistry, New York: Academic Press.

Howe, P.D., 1998, A review of boron effects in the environment, Biol. Trace Elem. Res. 66, 153–166.

Hunt, C.D., 1994, The biochemical effects of physiologic amounts of dietary boron in animal nutrition models, Environ. Health Perspect. 102(suppl. 7), 35–43.

Jansen, J.A., and Schou, J.S., 1984, Gastro-intestinal absorption and in vitro release of boric acid from water-emulsifying ointments, Food Chem. Toxicity 22(1), 49–53.

Jansen, J.A., Andersen, J., et al., 1984a, Boric acid single dose pharmacokinetics after intravenous administration to man, Arch. Toxicol. 55, 64–67.

REFERENCES (Continued)

Kabay N., Yilmaz I., Yamac S., Yuksel M., Yuksel U., Yildirim N., Aydogdu O., Iwanaga T., Hirowatari K., 2004, Removal and recovery of boron from geothermal wastewater by selective ion-exchange resins - II. Field tests, Desalination 167: 427-438.

Keren, R., and Bingham, F.T., 1985, Boron in water, soils, and plants, Adv. Soil Sci. 1, 229–276.

Koltuniewicz A. B., Witek A., Bezak K., 2004, Efficiency of membrane-sorption integrated processes, Journal of Membrane Science 239: 129-141.

Kunin, R., 1960, Elements of Ion Exchange, Reinhold Publishing Corporation, New York.

Kunin, R. and Preuss, A.F., 1964. "Characterization of a boron-specific ion exchange resin", Industrial and Engineering Chemistry: Product, Research and Development 3 4, pp. 304–306.

Kurihara M., Yamamura H. and Nakanishi T., 1999, High Recovery / High pressure Membranes for Brine Conversion SWRO Process Development and its Performance Data, Desalination 125: 9-15.

Liberti, L., Petruzelli, D., Hellferich, L., Millar, J. R., Passino, R., 1987, Kinetics of ion exchange with intraparticle rate control: Models accounting for interactions in the solid phase Reactive Polymers, 1:1-13.

Lovatt, C.J., and Dugger, W.M., 1984, Boron. In Biochemistry of the essential ultratrace elements, ed. E. Frieden, Vol. 3, pp. 389–421. New York: Plenum Press.

REFERENCES (Continued)

Magara, Y., Tabata, A., et al., 1998, Development of boron reduction system for sea water desalination, Desalination 118, 25–34.

Malik, A.U., Ahmad, S., Andijani, I. and Al- Fouzan. S., 1999, Corrosion behavior of steels in Gulf seawater environment, Desalination 123(2–3) 205–213.

Mannsville Chemical Products Corp, 1999, Chemical Products Synopsis—Sodium, http://www.mannsvillechemical.com.

Marinsky, A., 1966, Ion Exchange, Marcel Dekker, Inc., New York, Vol : 1.

Marston C., Busch M., Prabhakaran S., 2005. " A boron selective resin for seawater desalination" Paper for presentation at European Desalination Society Conference on Desalination and the Environment, Santa Margherita Ligure, Italy, 22-26 May 2005.

Matterson KJ., 1980 ,Borate ore discovery, mining and beneficiation. Sect. A3, vol 5, Suppl to Mellor's Comprehensive Treatise on Inorganic and Theoretical Chemistry (Thompson R, Welch AJE eds) Sect. A3, Vol 5.

Meacham, S.L., and Hunt, C.D., 1998, Dietary boron intakes of selected populations in the United States, Biol. Trace Elem. Res. 66, 65–78.

Moore, J.A., 1997, An assessment of boric acid and borax using the IEHR evaluative process for assessing human developmental and reproductive toxicity of agent, Reproduct. Toxicol. 11(1), 123–160.

REFERENCES (Continued)

Morgan V., 1980, Boron geochemistry. Suppl to Mellor's Comprehensive Treatise on Inorganic and Theoretical Chemistry (Thompson R, Welch AJE eds). Sect. A2, Vol. 5.

Murray, F.J., 1995, A human health risk assessment of boron (boric acid and borax) in drinking water, Regul. Toxicol. Pharmacol. 22, 221–230.

Nable, R.O., Banuelos, G.S., et al., 1997, Boron toxicity, Plant Soil 198, 181–198.

Nadav, N., 1999, Boron removal from seawater reverse osmosis permeate utilizing selective ion exchange resin, Desalination 124, 131–135.

New Zealand Ministry of Health, 2000, Drinking-water standards for New Zealand 2000. Wellington: Ministry of Health.

Newnham, R.E., 1994, The role of boron in human nutrition, J. Appl. Nutr. 46(3), 81–85.

Nielsen, F.H., 1994, Biochemical and physiologic consequences of boron deprivation in humans, Environ. Health Perspect. 7(suppl. 7), 59–63.

Oldfield, J.W. and Todd, B., 1999, Technical and economic aspects of stainless steels in MSF desalination plants, Desalination 124(1–3) 75–84.

Ozturk N. and Kavak D., 2005, Adsorption of boron from aqueous solutions using fly ash: Batch and column studies, Journal of Hazardous Materials B127, 81–88.

REFERENCES (Continued)

Parks J. L. and Edwards M., 2005, Boron in the Environment, Critical Reviews in Environmental Science and Technology, 35:81–114.

Pearce, F., 2004, Sea change for drinking water. New Sci. 22 (10 July).

Penland, J.G., and Eberhardt, M.J., 1993, Effects of dietary boron and magnesium on brain function of mature male and female Long-Evans rats, J. Trace Elem. Exp. Med. 6, 53–64.

Pillard, D.A., DuFresne, D.L., and Mickley, M.C., 2002, Development and validation of models predicting the toxicity of major seawater ions to the mysid shrimp, Americamysis Bahia. Environ. Toxicol. Chem. 21(10), 2131–2137.

Power, P.P., and Woods, W.G., 1997, The chemistry of boron and its speciation in plants, Plant Soil 193, 1–13.

Price, C.J., Carr, M.C., et al., 1990, Final report on developmental toxicity of boric acid (CAS No. 10043-35-3) in Sprague-Dawley rats. National Toxicology Program, National Institute of Environmental Health and Safety.

Price, C.J., Marr, M.C., et al., 1991, Final report on the developmental toxicity of boric acid (CAS No. 10043-35-3) in New Zealand white rabbits. National Toxicology Program, National Institute of Environmental Health and Safety.

Price, C.J., Marr, M.C., et al., 1994, Determination of the no-observable-adverse-effect-level (NOAEL) for developmental toxicity in Sprague-Dawley (CD) rats exposed to boric acid (CAS No. 10043-35-3) in feed on gestational d 0 to 20, and evaluation of postnatal recovery through postnatal day 21. Research Triangle Park, NC: Research Triangle Institute.

REFERENCES (Continued)

Recepoglu, O., and Beker, U., 1991, A preliminary study on boron removal from Kizildere/Turkey geothermal waste water, Geothermics 20(1/2), 83–89.

Redondo, J., Busch, M., De Witte J. P., 2003, "Boron removal from sea water using FILMTEC high rejection SWRO membranes", Conference on Desalination and the Environment – Fresh Water for All", 4-8 May 2003, Malta, published in Desalination 156.

Qadir, M., Boers, Th.M., Schubert, S., Ghafoor, A., Murtaza, M., 2003, Agricultural water management in water-starved countries: challenges and opportunities. Agric. Water Manage. 62, 165–185.

Qadir M., Sharma B.R., Bruggeman A., Choukr-Allah R., Karajeh F., 2006, Non-conventional water resources and opportunities for water augmentation to achieve food security in water scarce countries, Agricultural Water Management, Article in press.

Samatya, S., 2002, Removal of Boron from Aqueous Solutions by Using Chelating Ion Exchange Resins, MSc. Thesis, Ege University.

Samuelson, O., 1963, Ion Exchange Separations in Analytical Chemistry, Engineering Chemistry, Chalmers University of Technical, Sweden, John Wiley & Sons.

Semiat, R., 2000, Desalination: present and future. Water Int. 25, 54–65.

Soto F., Camacho E. M., 2005, Boron removal from industrial wastewaters by ion exchange: an analytical control parameter, Desalination 181: 207-216.

REFERENCES (Continued)

Sprague RW., l992, Boron. Metals and Minerals Annual Review, Metals Minerals, pt. 2; 106.

Stumm W. and Morgan J., 1981 Aquatic Chemistry, Wiley, New York.

Taniguchi, M., Fusaoka, Y., Nishikawa, T., Kurihara, M., 2004, "Boron removal in RO seawater desalination", Desalination 167.

Travis NJ, Cocks EJ., 1984, The Tincal Trail - A History of Borax. London: Harraps Ltd.

U.S. Environmental Protection Agency., 2003, Drinking water contaminant candidate list. 2003. http://www.epa.gov/safewater/ccl/cclfs.html.

Vadivelan V., Kumar K., 2005, Equilibrium, kinetics, mechanism, and process design for the sorption of methylene blue onto rice husk, Journal of Colloid and Interface Science 286: 90–100.

Vermeulen, T., Hiester, N.K, 1952, Saturation performance on ion Exchange and adsorption columns, Chemical Engineering Progress, 48:505-516.

Versar Inc., 1975, Preliminary investigation of effects on the environment of boron, indium, nickel, selenium, tin, vanadium and their compounds—Vol. I: Boron. Springfield, VA: U.S. EPA.

Voutchkov, N., 2004, The Ocean: a new resource for drinking water. Public Works 30–33.

Waggott, A., 1969, An investigation of the potential problem of increasing boron concentrations in rivers and water courses, Water Res. 3, 749–765.

REFERENCES (Continued)

Wells, N., and Whitton, J.S., 1977, A pedochemical survey; 3, Boron, N. Z. J. Sci. 20(3), 317–332.

Wester, R.C., Hui, X., et al., 1998, In vivo percutaneous absorption of boric acid, borax, and disodium octaborate tetrahydrate in humans compared to in vitro absorption in human skin from infinite and finite doses, Toxicol. Sci. 45, 42–51.

Woods, W.G., 1994, An Introduction to Boron: History, Sources, Uses, and Chemistry, Environmental Health Perspectives 102, Supplement 7.

World Health Organization., 1998, Boron. Environmental health criteria 204. Geneva: World Health Organization.

World Health Organization., 2003, Guidelines for drinking water quality. Boron. Geneva: World Health Organization.

Yılmaz Neval, 2003, Use of C_{14}^- and C_{16}^- Montmorillonites in Phenol Removal from Aqueous Media, MSc Thesis, Ege University, pp 117.

Yurdakoç M., Seki Y., Karahan S., Yurdakoç K., 2004, Kinetic and thermodynamic studies of boron removal by Siral 5, Siral 40, and Siral 80, Journal of Colloid and Interface Science 286 440–446.

Zagarodni, A., 1997, Seminar Notes, Ege University Chemical Engineering Department, Izmir.

CURRICULUM VITAE

Name: Sarper SARP
Date of Birth: April, 27, 1980
Place of Birth: Ankara, Turkey
Nationality: Republic of Turkish
Marital Status: Single
Adress: Kazım Dirik Mah. 165. Sok. No: 6 D:1
Bornova, İzmir, Turkey
Phone Number: +90 232 3881661
E-mail: sarper.sarp@gmail.com
Education: 1997-2004, BSc Degree in Chemical Engineering Department of Ege University, İzmir, Turkey
2004-2006, MSc Degree in Chemical Engineering Department of Ege University, İzmir, Turkey

Presentation in National and International Conferences:

1. IPEK, O., **SARP, S.**, YILMAZ, I., KABAY, N., YUKSEL, M., 2004. Boron removal from geothermal wastewaters by chelating resins and fibers. 6th National Chemical Engineering Congress, September 7-10, 2004 Ege University, Izmir, TURKEY (Poster Presentation, in Turkish)
2. **S.Sarp**, N.Kabay, Ö.Arar, Ö.Kırmızısakal, İ.Yılmaz, M.Yüksel, 2006. Removal of Boron from Seawater by Boron Selective Ion Exchange Resins, International Workshop On Frontiers And Interfaces Of Ion Exchange, June 11-15, Antalya, TURKEY (Poster Presentation)